



**FACULTY
OF MATHEMATICS
AND PHYSICS**
Charles University

DOCTORAL THESIS

Barbora Smolková

**Alteration of the redox signalling in liver cancer cells by
non-thermal plasma and laser irradiation**

Institute of Physics of the Czech Academy of Sciences

Supervisor of the doctoral thesis: Mgr. Oleg Lunov, PhD.

Study program: Physics

Specialization: Biophysics, Chemical and Macromolecular
Physics

Praha 2022

I declare that I carried out this doctoral thesis independently, and only with the cited sources, literature and other professional sources. It has not been used to obtain another or the same degree.

I understand that my work relates to the rights and obligations under the Act No. 121/2000 Sb., the Copyright Act, as amended, in particular the fact that the Charles University has the right to conclude a license agreement on the use of this work as a school work pursuant to Section 60 subsection 1 of the Copyright Act.

In Prague, March 25th 2022

.....

Author's signature

ACKNOWLEDGEMENT

During my PhD. study I have come through a huge transition, personal and professional. It has been a great journey full of interesting ideas, inspiring people, exceptional achievements but also days full of frustration and sleepless nights. Only now, when I am close to the end, I can realize that every unsuccessful exam or presentation, every failed experiment, every unpleasant situation, all the criticisms just helped me to become the person I am now. Here, I would like to thank to all the people who accompanied me during this path.

Firstly, I would like to thank to my colleagues from Institute of Physics for the opportunity to be a part of a very productive team of *dr. Oleg Lunov*. Thank you, *dr Oleg Lunov*, *dr. Alexandr Dejneka*, *Adam Frtús* and *Mariia Uzhytchak*! I can say without doubts that my lab-colleagues became my second family. In particular, I am thankful to my supervisor *dr. Oleg Lunov*, for his help with experimental work, borderless patience, inspiring and motivational discussions and trust in me. Thank you, for teaching me to think critically, to ask questions and finally to spot and call bullsh.t, not only in science.

Next, I would like to express my gratitude to *prof. Milan Jirsa* and his team from Institute for Clinical and Experimental Medicine (IKEM) for providing us the technical and scientific support over years. Particularly, to *dr. Mariia Lunova* for her patience, help with experimental work and time spent together not only in laboratory.

Last but not least, I would like to thank to my family and my friends for their support. Especially, I am thankful to my husband to be- *Adam*, for your love and understanding.

Title: Alteration of the redox signalling in liver cancer cells by non-thermal plasma and laser irradiation

Author: Mgr. Barbora Smolková

Department: Department of Optical and Biophysical Systems, Institute of Physics of the Czech Academy of Sciences

Supervisor: Mgr. Oleg Lunov, PhD., Department of Optical and Biophysical Systems, Institute of Physics of the Czech Academy of Sciences

Abstract:

Over the years, the implementation of physics-based techniques into medicine have contributed to the development of novel approaches for diagnostics and treatment. Recently, new promising therapeutic approaches, namely non-thermal plasma and low-power light (laser) therapy have gained attention for the treatment of various diseases. This dissertation thesis aims to critically assess the current knowledge in the field of plasma medicine and laser irradiation. In particular, it focuses on the interaction and molecular mechanisms of non-thermal plasma and laser light irradiation in 3 different hepatic cancer cell lines. We hope that our critical analysis will help researchers to overcome challenges and develop in the future better controlled, safer, and more robust NTP- and laser-based treatment modalities.

Keywords: hepatic cancer cells, non-thermal plasma, laser irradiation, oxidative stress, redox signalling

Název práce: Změna redoxní signalizace v buňkách rakoviny jater působením nízkoteplotního plazmatu a laserového ozařování

Autor: Mgr. Barbora Smolková

Katedra: Oddělení optických a biofyzikálních systémů, Fyzikální ústav AV ČR

Školitel: Mgr. Oleg Lunov, PhD., Oddělení optických a biofyzikálních systémů, Fyzikální ústav AV ČR

Abstrakt:

Aplikace fyzikálních metod jsou dlouhá léta významným prostředkem pro vývoj inovativních diagnostických a léčebných procesů v medicíně. V poslední době si pro svůj léčebný potenciál a vlastnosti získaly pozornost nízkoteplotní plazma a lasery o nízkém výkonu. Tato disertační práce shrnuje dosud známé informace v oblasti výzkumu nízkoteplotního plazmatu a laserové terapie. Práce se zaměřuje zejména na studium molekulárních mechanismů a efektů vzájemného působení nízkoteplotního plazmatu a laserového ozařování u tří buněčných linií rakovinných buněk jater člověka. Věříme, že analýza, kterou tato disertační práce představuje, bude přínosem pro budoucí výzkum a vývoj lépe ovladatelných a spolehlivých léčebných využití nízkoteplotního plazmatu a laserů o nízkém výkonu.

Klíčová slova: Buněčné linie rakoviny hepatocytů, nízkoteplotní plazma, laserové ozařování, oxidační stres, redoxní signalizace

TABLE OF THE CONTENTS

1. INTRODUCTION	1
1.1. Redox signalling in cells: Sources, targets and antioxidants.....	1
1.1.1. Role of oxidative stress in progression of different pathological conditions...	7
1.1.2. Oxidative stress and liver pathology	9
1.1.3. Redox balance modulation as a therapeutic approach.....	11
1.2. Nonthermal plasma interaction with cancer cells	13
1.2.1. Generation and characterization of non-thermal plasmas	13
1.2.2. Possible mechanisms of action	15
1.2.3. Plasma- cancer cells interaction.....	17
1.2.4. Biomedical applications of non-thermal plasmas	20
1.3. Laser-light interaction with living cells.....	22
1.3.1. Characterisation and production of light used in biomedicine.....	22
1.3.2. Light-cells interaction	23
1.3.3. Mechanisms of action of the non-specific laser light interaction	25
1.3.4. Biomedical applications of light-based technologies.....	26
1.4. Challenges and perspectives	28
2. AIMS	30
3. EXPERIMENTAL PART-METHODS	33
3.1. Cell cultures.....	33
3.2. Protein extraction and Western blot analysis.....	33
3.3. Microscopy	34
3.4. Spectro-fluorometric analysis	36
3.5. Statistical analysis.....	36
4. EXPERIMENTAL PART-RESULTS	37
4.1. Plasma interaction with living cells	37
4.1.1. Characterization of plasma device	37
4.1.2. Analysis of cell viability post NTP treatment.....	40
4.1.3. Detection of cellular ROS and Superoxide	41
4.1.4. Analysis of mitochondria post NTP treatment.....	43
4.1.5. Detection of apoptotic cell death.....	45
4.1.6. Analysis of cellular signalling post plasma treatment.....	47
4.2. Laser light irradiation with living cells.....	50
4.2.1. Laser light characterization	50

4.2.2.	Analysis of cell death post laser irradiation	52
4.2.3.	Analysis of mitochondria post laser irradiation	54
4.2.4.	Effects of laser irradiation on mitochondrial electron transport chain	57
4.2.5.	Up-regulation of Bcl-2 protein stabilized the mitochondria and protected cells from cell death	62
5.	CONCLUSIONS	66
	BIBLIOGRAPHY	68
	LIST OF FIGURES	79
	LIST OF TABLES	81
	LIST OF ABBREVIATIONS	82
	LIST OF PUBLICATIONS:	84
	LIST OF APPENDICES	86

1. INTRODUCTION

1.1. Redox signalling in cells: Sources, targets and antioxidants

Reactive oxygen species (ROS) are highly reactive oxygen containing reactive chemical species, formed by electronic excitation or by redox reactions. ROS can be classified into two groups, non-radical, which are chemically reactive, but do not contain free electrons and free radical species with one or more unpaired electrons [1, 2]. Moreover, ROS can react with other molecules referred to as reactive nitrogen species (RNS), in order to form oxidants. Both ROS and RNS are involved in signal transduction in living cells [3, 4]. Depending on the concentration, RONS can promote or suppress cellular proliferation, growth, differentiation, or induce an irreversible oxidative damage activating cell death signalling [1, 5].

Examples of the selected biologically relevant RONS are combined in the Table 1, together with their source, cellular targets and functions (Table 1). However, the term reactive oxygen species does not represent the chemical compound or molecule, but rather “*it is a collective term for a number of related molecules with vastly divergent reactivity*” [2]. Thus, it is needed to specify the particular RONS type wherever possible.

Table 1: Major types of reactive oxygen and nitrogen species involved in the biological systems signalling.

	Designation	Cellular Targets	Functions	Source	Ref.
Non-radicals	Hydrogen Peroxide (H ₂ O ₂)	Proteins Pr-(Cys)-S-	Signal transduction Cellular proliferation, differentiation, migration, Angiogenesis Inflammation Growth arrest and Cell death	NOX, mitochondria	[1, 2]
	Singlet molecular oxygen (¹ O ₂)	DNA (guanine), Unsaturated lipids Proteins	Defence mechanisms used by phagocytic cells against pathogen Liperoxidation process Cell death	Reaction catalysed by Myeloperoxidase/ Lipoxygenases H ₂ O ₂ with or O ₃ with HOCl biomolecules	[6]

		Pr-(Met)/ (His)/(Trp)	Signal transduction	Photosensitization reactions	
	Organic hydro- peroxides (ROOH)	DNA Proteins Lipids	Signal transduction Immune response Ferroptosis	Form in lipid peroxidation from polyunsaturated fatty acids (PuFas) and sterols	[2]
	Ozone (O ₃)	Lipid Proteins	Immune response Cell death and inflammation Oxidative stress in lungs	Air pollution Some atmospheric conditions White blood cells	[2, 7]
	Hypochlorous acid and hypobromous acid (HOCl and HOBr)	DNA Proteins Pr- (Met)/(Cys)	Immune response Wound healing Microorganisms' deactivation	From H ₂ O ₂ by myeloperoxidase in the phagocytic vacuoles of the neutrophils	[2, 8]
Free radicals	superoxide anion radical (O ₂ ⁻)	Proteins Pr-[4Fe-4S]	Signal transduction (From proliferation to cell death)	NOX, mitochondria	[2]
	Hydroxyl radical (·OH)	Proteins Pr-(Cys)-S- Lipids	Lipid peroxidation Signal transduction	Fenton reaction	[2]
	Peroxyl radical (ROO·)	Proteins Lipids	Lipid peroxidation	from polyunsaturated fatty acids (PuFas)	[2]
	Nitric oxide (NO·)	DNA Proteins Pr-(Tyr)	Vasodilatation Signal transduction Immune response Regulation of nervous system Nitrosylation	from L-arginine by NOS (eNOS, nNOS, iNOS)	[2-4]
	Peroxynitrite (ONOO ⁻)	DNA Lipids Proteins Pr-(Tyr)	Pathogen deactivation Oxidative damage Cell death	diffusion-limited reaction of NO· with O ₂ ⁻	[2-4]

From the Table 1, one can clearly see that RONS are participating in a number of cellular processes, ranging from cellular proliferation and death, to immune response and pathogen deactivation. However, before discussing the functions in more details, we have to reveal where are the ROS coming from.

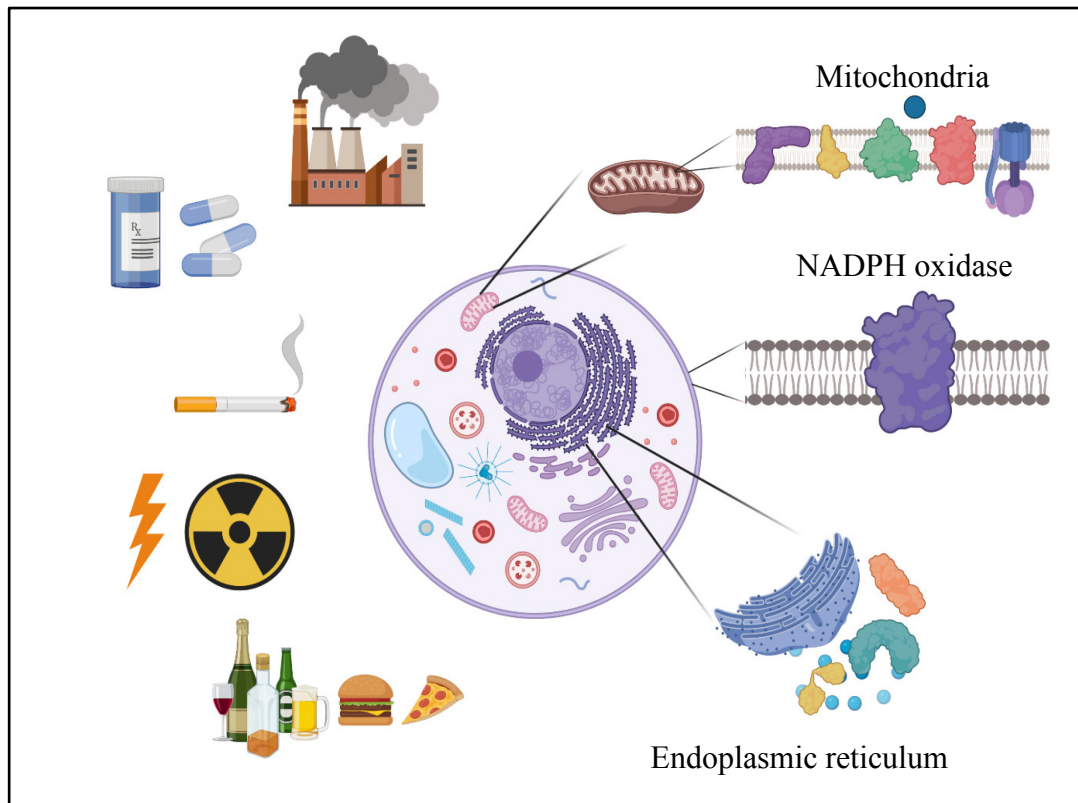


Figure 1 Schematic illustration of exogenous and endogenous sources of ROS. The various factors can influence the ROS levels in the cells. On the left side, to the exogenous sources belong air pollution and heavy metals, drugs, tobacco smoke, ionizing radiation, UV, X-ray and lifestyle. On the right side, the major endogenous sources represent the mitochondria, NOX localized to cellular membranes and the endoplasmic reticulum. Created with BioRender.com

RONS can be produced inside the cells as a by-product of the cellular aerobic metabolism [1] (Fig.1). It is widely accepted that primary intracellular source of ROS are mitochondria and their electron transport chain (ETC). In ETC, electrons from nicotinamide adenine dinucleotide phosphate (NADPH) and flavin adenine dinucleotide (FADH₂) flow through series of carriers, complexes I, II, III, IV, V, cytochrome c and ubiquinone. This results in the reduction of 4 electrons of O₂ to H₂O₂ during oxidative phosphorylation. Concomitantly, protons are moved from the mitochondrial matrix to the intermembrane space forming the electrochemical gradient across the inner membrane [5]. Electron leakage, as a result of insufficient reduction or in a controlled manner under physiological conditions, leads to the formation of

H_2O_2 and $\text{O}_2^{\bullet-}$ and its subsequent conversion to other ROS [1, 5]. Moreover, ROS can be produced in endoplasmic reticulum during oxidative protein folding. Another important source of ROS are NADPH oxidases (NOXes), enzymes localized to cellular membranes. NOXes are key component of the phagocytic cells used for pathogen killing during the immune response [5]. Additionally, ROS can be produced as secondary products of some biochemical reactions, such as activity of superoxide dismutases, myeloperoxidases, in prostaglandin synthesis by cyclooxygenases, during β -oxidation of fatty acids in peroxisomes, by detoxification of drugs by cytochrome P450 or by Fenton reaction [1, 2, 5, 9] (Table 1). Moreover, reactive oxygen and nitrogen species can be generated and subsequently accumulated as a result of the exposure to a number of environmental factors, including the air pollution, tobacco smoke, ionizing radiation, UV, X-rays, heavy metals, drugs and even certain psychological stressors [5](Fig.1).

ROS are very reactive and can reversibly or irreversibly modify the different range of biomolecules, including DNA, proteins and lipids, and thus alter their functions. The thiol-based modification of target proteins is the main mechanism by which RONS regulate redox signalling in cells [2, 10]. A closer look at the data combined in the Table 1 indicates that proteins containing cysteine residues are very susceptible to oxidation. ROS can cause cysteine modifications, such as glutathionylation, nitrosylation, persulfidation or formation of intramolecular and intermolecular disulphide bridges that affects the protein functions [2, 10]. Besides cysteine thiols, residues of other amino, such as tyrosine, methionine, arginine, lysine, proline and iron-sulphur (4Fe-4S) clusters are ROS interaction targets [2, 5]. Additionally, excessive oxidative stress, induced by ROS mediated fatty acids peroxidation, changes the integrity of lipid bilayer and subsequently leads to cell death. Moreover, DNA functionality and stability can be greatly affected by ROS activity. Especially, the oxidation of guanine and adenine have an influence on the DNA methylation, telomere length and can contribute to the ROS-triggered tumorigenesis [5].

Mitochondria are complex double-membrane, semiautonomous organelles involved in many crucial cellular functions (64-66,74)[11-14]. Mitochondria consist of the outer membrane (OMM), intermembrane space, inner membrane (IMM), cristae structures, which are formed by protrusion of IMM and matrix (Fig.2). The main role

of the mitochondria is the ATP production in the process of oxidative phosphorylation and generation of NADH in tricarboxylic acid cycle (TCA). Oxidative phosphorylation takes place on IMM, whereas the tricarboxylic acid cycle occurs in the mitochondrial matrix [15]. Besides its function in energy conversion, mitochondria also regulate the redox homeostasis, calcium signalling and cell death[11-13, 15, 16].

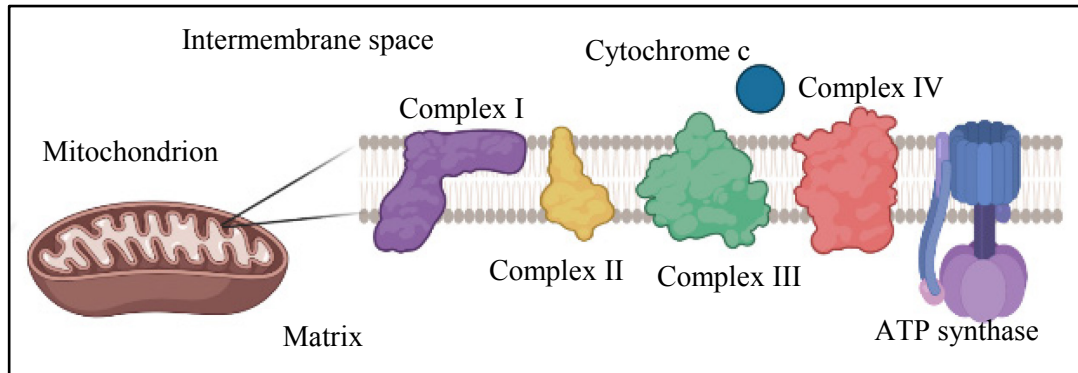


Figure 2 Schematic illustration of electron transport chain of mitochondria. Created with BioRender.com

Mitochondria are dynamic structures that can change their shape and morphology during cell cycle, depending on metabolic state or in a response to various stimuli in the processes called fission and fusion [16, 17]. Under normal physiological conditions, mitochondria are tubular and continuously divide and fuse. However, under stress stimuli, especially under oxidative stress, mitochondria become roundish, forming giant spheres or hyperfused structures [17]. The balance between fission and fusion is crucial for maintenance of the normal mitochondrial homeostasis. These processes are tightly regulated by specific proteins, e.g., Drp1, Mff, Fis1, MIEF1/MiD51, MIEF2/MiD49 (regulate fission) and OPA1, Mfn1, and Mfn2 (regulate fusion) [16]. Moreover, mitochondrial dynamics is associated with mitochondrial quality control mechanism. It has been shown that the mitochondrial fusion results into renewal of impaired mitochondria by joining of compartments of healthy and damaged mitochondria [18]. However, when the damage is extensive, dysfunctional mitochondria are removed from the cells in the process known as mitophagy, mitochondrial autophagy [19, 20]. It is worth noting that recently new mitochondrial quality control process has been described in migrating cells, known as mitocytosis [21]. During mitocytosis, damaged mitochondria are transported to the periphery of the cells and released in vesicles called migrasomes [21].

Moreover, mitochondrial fission is associated with segregation of mitochondria during cell division [14] and also with cell death activation [11, 16, 22]. In general, mitochondria are crucial regulators of the intrinsic apoptotic pathway. The mitochondrial outer membrane permeabilization (MOMP) driven by proteins BAX and BAK of B cell lymphoma 2 (Bcl-2) protein family is required for the apoptosis execution. This leads to cytochrome c release from mitochondria to cytosol and its binding to adaptor molecule apoptotic peptidase activating factor 1 (APAP1) and formation of complex called apoptosome. Further, apoptosome cleaves the caspase-9, which activates the executioner caspases 3/7 and triggers the apoptosis [22]. Besides their function in apoptosis, mitochondria are also involved in the other types of regulated cell death, such as necroptosis, ferroptosis and pyroptosis [22]. Dysregulation of mitochondrial homeostasis and changes in their function are linked with development of different types of diseases, including diabetes, neurodegenerative disorders, heart failure, changes related to aging and cancer [23, 24]. Especially, excessive ROS production and oxidative stress, MOMP and formation of mitochondria permeability transition pore (MPTP), impairment of calcium homeostasis and inflammation are contributing to the majority of pathologies [23, 24]. Thus, it is not surprising that, recently, several therapeutical approaches have been developed for selective targeting of mitochondria [25]. Nevertheless, despite the extensive research in this area there is still a number of challenges that has to be solved[25].

ROS act as double-edge sword in cells, at low levels can positively regulate cellular proliferation and growth. However, the increase in the ROS production and subsequent decrease of the scavenger molecules impair the cellular redox balance and induce oxidative stress, that may result into the cell death [2, 9]. In order to maintain cellular homeostasis, eukaryotic cells developed several mechanisms to regulate ROS generation and their levels at physiological concentrations (Table 2).

Table 2: Enzymatic and non-enzymatic antioxidants involved in the ROS regulation.

	Antioxidant	Function	Ref.
Enzymatic Antioxidants	Catalase	Decomposition of H ₂ O ₂ to water and oxygen	[26]
	Glutathione peroxidase (GPx)	Reduction of H ₂ O ₂ to water Reduction of lipid peroxides to alcohols	[27]

	Superoxide dismutase (SOD1, SOD2, SOD3)	Dismutation of $O_2^{\bullet-}$ to H_2O_2 and to oxygen	[28]
	Thioredoxin (Trx)	Redox signalling control Restoration of eNOS function	[29, 30]
	Heme oxygenase (HO)	Degradation of heme to CO, biliverdin/bilirubin, free ferrous iron	[31]
	Peroxiredoxins (Prx)	Reduction of peroxides	[29, 30]
Non-Enzymatic Antioxidants	Glutathione	Maintain the redox balance in cells Glutathionylation	[30]
	Uric acid	ROS scavenger	[29]
	Bilirubin	ROS scavenger	[31]
	Vitamin C and E	ROS scavengers	[29]
	N-acetylcysteine	ROS scavenger Precursor of Glutathione	[32]

In a series of reactions, RONS are reduced to more stable and less reactive form by antioxidants [29]. The knowledge of antioxidants action is crucial in order to reveal the subcellular mechanism of ROS. As it is seen from the Table 2, there are two subtypes of antioxidants, enzymatic or non-enzymatic involved in the ROS scavenging. Enzymatic antioxidants, such as catalase, glutathione peroxidase, superoxide dismutase, thioredoxin, heme oxygenase and peroxiredoxins act selectively and convert the specific ROS into less reactive product [33, 34].

1.1.1. Role of oxidative stress in progression of different pathological conditions

The increased production of RONS together with reduced capacity of antioxidant system may lead to disruption of redox signalling and induction of oxidative stress. It is widely accepted that oxidative stress is associated with pathophysiology of many diseases, including cardiovascular and neurodegenerative diseases, ischemia-reperfusion injury, many metabolic disorders and cancer [1, 2, 9, 35, 36]. Indeed, cancer cells display higher rate of aerobic glycosylation accompanied with oxidation of pyruvate in mitochondria, known as the Warburg effect [37]. Moreover, due to transformation in metabolism and signalling, cancer cells have endogenously higher levels of ROS in comparison with normal cells [1] (Fig.3). As noted above, certain

ROS levels may alter the structure and function of cellular macromolecules and thus induce the mutations leading to initiation and progression of cancer. However, compelling evidence suggests that, excessive ROS levels can suppress the tumour growth and metastasis spreading [38, 39].

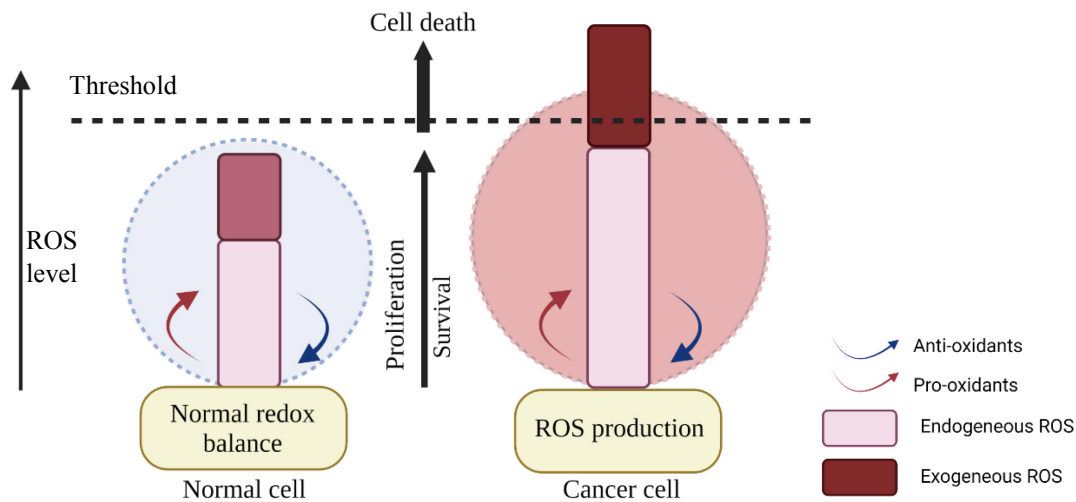


Figure 3 Comparison of the redox status in normal and cancer cells. Adapted from ref.[1]
Created with BioRender.com

Number of factors regulates the reprogramming of the redox signalling and metabolism in cancer cells. Because of the increased rate of proliferation, cancer cells require more extensive ATP production, that leads into higher ROS accumulation. In order to manage the oxidative stress, cancer cells need to adapt the antioxidant system [1]. Keap1/Nrf2 pathway is one of the major regulators of the redox homeostasis [40]. Under normal conditions, Nrf2 binds to Keap1 and is localized in cytosol, where it is ubiquitinated and degraded in proteasome. Contrary, during oxidative stress cysteines of Keap1 are oxidized, which leads to Nrf2 dissociation from Keap1 and its translocation into the nucleus [41]. In the nucleus, Nrf2 binds to antioxidant responsive elements (AREs) and triggers the expression of genes involved in the detoxification and oxidative stress scavenging, e.g. glutathione and thioredoxin [40]. Due to Nrf2 function in redox balance maintaining, it has been widely accepted that Nrf2 act as tumour suppressor [42]. However, recent studies have shown that the Keap1/Nrf2 pathway is contributing to cancer metabolic rewiring and progression [43, 44]. It is worth noting that many cancer types possess different mutations in *KEAP1* and *NRF2* genes, that supports their association with tumorigenesis [45-47]. Moreover, the most frequently mutated gene in human cancer is *TP53*, occurring in almost half of all tumours [48]. The vast majority of the mutations are missense, localized in the DNA-

binding domain, resulting into the expression of dysfunctional protein [49]. Normal wild type of p53, besides its function as genome guardian, is involved in redox homeostasis[50]. Depending on the conditions in the cell, p53 may trigger the expression of anti-oxidant genes, such as GPx1, GLS2, TIGAR, p21 and SESN2, or pro-oxidants genes, such as Puma, Bax, Noxa, PIG3, FDXR, and SCO2 [50]. On the other hand, mutant p53 (mutp53) stimulates the cancer progression and promotes metastasis and chemoresistance [49]. Further, in cancer cells, mutp53 raises the glucose uptake and shifting the cellular metabolism towards aerobic glycolysis[51]. Moreover, to induce the transcription of antioxidant molecules, mutp53 has the ability to interact with Nrf2 protein and thus protect the cancer cells from oxidative stress and cell death [49, 50]. It is worth mentioning that mutated p53 is very often connected with poor patients' prognosis in many cancer types, including hepatocellular carcinoma[52].

1.1.2. Oxidative stress and liver pathology

The liver is an important organ, responsible for the detoxification of xenobiotics, drugs and alcohol. ROS production is a typical by-product of such detoxifications as a result of series of oxidative reactions. In the liver, RONS are produced by mitochondria and cytochrome P450 in the hepatocytes; and by activation of NADPH oxidases in neutrophils and Kupfer cells [53]. Malfunction of physiological processes of the liver may lead to redox imbalance and oxidative stress. It is widely accepted that oxidative stress disrupts the normal liver function and largely contributes to the development of many metabolic and proliferative liver diseases [53]. Correlation between liver damage and impaired redox homeostasis has been shown in many reports involving patients with different diagnosis [54, 55].

Non-alcoholic fatty liver disease (NAFLD) is one of the most common chronic liver conditions in Western nations [36]. The main cause of NAFLD is the increased triglycerides accumulation in the liver. Moreover, recent studies suggest that oxidative stress, especially ROS produced by fatty acid oxidation, β - and ω - oxidation are contributing to the NAFLD development [56]. Under certain conditions, NAFLD can be transformed into more aggressive non-alcoholic steatohepatitis (NASH), which is accompanied with inflammation, liver injury and fibrosis [56]. Different factors are contributing to the NASH progression, including lipogenesis, insulin resistance, mitochondrial accumulation of cholesterol, endotoxemia, oxidative stress and others

[53, 56-58]. Moreover, drug misuse or overuse may lead to drug-induced liver injury (DILI) [59]. Further, NASH may develop into cirrhosis and eventually hepatocellular carcinoma (HCC) [57]. The liver cancer is the sixth most frequently occurring cancer worldwide [60, 61]. 90% of all cases are hepatocellular carcinoma with different aetiology. There are many risk factors that are contributing to the pathophysiology of HCC, such as genetic predisposition, cirrhosis, alcohol, obesity, diabetes mellitus, metabolic-related NASH or hepatitis B (HBV) and hepatitis C (HCV) virus infections (Fig.3)[60, 61]. During the HCC progression, hepatocytes gather different chromosomal aberrations and DNA mutations. The most common are the mutations in TERT promoter leading to telomerase activation. In addition, mutations accumulate in genes involved in the cell cycle control, proliferation and metabolism regulation, e.g., TP53, PTEN, Wnt- β -catenin signalling pathway, AKT-mTOR and MAPK pathways [52]. It is worth noting here that hypoxia promotes the tumour growth, angiogenesis, survival, spreading and invasiveness of cancer cells [53]. Specifically, the production of hypoxia-induced mitochondrial ROS may lead to activation of NF- κ B and HIF-1 α [62, 63] and thus contribute to the cancer progression. On the other hand, excessive ROS generation post glutathione depletion may shift hypoxia from a pro-survival to a pro-death by activating necrosis [64]. Additionally, changes in cholesterol metabolism, especially cholesterol accumulation in mitochondria, support the solid tumour growth by shifting cancer metabolism towards aerobic glycolysis [63] and contribute to the resistance to chemotherapy[65]. Moreover, malfunction of iron metabolism and its accumulation in the liver is associated with oxidative stress in hereditary hemochromatosis and other liver diseases[66]. Understanding the specific signaling pathway is essential for the successful development of therapeutic approach.

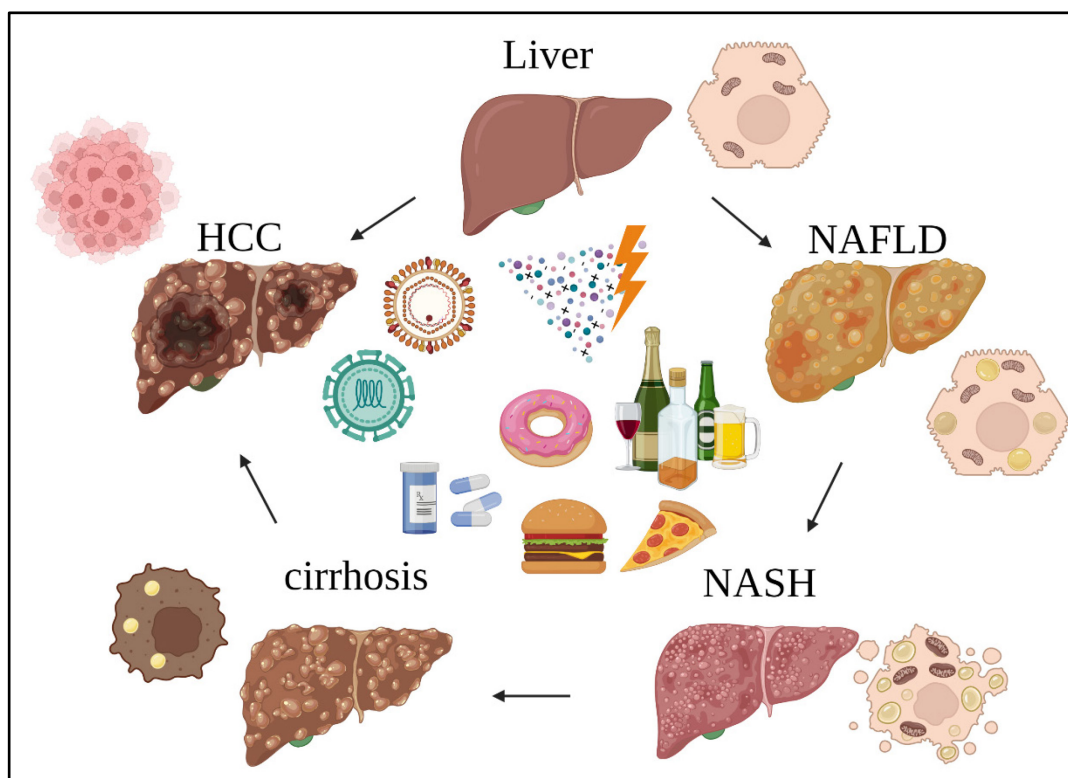


Fig. 4 Different stages of liver pathology. Arrows indicates progression of liver damage. Different factors contributing to the HCC. Created with Biorender.com.

1.1.3. Redox balance modulation as a therapeutic approach

We may conclude from previous chapters, that ROS and oxidative stress play crucial role in both normal functions of cell and different pathological conditions. Therefore, it is not surprising that ROS-mediated signalling and redox modulation are being utilized in certain therapeutic strategies [1, 39]. For example, cancer cells possess higher basal level of ROS and impaired redox state (Fig.3). Hence, the use of exogenous antioxidant may inhibit the tumour growth and stop the cancer spreading. It has been shown that the vitamin E supplements may potentially decrease the liver cancer risk [67]. However, other studies indicate that antioxidants action contribute to the tumorigenesis and development of drug resistance [68, 69]. Alternatively, the depletion of ROS may lead to cell death inhibition and tumour progression [68]. It is worth noting here that in order to adapt to redox changes, cancer cells may induce the activation of redox sensitive pathways, such as Nrf2, NF- κ B, HIF1, c-JUN and thus increase endogenous levels of antioxidant and pro-survival molecules [1]. Thus, the elevation of oxidative stress by exogenous ROS-producing agents simultaneously with antioxidant system inhibition might be an effective therapeutic strategy in selective killing of the cancer [1].

Currently, there is a number of agents modulating the redox system of cancer cells under the investigation in clinical trials or already approved by the FDA and used in clinic (Table 3). Moreover, as the research is progressing, new promising therapeutic approaches have emerged, such as non-thermal plasma treatment and photodynamic therapy [70, 71].

Table 3: Selected therapeutic approaches used for cancer treatment modulating the redox system.

Treatment entity	Type of Cancer	Mechanism of action	Ref.
5-fluorouracil (5- FU)	Colon, rectal and head-neck cancer	Elevation of O ₂ ⁻ level Incorporation into DNA/RNA	[72]
Anthracyclines (Doxorubicin, daunorubicin or epirubicin)	Various types of cancer	Generation of free radicals via ETC and Fenton reaction Inhibition of telomerase II	[73]
NOV-002	HER2-negative breast cancer	Changes in glutathione homeostasis	[74]
Sulfasalazine	Pancreatic and lung cancer	Inhibitor of cysteine/glutamate transporter XCT	[75, 76]
Cisplatin	Ovarian cancer Non-small lung cancer	Changes in ETC activity Production of ROS	[77]
2-methoxyestradiol (2-ME)	Neuroblastoma	Generation of free radicals Loss of mitochondrial membrane potential	[78]
G202	Prostate cancer	Increased level of ROS and calcium	[79]
Celecoxib	Prostate cancer	ER-mediated ROS production Inhibition of cyclooxygenase 2 (Cox2)	[80]
Bortezomib	Head and neck squamous cell carcinoma	ER-mediated ROS production	[81]
Arsenic trioxide	Myeloma, Leukemia	Generation of free radicals Inhibition of cellular respiration	[82]
Ionizing Irradiation	Various types of cancer	Breakage of the chemical bonds by irradiation	[83]

	Generations of free radicals and ROS		
Non-thermal Plasma	Various types of cancer	ROS generation	[70]
Photodynamic therapy (PDT)	Various types of cancer	Effects of light and photosensitising molecule	[71]

Currently, physics-based treatment modalities represent provocative and leading-edge developments of novel therapeutic strategies [84, 85]. From Table 3 one can clearly see that there is a number of physics-based approaches aimed to modulate redox balance. In following chapters, we will overview actively researched external physical cues intended to be applicable as therapeutic strategies for modulation of redox balance, i.e., non-thermal plasma and laser irradiation. We selected those physical cues because they are actively researched and hold great opportunities for the development of future therapeutic modalities. However, those approaches need to prove their effectivity in evidence-based medicine (EBM) controlled health care systems.

1.2. Nonthermal plasma interaction with cancer cells

1.2.1. Generation and characterization of non-thermal plasmas

In 1879, William Crookes described the *plasma* as fourth state of matter for the first time [86]. With increased energy, the form of matter converts from solid to liquid, to gas and to plasma (Fig.4). The term *plasma* has been introduced into field of physics by Langmuir and Tonks in 1929 [87]. Plasma is defined as quasi-neutral ionized gas, consisting of charged particles and atoms. Depending on the temperature of the particles, plasma can be classified into high-temperature (HTP) and low-temperature (LTP). Further, LTP can be subdivided into thermal and non-thermal [88]. The thermal plasma can reach the thermodynamic equilibrium because the temperatures of heavy particles and electrons are very similar. In non-thermal plasma the temperature of heavy particles is lower in comparison with the electron temperature [89]. Thus, the temperature of whole system is less than 40°C. This type of plasma has been applied for various biomedical applications (e.g., wound healing, bacteria eradication, dental hygiene, blood coagulation, angiogenesis suppression, cancer treatment [86, 90-92] due to treatment of living cells or tissues without inducing the thermal injury [86].

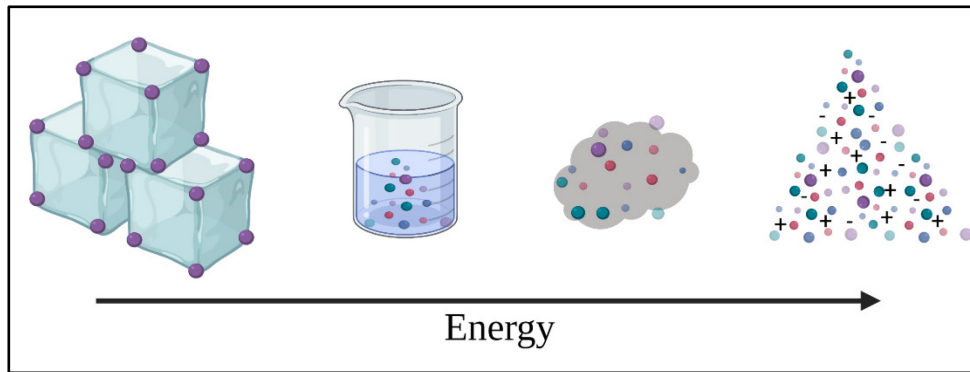


Figure 5 Four states of matter. From the left solid, liquid, gas and plasma. Created with Biorender.com.

Ionization, the process of ions formation, by which the neutral atoms loss or gain the electrons, is needed for plasma generation. Neutral gas is ionized by using various forms of energy e.g., thermal or electrical energy, UV light, gamma or X-ray electromagnetic radiation[93]. Different methods of non-thermal plasma generation have been developed for biomedical applications. The most commonly used methods are dielectric barrier discharge (DBD) and atmospheric pressure plasma jet (APPJ) [88]. Briefly, DBD consists of two metal electrodes that are covered by dielectric material. Gas is ionized to plasma in between high voltage electrode needed for the discharge and the grounded one[86]. Nowadays, many different configurations and device settings have been developed for NTP generation. One of them is so called floating-electrode DBD (FE-DBD), where the second electrode is replaced by living tissue or another sample allowing direct application [94]. DBD devices have shown promising results in effective blood coagulation and bacterial decontamination[94, 95]. However, it is worth noting that direct application of high voltage to the cells or tissue may alter their functionality. This issue is prevented in APPJ, another regularly used plasma device in biomedical applications [88, 89, 96]. The main advantage of APPJs is the scalability of the jet, which enables changes in size, working gas or in physical parameters (e.g., voltage) [97]. Despite the huge variability of settings, principle stays relatively the same; plasma is generated between two electrodes and carried in a gas flow to the desired area. Many different types of APPJs have been developed, from small plasma needles and pencils to big plasma torches [98, 99]. Scalable size of APPJs enabled their effective use in treatment of small areas and cavities and also in large-scale treatments using multiple jets approach [99, 100]. Ar-based kINPen, the most studied APPJ device, showed a great potential in wound healing, bacterial decontamination and tissue regeneration [70]. It is worth noting that

kINPen MED received CE certification as a medical device for the treatment of wound and skin diseases associated with pathogens in 2013 [70].

1.2.2. Possible mechanisms of action

As noted above plasma is a chemical cocktail consisting of uncharged particles, ions, UV photons and reactive oxygen and nitrogen species. Nowadays, there is a consensus in scientific literature that complexity of plasma and synergistic effect of active particles are responsible for plasma mechanism of action [70, 88, 89, 101]. However, it is worth mentioning that the settings of physicochemical parameters of plasma devices greatly affect biological outcomes of NTPs. Among those parameters are values of voltage, frequency, input power working gas, flow rate, mode of plasma generation and exposure time [89, 90, 102-104]. Additionally, the used cellular or animal model also play crucial role in studies assessing the plasma effects. Despite the fact, that number of studies have shown the positive effects of NTP in various biomedical applications, the precise mechanism of action remains elusive. Based on previous studies we can conclude that there are 3 major factors involved in the plasma-cell interactions, namely UV radiation, RONS and charged particles [89, 90, 102-104]. It is worth noting that, effects of UV radiation and charged particles are minimal by NTP treatment of eukaryotic cells [105].

Bactericide properties of UV light have been used for sterilization in biomedicine over decades [106]. It is generally known, that UV radiation at 260 nm may cause irreversible damage in DNA structure by formation of pyrimidine dimers. Moreover, longer exposure to higher doses of UV may lead to increased rate of mutations and eventually to cell death. Thus, it was logical to explain the plasma induced bacterial damage as a result of UV radiation[107]. We and others have shown no or only a minor impact of plasma derived UV photons on microorganisms' decontamination [108, 109]. It is worth mentioning here that it is challenging to generate UV light with energy sufficient to induce any harmful effects by atmospheric pressure plasma production[86]. Power measurements of NTP generated UV revealed that the power density of the emitted UV light is $3 \pm 1 \mu\text{W}/\text{cm}^2$ for He-based NTP and lower than $1 \mu\text{W}/\text{cm}^2$ for air-based NTP when using discharges lower than 10kV [104, 110]. To induce any effect on living cells or tissues we would need to use UV radiation with at least one order of magnitude higher values [111]. On the other hand, other studies highlighted the UV as major agent inducing bacterial cell death post NTP

treatment [112]. This brings us to the main challenge in the plasma field, which is the huge variability of device settings used for plasma generation, what makes the direct comparison of results very difficult.

Another important aspect, especially in plasma-induced bacterial decontamination is the electrostatic disruption of bacteria wall and accumulation of charged particles on surface of bacteria [113]. Ions excessively accumulating on surface of bacteria may cause the physical disruption of bacterial wall resulting in leakage of the internal compartments and subsequent cellular death [89, 113, 114]. Such effect of charged particles may be particularly advantageous by direct NTP treatment. Direct plasma treatment mode showed higher antimicrobial efficiency over indirect plasma treatment [115].

Reactive oxygen and nitrogen species are other important components of plasma affecting the biomolecules [116-119]. The most abundant RONS in non-thermal plasma are superoxide, hydrogen peroxide, ozone, singlet oxygen, hydroxyl and organic radicals, nitric and nitrogen oxides, and peroxyxynitrite [70, 120]. It must be noted that RONS composition of plasma is very complex and can be extremely various. It has been shown that there are more than 96 chemical reactions in the air NTP with additional number of RONS, generated by plasma interaction with liquid environment [121]. In general, RONS can be classified as long-lived (O_3 , H_2O_2 , NO_2^- , NO_3^-), and short-lived ($\bullet OH$, O , O_2^- , $^1O^2$, $NO\bullet$, $NO_2\bullet$). Yet, the lifetime of long-lived species does not exceed the range of milliseconds [105, 120, 122, 123].

Further, the penetration depth of NTP is quite low, up to 2 mm *in vitro* and only up to ~400 μm in *in vivo* models [105]. Moreover, the penetration depth of plasma is strictly dependent on the treatment time and other physical parameters [105, 122]. Thus, the mechanism of action of plasma-mediated ROS has been proposed as a combination of several follow-up events [105]. Due to the relatively short lifetime and high reactivity, plasma-mediated ROS interact with biomolecules and form ROS intermediates. Further, ROS intermediates act as signalling molecules inside the cells and are primarily responsible for redox system modulation induced by NTP [105].

The majority of the studies agrees that plasma generated RONS are significant contributors to the eukaryotic cell's response to NTP treatment [116-119]. This is not surprising because RONS are involved in many cellular processes, from cell

proliferation, growth to activation of cell death [1, 91, 124-126]. It is worth mentioning that the outcome is dependent on the RONS concentration and exposure time [2, 9]. The low dosage of compound (RONS) has positive effect and stimulates cell proliferation whereas the higher dosage induces toxic effects followed by cell death. This phenomenon is called hormesis [105, 127]. Various studies described the hormetic response to plasma mediated ROS in different cell lines [105]. Moreover, Privat-Maldonado et al proposed hormetic response as a reason for NTP utilization in different areas, from wound healing to cancer treatment [105].

1.2.3. Plasma- cancer cells interaction

During last three decades, non-thermal plasma effects have been demonstrated on various types of prokaryotic and eukaryotic cells [103, 104, 106] [116-119] [112, 128-131]. NTP may alter cellular signalling on different levels, from inhibition of proliferation to inducing distinct types of cell death [116-119]. Moreover, growing number of studies showed that NTP may preferentially kill cancer cells without damaging the surrounding cells and tissue [131-133]. Overview of selected studies showing the NTP effects on different cancer types *in vitro* and *in vivo* is summarized in the Table 4 (Table 4).

Table 4: Summary of NTP interaction with cancer models *in vitro* and *in vivo*.

Type of device	Working gas	Voltage	Cancer Model	Signalling events	Ref.
DBD	Helium with 0.25% of oxygen	Vp-p~28 kV	hepatocellular carcinoma cells Bel7402 5-FU-resistant Bel7402/5FU	Signs of apoptotic and necrotic cell deaths	[134]
Spray-type AP NTP system	Helium and oxygen	2 kV minimum 13 kV maximum	head and neck cancer cells FaDu and SNU1041, SCC, SNU899, HN9	Apoptotic cell death via MAPK-mediated mitochondrial ROS	[135]
APPJ	Air	2 kV	blood cancer cells U937, THP1, RAW264.7	Apoptotic cell death	[136]
APPJ	Argon	N.A.	36 tumour cell lines	Correlation of cell metabolism	[137]

				to resistance to NTP	
APPJ	Argon	2–6 kVpp	Glioblastoma cells U87, U251 and LN229	Decreased viability post plasma- activated PBS	[138]
DBD	Helium	Inpute voltage 5V	17 tumour cell lines	Apoptotic cell death in p53- mutated cancer cells	[139]
DBD	Synthetic Air and Oxygen	13 kVpp	Melanoma and pancreatic cancer cells PANC-1, Hmel1 MM, HBL MM	ICD	[140]
DBD	Air	Inpute voltage 10 kV	triple negative breast cancer cells MDA-MB-231 MDA-MB-453 and normal cells MCF10A	Apoptotic cell death in cancer cells	[141]
DBD	Oxygen	29 kV	THP-1, A549 in co- culture	ICD	[142]
APPJ	Argon	N.A.	Jurkat, U-937	Apoptotic cell death	[143]
APPJ	Argon	a sinusoidal voltage with a frequency of 1 MHz	C57BL/6 mice Pancreatic cancer cells	Apoptotic cell death in tumour tissue	[144]
APPJ	Oxygen or nitrogen	24 kV	CD2F1 and C57BL/6 mice	Inhibition of tumour growth	[145]
DBD	Argon	17 kV	Melanoma cancer cells C57BL/6J mice	ICD	[146]
APPJ	Argon Argon/Oxygen Helium Helium/Oxygen	N.A.	Melanoma cancer cells C57BL/6 mice	ICD	[147]

The selectivity of treatment is crucial for setting up an efficient and safe cancer treatment. Different hypothesis has been suggested to clarify greater susceptibility of cancers towards plasma (Fig.6) [131, 133, 148-150].

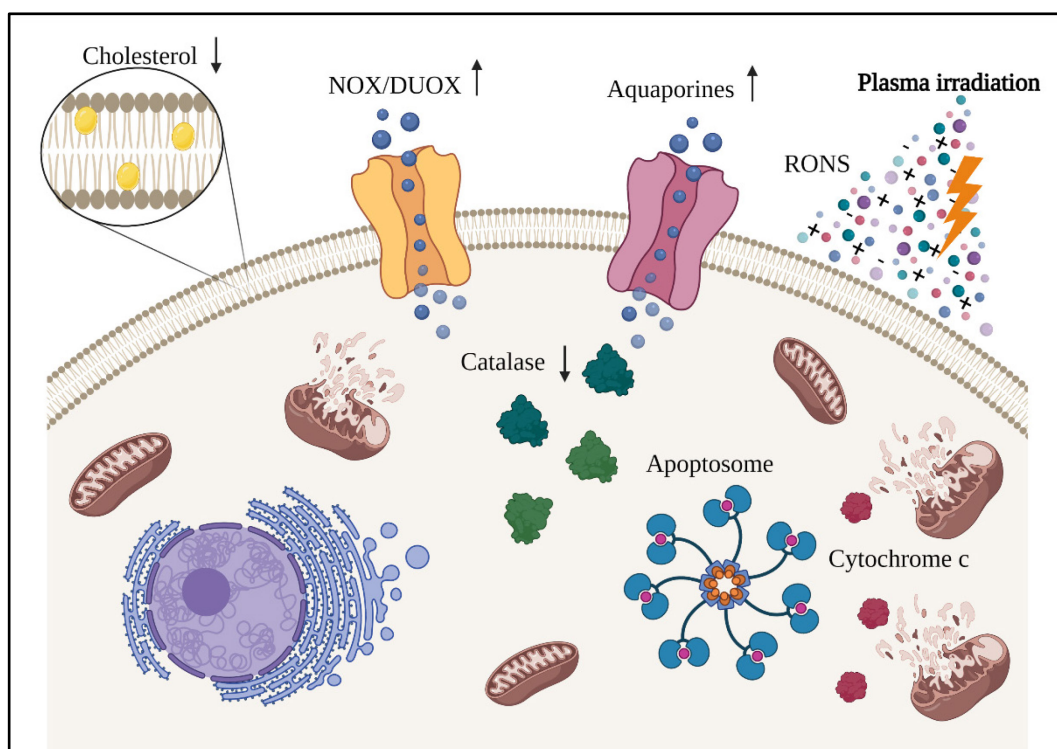


Figure 6 Schematic illustration of the potential mechanism of non-thermal plasma in cancer cells. Scheme was created with Biorender.com

As noted above, cancer cells display altered energy metabolism and changes in redox signalling. Specifically, cancer cells possess higher basal level of ROS in comparison to normal cells [1]. Thus, different studies postulated that using of ROS-generating agent, such as non-thermal plasma, would result in selective cancer killing [148, 149]. However, this turned out not to be always the true, because cancers are very heterogeneous and may adapt to oxidative stress by enhancing their antioxidant systems [1]. Another possible explanation of plasma selectivity towards cancer cells is based on different expression of catalase and aquaporins in cancers[148]. Some cancer cells possess elevated expression level of aquaporins, i.e., transporters of H_2O_2 and water[151]. During the NTP treatment, plasma-derived H_2O_2 may penetrate into cancer cells at higher rate in comparison with normal cells and thus may potentially induce higher oxidative damage [148]. Particularly, it is notable in the cancer cells with decreased anti-oxidant enzyme expression, such as catalase. However, the levels of catalase expression in cancer cells may greatly vary among different cancers [152]. Similarly, it has been proposed that higher expression of redox enzymes, such as

NADPH oxidases (NOX) and dual- oxidases (DOUX), on cancer cell membrane is contributing to higher sensitivity of cancers to NTP, by enhancing the toxic effects of NTP-mediated ROS [150]. Recently, Bekeschus et al revealed in their study by using 36 cancer cell lines that neither the aberrant expression of aquaporins nor redox-related enzymes could explain the cancer cells susceptibility towards plasma treatment [137]. Contrary, they observed higher resistance to NTP- treatment. However, the major limitation of this study is that they compared just the absolute expression levels of aquaporins and enzymes, not their activity. In addition, Bekeschus et al proposed another hypothesis, that the decreased cholesterol content of tumour cell membranes may provide a gateway for sensitization of tumours to plasma-mediated oxidation and resultant cytotoxicity [137]. Surprisingly, the study found correlation of the cholesterol level and metabolic activity with NTP treatment resistance of cancer cells [137].

This brings us to the conclusion that despite the years of research, biochemical and cellular foundations of NTP action remain still not fully understood. Understanding the precise molecular mechanisms of action of drug or treatment is crucial for successful implementation into clinical practice [153, 154].

1.2.4. Biomedical applications of non-thermal plasmas

Over the years, non-thermal plasma has shown promising results in different areas of biomedicine, ranging from microorganisms' decontamination, wound healing, dental hygiene, blood coagulation, medical devices sterilization to cancer treatment [70, 155]. Despite the wide range of biomedical applications of plasma, so far only pathogen-based skin diseases treatment and wound healing found the real application in the clinic [70, 156]. Positive effects of NTP treatment on chronic wounds of patients have been shown in different randomized clinical trials [157, 158]. Especially, APPJ device kINPen developed by the INP Greifswald, Germany is one the most used and studied plasma devices in biomedicine [70]. In 2013, kINPen MED received CE certification as a medical device for the treatment of wound and skin diseases associated with pathogens [70]. Nowadays, there are more commercially available NTP devices used in clinical research [70]. Besides this success, other potential applications of NTP in biomedicine are currently under the investigation. In recent years, compelling evidence proposed NTP as a new safe potential tool for targeted cancer treatment [155, 159]. It has been shown that plasma treatment may induce the immunogenic cell death in cancer cells[140, 142, 160]. However, it is worth noting that the vast majority of the

studies showed the activation of damage- associated molecular patterns (DAMPs) only *in vitro*, without direct validation in *in vivo* models [161]. Various pre-clinical studies confirmed that NTP treatment may selectively target the tumour cells or reduce the metastatic spreading [137, 162]. It is clear that synergistic effect of plasma mediated RONS is responsible for the anti-cancer activity of NTP [148, 149]. Dysregulation of redox status of the tumour cells showed promising results in targeted cancer treatment [1]. Recently, several studies used NTP in combination with conventional chemotherapy or with other novel techniques [163, 164]. Kaushik et al showed that plasma treatment in combination with glycolysis inhibition induce cell death in blood cancer cells [136]. Moreover, Rasouli et al proposed the combination of NTP with specific nanoparticles as a potential cancer treatment [164].

Despite that substantial progress, there is still a number of questions needed to be addressed. One of them is the delivery of plasma inside the body to the target place [70]. Recently, plasma- treated solutions (synonyms plasma-activated solutions, plasma-enriched solutions...) have gained increasing attention [138, 165]. However, the composition, shelf life and generation of such solutions have to be carefully evaluated [164]. Another big challenge, which we highlighted above, is the huge variability of plasma devices used in biomedical applications. Standardization of the protocol for plasma treatment will contribute to the faster transition towards potential clinical application [166]. Even though, non-thermal plasma has shown potential in cancer treatment, further research is essential in order to reveal the precise mechanisms of action in specific tumour types.

1.3. Laser-light interaction with living cells

1.3.1. Characterisation and production of light used in biomedicine

Light is a part of electromagnetic radiation (ER), ranging from gamma rays to radio waves [167]. As one of the first, in 19th century, Niels Finsen showed the positive effects of UV-induced phototherapy for treatment of lupus vulgaris [71]. Over the years, a wide spectrum of electromagnetic waves has been routinely used for diagnostic or treatment in medicine, from X-rays, gamma rays in computed tomography (CT) to radio waves in magnetic resonance imaging (MRI) [71]. Thus, it is not surprising that different applications of light, with its very low photon energy (0.5-3eV) and non-ionizing properties, are under the investigation [71]. Three major directions of light-based applications have been established, namely laser surgery, optical diagnosis and light-activated therapy [71]. In this thesis, we will focus more closely on photobiomodulation (PBM) or low-level laser (light) therapy (LLLT) and lasers used in microscopic imaging. Of note, in a laser system, light is emitted in a process of optical amplification involving stimulated emission of photons. This light is characteristic by its temporal and spatial coherence [167]. In contrast to laser surgery, where the photothermal effects are used, in LLLT the major effect is induced by photochemical interactions [71]. However, it is worth noting that number of factors may affect the desired outcome, including wavelength, source of the light, treatment time, power density (irradiance), energy density (fluence), spot size, tissue absorption characteristics [168]. In general, two categories of low power lasers (power of 0.001-0.1W) have been used for photobiomodulation: low optical intensity ($<10\text{W}/\text{cm}^2$) and high optical density ($\gg 10\text{ W}/\text{cm}^2$, $\sim\text{kW}/\text{cm}^2$) lasers [71, 123, 167, 169, 170]. Moreover, different values of fluence, energy density, have been reported in various studies, ranging from 1 to $50\text{ J}/\text{cm}^2$ [168]. It has been shown that this level is adequate for induction of photochemical effects [71]. Additionally, higher fluence will substantially increase the temperature of the treated tissue. Thus, in order to prevent the thermal damage, fluence lower than $1\text{ J}/\text{cm}^2$ is used for biomedical applications [71]. Another very important factor affecting the efficiency of the treatment is penetration depth, which is directly dependent on the wavelength of used light. Especially in the skin, the effective penetration depth at which the incident optical density decreases to $\sim 37\%$ is around $50\text{-}100\mu\text{m}$ for the UV and blue light (400-450nm), $\sim 200\text{-}800\mu\text{m}$ for the green light (500-550nm) and 1-3mm for red and near infra-red light (NIR) (600-1350nm) [71, 123]. It is worth noting that the penetration depth of

infra-red light above 2000nm is around 50-100 μ m because of the high light absorption by water [71, 123]. For this reason, the NIR light found utilization in many areas of biomedicine.

1.3.2. Light-cells interaction

Light is directly involved in many important physiological processes, from vision, colour perception, circadian rhythm, metabolism of vitamin D and others [71]. Especially, vision is a very complex process by which light stimuli are collected and converted into electrical signal in the eyes and transmitted through optic nerves to the brain. For this purpose, human eye has specialized cells (rods and cones) containing specific photoreceptor proteins involved in the photons absorption [71]. However, recent studies showed that even cells without photoreceptors cells might interact with light non-specifically [171-178]. In general, photons of light are interacting with biological tissue and cells by two processes classified as scattering and absorption [71]. As the light is absorbed, energy of photons is transformed into vibrational or electronic energy of the absorbing molecule. The part of the energy which is emitted in the form of luminescence. Moreover, the scattering might influence propagation path, polarization and spectrum of incident light. Both light absorption and scattering are used as a basement for optical imaging methods [71].

Over the years, it has been shown that low power light can affect cells on different levels [169, 171-173, 179]. Overview of selected studies showing the effects of low power light on different models *in vitro* and *in vivo* is summarized in the Table (5).

Table 5: Summary of interactions of low power light on different biological models *in vivo* and *in vitro*.

Properties of light source	Model	Main outcome	Ref.
He-Ne laser 633 nm Fluence of 120 J/cm ² Output power 4.3 μ W	human lung adenocarcinoma cells (ASTC-a-1)	Mitochondria-mediated apoptotic cell death	[180]
LED light at 620 nm Fluence of 2 J/cm ² Output power N.A.	human umbilical cord mesenchymal stem cells (hUMSCs)	Enhanced cell proliferation and osteogenic differentiation	[172]
LED light at 530 nm Fluence N.A. Output power N.A.	human orbital fat stem cells (OFSCs)	Enhanced OFSCs migration	[173]

<p>Laser diode 655 nm At power 1 mW power density at a distance of 500 μm 18.7 kW/cm² 46 μW, the power density was 0.8 kW/cm² Fluence N.A. Output power N.A.</p>	<p>Human hepatocellular carcinoma cells Huh7</p>	<p>Low dose laser irradiation [169] led to apoptotic cell death Higher dose led to CypD-related necrosis</p>
<p>Laser at 810 nm Various irradiances (W/cm²) Fluence N.A. Output power N.A.</p>	<p>Human dermal keratinocytes (HaCaT) human normal oral keratinocytes (NOKSI) 57BL/6NCr male mice</p>	<p>ROS and thermal damage [175] Endoplasmic reticulum - mediated stress response</p>
<p>InGaAlP diode laser at 660nm, 30 mW Fluence of 0.5 J/cm², 16 s and 1.0 J/cm², 33 s Output power N.A.</p>	<p>Human periodontal ligament stem cells (hPDLSC)</p>	<p>Enhanced proliferation [171]</p>
<p>GaAlAs laser diode at 810nm Fluence of 0.3 J/cm², 3 J/cm², 30 J/cm² Output power N.A.</p>	<p>hDSCs and a rodent pre-odontoblast cells Rats (Sprague-Dawley) Mice C57B6/129SVJ/FvBN</p>	<p>ROS production [174] Differentiation of cells <i>in vitro</i> Dentin regeneration <i>in vivo</i></p>
<p>Diode laser at 810nm power density at 1 mW/cm² -30 mW/cm² Fluence of 0.003, 0.03, 0.3, 3 and 30 J/cm² Output power N.A.</p>	<p>Murine embryonic fibroblasts</p>	<p>ROS production and [176] NF-kB activation</p>
<p>660nm fluence of 5 J/cm², and power density of 11.2 mW/cm² 830nm fluence of 5 J/cm², and power density of 10.3 mW/cm² Output power N.A.</p>	<p>WS1 human skin fibroblast cells</p>	<p>Increased diabetic wound [177] healing</p>
<p>LPLI at 810nm</p>	<p>human oral cancer OC2 cells</p>	<p>ROS production [178]</p>

Fluence from 10 to 60 J/cm² Output power N.A.	human gingival fibroblast (HGF) cells	Activation of cell death in cancer cells
---	--	---

Detailed analysis of the table 6 shows that studies using light sources with lower optical density (<10W/cm²) reported various “*positive*” effects on tested models, from stimulating of proliferation and differentiation to decreasing the cellular viability and cell death activation in cancer cells [169, 171, 172, 178, 179]. On the other hand, utilization of low power light with high optical density (>>10 W/cm², ~kW/cm²) induced phototoxic damage and ROS- mediated cell death [167, 169, 175, 176, 180]. One can see the big variability of the outcomes depending on the used parameters. This brings us to the similar problems and discrepancies as in non-thermal plasma field, namely variability in the used parameters, difficulties in direct comparison of the outcomes and lacking precise mechanism of action.

1.3.3. Mechanisms of action of the non-specific laser light interaction

Many studies have shown that low power light may affect the cells and tissues on molecular level[169, 171-176, 178-180]. However, it is worth noting that physical parameters and the used cellular or tissue model can greatly influence the desired treatment outcome [168]. Despite the years of research on low power laser light, the precise mechanisms of action of nonspecific light interaction with cells are not fully understood. Based on the current knowledge several hypotheses have been discussed in the scientific literature (Fig. 7) [71, 167, 181].

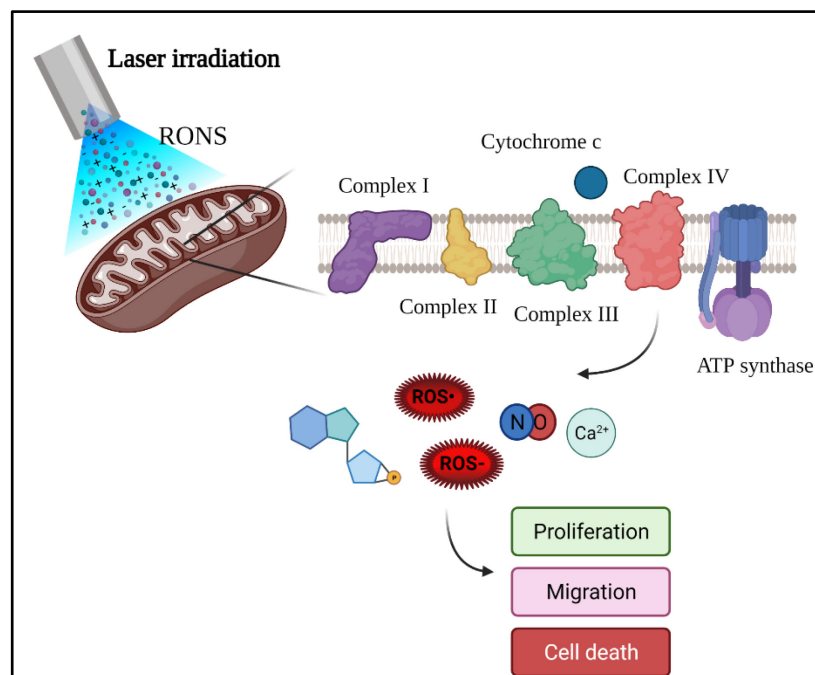


Figure 7 Scheme of the potential mechanisms of laser light non-specific interaction with cells. Scheme was created with Biorender.com.

Low power light irradiation may trigger series of photochemical reactions in the cells [71, 167, 182]. At the cellular level the photons of light are absorbed by various endogenous chromophore molecules [167, 182]. Recently, numerous studies proposed chromophores of mitochondria as the major sensor of low power light [167, 181]. In particular, complex IV known as cytochrome c oxidase (COX) has been identified as the main photo-acceptor of LLLT by comparison of the absorption spectra of mitochondrial complexes to the spectra of light used in PBM [183]. Indeed, COX shows two absorption peaks, one in the blue spectral range about 380-420nm and second one corresponding to the red spectral region about 600-660nm [71, 184]. In fact, COX is a terminal enzyme of electron transport chain catalysing the reduction of molecular oxygen to water [185]. It has been shown that photobiomodulation may increase the ATP production, mitochondrial membrane potential, cyclin adenosine monophosphate (cAMP) and ROS generation [167, 181]. Especially, photodissociation of nitric oxide (NO) from its binding sites on heme iron of cytochrome c and copper centres from COX caused by photons might be responsible for those effects [181]. Another hypothesis involves mitochondrial retrograde signalling as a possible mechanism of light-cells interaction [186]. Number of signalling events are triggered by increased generation of ROS, cAMP, Ca^{2+} and NO resulted from photons absorption by COX in mitochondria [186]. ROS, cAMP, Ca^{2+} act as signalling molecules in the cell and activate transcription factors, which leads to the increased expression of genes linked to cellular proliferation and migration [167, 181, 186]. On the other hand, when higher fluence (120 J cm^{-2}) was used, light irradiation led to COX inhibition, following by excessive ROS production and mitochondrial induced cell death in cancer cells [187]. Additionally, it has been shown that Ca^{2+} dependent “transient receptor potential” (TRP) channels are sensitive to light [184]. However, the precise function of TRP channels in PBM is not completely understood [181].

1.3.4. Biomedical applications of light-based technologies

The ability of light to induce biological response led to development of light-based biomedical techniques. Light-based technologies have shown promising results in various clinical applications, ranging from imaging, diagnostics, surgery and treatment of different diseases [71]. Nowadays, optical technologies are routinely used in imaging and diagnostics allowing real-time visualization of cells or tissues at high

resolution [71]. Number of optical techniques have been implemented into the clinical practise, ranging from light microscopy, spectroscopy-based methods, flow cytometry, endoscopy to usage of super-resolution confocal microscopes [71]. Additionally, laser surgery has become a routine technique in different areas of medicine, including ophthalmology, dermatology and aesthetic medicine, gastroenterology, urology, otolaryngology and cardiology [71]. It is worth noting that laser surgery uses in principle photothermal effects of the laser light [71]. On the other hand, LLLT or so called “cold therapy” uses lasers or LEDs with low power density in order to avoid heating of the tissue [167]. Numerous studies have demonstrated the positive outcome of LLLT in wound healing and tissue regeneration; pain reduction and inflammation, for review see [167]. It has been shown that LLLT may promote wound healing by enhanced migration of immune cells to the wound site together with increased activity of fibroblasts stimulating collagen production and neovascularization [167, 188]. Contrary, other studies indicate only minor or no significant impact of LLLT on wound healing[189, 190]. Indeed, there is a lack of properly designed clinical trials assessing the LLLT effects on wound healing. Moreover, the achieved results are non-consistent and often contradictory. In fact, a big variability of the parameters used in LLLT makes the direct comparison of the results very difficult. In addition, LLLT has been proposed as a therapy for pain relief in patients with chronic pain [167] and for treatment of various neurological conditions [167]. However, carefully designed randomized controlled studies and meta-analysis are needed in order to proof the effectivity of LLLT in clinic. Recently, new applications of laser light in combination with nanoparticles carrying light- triggered drugs have gained attention in cancer treatment [191, 192]. Even though, LLLT showed a potential by treatment of various conditions, further research is essential for better understanding of the precise mechanism of action. Better knowledge of light- cells interaction together with standardization of the treatment parameters may accelerate the clinical transition [71, 167].

1.4. Challenges and perspectives

The application of physics-based techniques into medicine have contributed to the development of novel approaches for diagnostics and treatment [84, 85]. Discoveries of X-rays and radioactivity, invention of optical techniques and developments in electrical engineering and computer technologies caused a revolution in many areas of modern medicine [84, 85]. Nowadays, new physics-based technologies are under the investigation as promising tools for diagnostic and therapeutic strategies [85, 123]. However, in order to reach the real clinical application, they have to comply with the high standards of evidence-based medicine [193]. Figure 8 is summarizing the major challenges in both fields based on [Appendix III](#) and [IV](#).

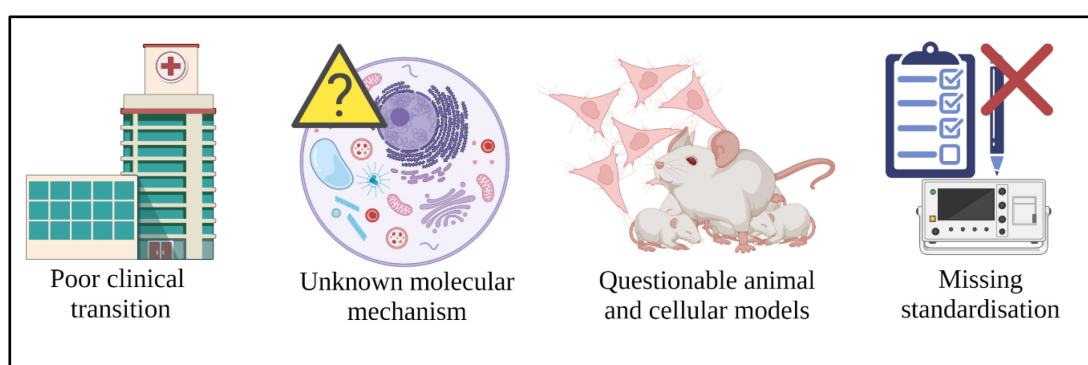


Figure 8 Major challenges in the field of plasma medicine and laser therapy. Created with Biorender.com

Firstly, the molecular and cellular mechanism of action of both non-thermal plasma and laser irradiation remains elusive [120, 123, 167, 181]. Indeed, ROS are involved in the cellular response to both NTP and laser irradiation. However, one has to remember that ROS is just collective name for numerous molecules involved in many molecular processes [1, 2]. In fact, target verification and knowledge of precise molecular mechanism are essential for successful clinical implementation of any drug or treatment modality [120, 153, 154, 194]. Drug approval is very costly and time-consuming process; thus, the known mechanism of action may save money and time during clinical trials [120, 154, 194]. Understanding the mechanisms of drug/treatment action at the molecular level has far going implications. It helps to optimize the therapeutic window of a treatment; enables better dosing for a patient; stratifies clinical trials; saves the lives of patients. Additionally, it may help by the identification of side effects and their prevention. In fact, only few studies on NTP and LLLT discussed the possible side effects of treatments [120, 167].

Another big challenge is the usage of questionable cellular and animal models. It has been shown that more than 20% of cell lines are misidentified due to cross-contamination [195]. Thus, the authentication of the cell lines and regular testing of mycoplasma contamination, the most common infection of cells, are crucial for achieving of the reproducible and reliable results [196, 197].

Furthermore, there is a huge variability in the design of NTP and lasers used in biomedical applications [123, 167]. This variability in physicochemical parameters of NTP and laser irradiation is directly affecting the biological response to the treatment [120]. The achieved results are very often non-consistent and contradictory. This makes direct comparison of isolated studies very challenging. Thus, standardization of the protocols and clear definition of the dosage for both plasma and laser treatments will contribute to the faster transition towards potential clinical application [70, 120, 123, 166, 167].

2. AIMS

Over the years, the implementation of physics-based techniques into medicine have contributed to the development of novel approaches for diagnostics and treatment. Recently, new promising therapeutic approaches, namely non-thermal plasma and low-power light (laser) therapy have gained attention for treatment of various diseases. During the last decade the number of publications and citations in the fields of biomedical applications of NTP and LLLT is remarkably raising (Fig. 9, 10). However, the quality of research outputs is more important than the total number of published papers. So far, research outputs of biomedical applications of NTP and LLLT show relatively modest overall quality, accounting for metrics of journals where relevant studies are published (Fig. 9, 10) and overall scientific quality of outputs [120, 123] **Appendix III, IV.**

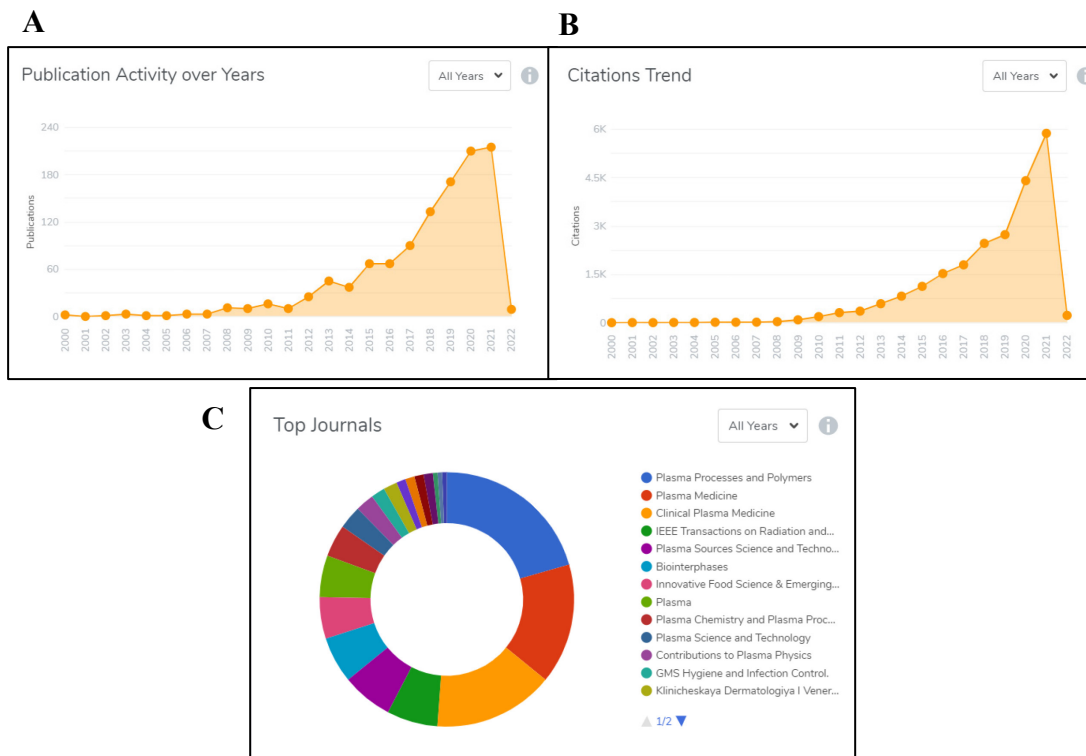


Figure 9: Graphs of publication activity (A), citations trend (B) over years and selection of the top journals (C) in the field of plasma medicine. Adapted from the <https://www.wizdom.ai/>

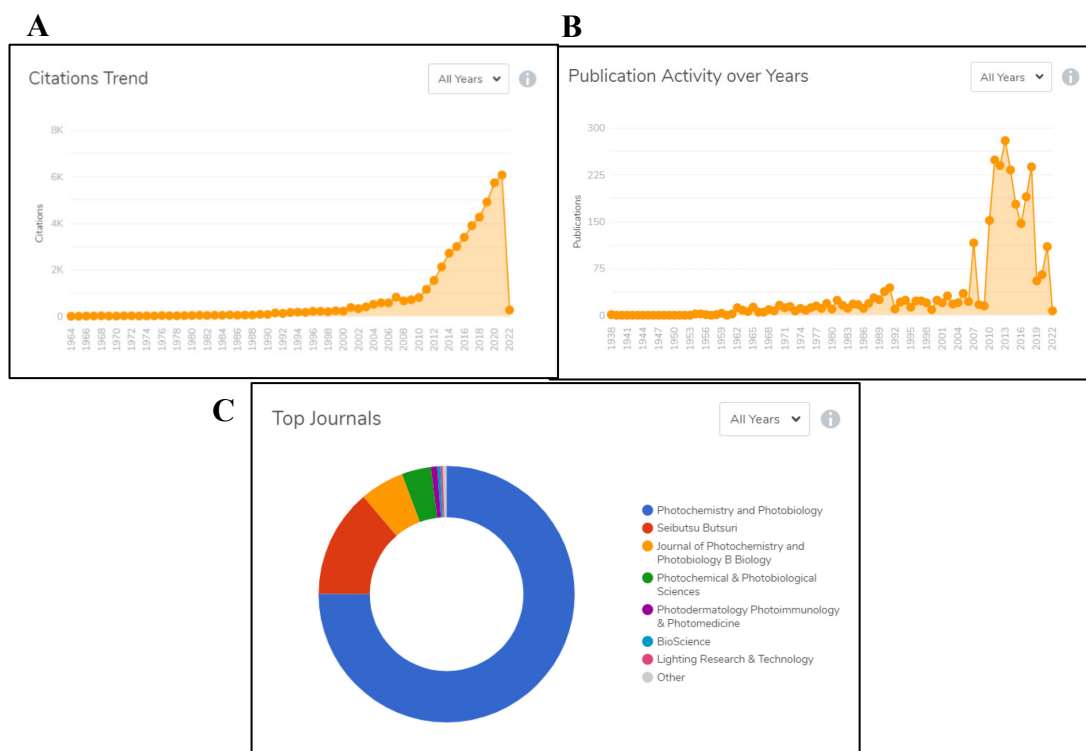


Figure 10: Graphs of publication activity (A), citations trend (B) over years and selection of the top journals (C) in the field of photochemistry and photobiology. Adapted from the <https://www.wizdom.ai/>

Despite the recent progress of the research on non-thermal plasma and low level power light (lasers) in various biomedical applications, there is still a lot of challenges that needed to be addressed. There are challenges with standardization of treatments, authentication and usage of cell models, lack of no meta-analysis of clinical outputs. Crucially, there is still fragmental knowledge on potential cellular and subcellular targets and mechanisms affected by NTP and LLLT. In fact, the lack of a clear understanding of how the drug and/or treatment works at cellular and molecular level may lead to dramatic outcomes [194].

This dissertation thesis aims to critically assess the current knowledge in the field of plasma medicine and LLLT. In particular, it focuses on the interaction and molecular mechanisms of non-thermal plasma and laser light irradiation in 3 hepatic cancer cells, namely Alexander (PLC/PRF/5), HepG2 and Huh7.

The work is divided into two parts. Firstly, it aims to analyse the effects of air non-thermal plasma on Alexander, HepG2 and Huh7 cell lines. The main goal of this part is the identification of the key molecular targets and description of the cellular signalling affected by NTP treatment. Second part of the thesis aims to describe the

impact of high-fluence low power laser irradiation of different wavelengths (398nm, 505nm, 650nm) on Alexander, HepG2 and Huh7 cells. It aims to reveal the molecular foundations mediating cell-laser nonspecific interactions.

We hope that our critical analysis will help researchers to overcome challenges and develop in future better controlled, safer, and more robust NTP- and laser-based treatment modalities.

3. EXPERIMENTAL PART-METHODS

The presented study is cross-disciplinary and therefore demanding in methodology. Wide range of methods were used in order to achieve the proposed aims. We briefly list here major points and description of the used methodology. The more detailed description and extended materials and methodology part can be found in already published papers [198, 199], [Appendix I, II](#).

3.1. Cell cultures

Human hepatocellular carcinoma cells Huh7 (Japanese Collection of Research Bioresources, JCRB) and Alexander (PLC/PRF/5) (American-Type Culture Collection, ATCC) and human hepatoblastoma cell line HepG2 (ATCC) were used for all experiments. Briefly, cells were cultivated in Eagle's minimal essential medium (EMEM, ATCC) supplemented with 10% fetal bovine serum (FBS, Thermo Fisher Scientific) and with Penicillin/ Streptomycin (Thermo Fisher Scientific) according to manufacturer's recommendations. Cells were maintained in a humidified atmosphere with 5% CO₂ at 37°C. Medium was changed once a week. All cell lines were routinely tested for mycoplasma contamination using the MycoAlert Mycoplasma Detection Kit (Lonza).

3.2. Protein extraction and Western blot analysis

In order to reveal the cellular signalling on protein level we isolated the proteins extracts as follows. RIPA buffer (Merck Millipore) supplemented with protease and phosphatase inhibitor cocktails (Sigma Aldrich) was used for extraction of whole cell lysates according to manufacturer's instructions and our previously published protocols [198, 199], [Appendix I, II](#). Briefly, cells were collected from the plates by scraping, spun down at 500g for 5 min, washed with PBS and once again spun down at 500g for 5min. After, the pellet of cells was resuspended in 50µl of RIPA buffer containing inhibitors and incubated at 4°C for 30 min. After incubation, samples were spun down at 15 000g for 10min and supernatants were collected. Concentration of the extracted lysates was determined by using Micro BCA (Bicinchoninic acid) assay. Equal amount of protein lysates was separated by SDS-PAGE (sodium dodecyl sulphate- polyacrylamide gel electrophoresis). After, the samples were transferred to the polyvinylidene fluoride (PVDF) membranes. Later, membranes were blocked with suitable blocking buffer for 1h at RT, following the incubation with primary antibodies against target proteins overnight at 4°C and by incubation with appropriate secondary

antibody for 1h at RT. The precise catalogue numbers, dilutions and clones are specified in the [Appendix I, II](#). For the signal detection, imaging system GBOX CHEMI XRQ (Syngene) was used. Chemiluminescence was detected by GeneTools acquisition software (Syngene). GeneTools (Syngene) and ImageJ (NIH) software were used for densitometric quantification of the blots.

3.3. Microscopy

Different types of microscopic techniques have been used in this work.

The routine observation of the cellular morphology has been done by optical light microscopy using IM-2FL epi-fluorescent system (Optika Microscopes). This system is equipped with light source type X-LED8 with white 8W LED, mercury burner 100W HBO, brightfield, phase contrast and fluorescence filters UV, B and G. In particular, fluorescence enables visualization of the cellular compartments with high sensitivity and specificity. IM-2FL epi-fluorescent system (Optika Microscopes) has been used for detection of apoptosis by the Dead Cell Apoptosis Kit (Thermo Fisher Scientific) and for visualization of cells in clonogenic survival assay in [Appendix I](#).

In order to visualize the cells at better resolution two types of confocal microscopy have been utilized. Firstly, Nikon Diaphot 200 microscope (Nikon) in combination with the BioRad MRC 1024 laser scanning imaging system (Bio-Rad) equipped with a Krypton/Argon laser, which creates three excitation lines co-aligned at 488nm, 568nm, 647nm. Eppendorf micromanipulator 5171 (Eppendorf) adjusted to the Nikon Diaphot 200 microscope (Nikon) was used for precise manipulation with taper in [Appendix II](#). Fluorescent images were acquired by acquisition software Lasersharp 2000 v5.2 (BioRad). ImageJ system (NIH) and Laser-Sharp 2000 software (BioRad) have been used for image processing and quantification.

This system was utilized in the following experimental work in [Appendix I](#):

- Detection of intracellular ROS and Superoxide using Cellular ROS/Superoxide Detection Assay Kit (Abcam)
- Visualization of mitochondrial membrane potential by JC-1 (TFS) and detection of mitochondrial related ROS by MitoTracker® red CM-H2XROS (TFS)
- Activity of Caspase 3/7 by CellEvent™ Caspase-3/7 Green Assay Kit (TFS)

And in [Appendix II](#):

- Visualization of mitochondrial membrane potential by JC-1 (TFS) and detection of mitochondrial related ROS by MitoTracker® red CM-H2XRos (TFS)
- Visualization of lysosomes by acridine orange (TFS) and assessment of endoplasmic reticulum stress by thioflavin T
- Analysis of cellular viability by the fluorescent live/dead cell assay kit (TFS)

More detailed description of experimental setup, materials, including catalogue numbers, used dilutions, concentrations and appropriate timing is described in [Appendix I, II](#).

Further, a brand-new high resolution spinning disk confocal microscopy IXplore SpinSR (Olympus) has been used in order to visualize the cells at great details. The system consists of two major parts, inverted microscope IX83 (Olympus) and spinning disc confocal unit CSUW1-T2S SD (Yokogawa). For the fluorophores excitation 3 different wavelengths were used, 405nm, 488nm and 561nm laser diodes. Confocal images were taken at a definition of 2048 x 2048 pixels or eventually at a definition 1024 x 1024 for super-resolution images and captured by two digital CMOS cameras ORCA-Flash4.0 V3 (Hamamatsu). Fluorescent confocal images were acquired by acquisition software cellSens (Olympus). ImageJ software (NIH) was used for image processing and quantification. More detailed description of the imaging system can be found in [199, 200].

This system was utilized in the following experimental work in [Appendix II](#)

- Mitochondrial dynamics by MitoTracker Red (TFS)
- Imaging of Annexin V (Dead Cell Apoptosis Kit, TFS) and caspase-3 (caspase-3 inhibitor VAD-FMK conjugated to FITC, Abcam)
- Evaluation of mitochondrial permeability transition pore m(PTP)
- Assessment of transient transfection efficiency

More detailed description of experimental setup, materials, including catalogue numbers, used dilutions, concentrations and appropriate timing is described in [Appendix II](#).

3.4.Spectro-fluorometric analysis

In order to measure the absorbance, luminescence or fluorescence signal of the higher number of samples at the same time in the plate Tecan microplate reader SpectraFluorPlus (Tecan) was used. This system enables using different combinations of filters for excitation, emission or absorbance.

This system was utilized in the following experimental work in [Appendix I](#):

- Cell viability using WST-1 assay (Roche)
- Measurement of protein concentration by micro-BCA assay (TFS)
- Detection of intracellular ROS and Superoxide using Cellular ROS/Superoxide Detection Assay Kit (Abcam)
- Lysosomal stability assay (TFS)
- Activity of Caspase 3/7 by CellEvent™ Caspase-3/7 Green Assay Kit (TFS)

And in the following experiments in [Appendix II](#):

- Cell viability using WST-1 assay (Roche) or AlamarBlue reagent (TFS)
- Measurement of protein concentration by micro-BCA assay (TFS)

Additionally, Tecan microplate reader SpectraFluorPlus was used for the detection of luminescence by testing for mycoplasma contamination using MycoAlert Mycoplasma Detection Kit (Lonza). More detailed description of experimental setup, materials, including catalogue numbers, used dilutions, concentrations and appropriate timing is described in [Appendix I, II](#).

3.5.Statistical analysis

Quantitative results are presented as \pm SEM. Sample size was determined by using statistical approach previously published in [201]. The statistical significance of differences between the groups was determined using ANOVA with subsequent application of either Fisher's, LSD or Newman-Keuls test. Differences were considered statistically significant at $*P < 0.05$. Detailed description of statistical analysis is described in [Appendix I, II](#).

4. EXPERIMENTAL PART-RESULTS

The chapter Results of this thesis is divided into two parts based on the proposed aims. First part focuses on the interaction of air non-thermal plasma with 3 hepatic cancer cell lines. It describes the non-thermal plasma device used for treatment of the cells, its physical and chemical parameters. Further, this part is dedicated to the identification of key cellular signalling and molecular targets in the hepatic cells post non-thermal plasma treatment ([Appendix I](#)). The second part of the Results describes the interaction of hepatic cancer cells with laser irradiation of different wavelengths. Moreover, this part focuses on the identification of cellular signalling and identification of the key molecular target in hepatic cells post laser irradiation ([Appendix II](#)).

4.1. Plasma interaction with living cells

4.1.1. Characterization of plasma device

In order to produce non-thermal plasma for biomedical application we designed the single jet non-thermal plasma system described previously [103, 104, 108, 114]. Figure 11 describes the designed plasma system, illustrating images of torch and schematic diagram of plasma nozzle (Fig. 11A,B,E). The specific outline of the device allows modifications in the plasma composition simply by the using of different types of gases, e.g. He, air, Ar [103, 104]. In fact, chemical composition of the plasma may greatly affect the resulted cellular signalling [104]. Thus, in order to assess the chemical composition, in terms of radicals and particles, of produced air and He plasma we used the optical emission spectroscopy (OES) [103]. One can see from the spectra the differences in composition of Air and He plasma. In air plasma observed peaks correspond to nitrogen and oxygen molecules (Fig. 11C), whereas in He plasma, peaks correspond to OH, He, O and other active molecules (Fig. 11D)[103]. Detailed description of method is provided in [103].

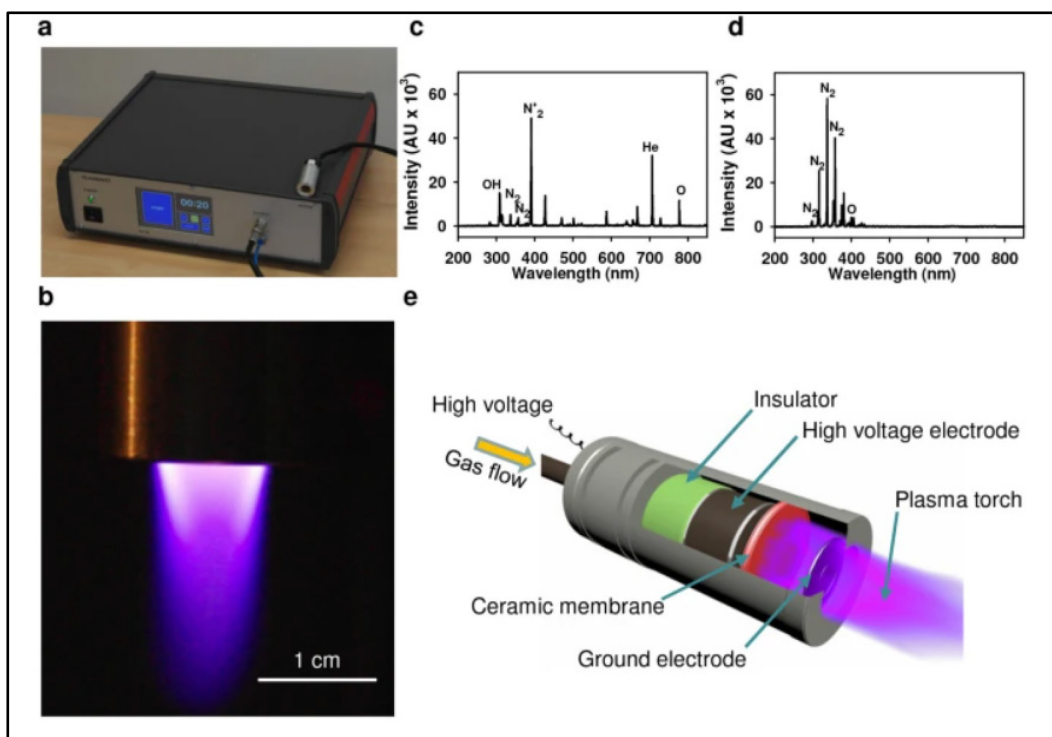


Figure 11: Schematic illustration and the physicochemical parameters of plasma device. (A) Photograph of the plasma system. (B) Plasma torch. Optical emission spectrum of (C) helium and (D) air plasma. (E) Scheme of plasma nozzle. Reprinted from open access article [103] under the terms of the Creative Commons Attribution License.

Further, we analysed the air and He plasma composition by using the Fourier transform infrared spectroscopy (FT-IR) (Fig 12). Moreover, we compared the spectra of air and He plasma with spectrum of ozone, the most abundant chemically active molecule of plasma (Fig 12)[104].

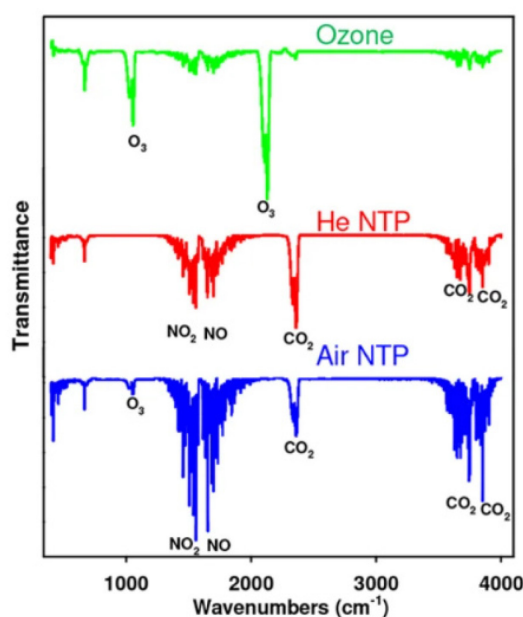


Figure 12: FT-IR spectra of air, helium NTPs and ozone. Reprinted from open access article [104] under the terms of the Creative Commons Attribution License.

It is worth noting that OES and FT-IR spectra confirmed a high chemical complexity of produced plasma [103, 104]. Another important issue discussed in the literature is the penetration depth of plasma, which is greatly dependent on the used physical parameters [105, 122]. Therefore, we generated tuneable devices allowing production of “high” and “low” voltage plasma. The detailed physicochemical parameters of low voltage (LV) and high voltage (HV) plasma device are shown in the Table 6.

Table 6 Physicochemical parameters of the low voltage and high voltage plasma devices.

Physical Parameters (unit)	High voltage (HV)	Low voltage (LV)
Current amplitude (mA)	125	224
Ion density m⁻³	$2.03 \cdot 10^{17}$	$2.33 \cdot 10^{18}$
Frequency (kHz)	22	250
Gas flow (L min⁻¹)	4	4
Operating voltage amplitude (V)	4740	725
Phase shift (o)	-24	21
Pulse duration (μs)	1	1
Real part of impedance (kΩ)	34.64	3.02
Rise-time of pulse (μs)	0.08	0.2

In order to see the penetration ability of produced plasma we analysed the distribution of ions of He, N, O during plasma production in two bacterial models [202]. Stopping and range of ions in matter (SRIM) stimulations revealed a distinct distribution for each ion (Fig. 13). As it is seen from the Figure 13, He ions were able to penetrate at higher extend into bacterial wall of gram-negative bacteria in comparison with N and O ions. On the other hand, all ion types accumulated in thick layer of peptidoglycan of gram-positive bacteria [202].

Summarizing characterization of plasma, we can state that the resultant physicochemical composition of NTP grossly varies depending on used gas composition, power, discharge voltage, gas flow rate, jet length, and voltage frequencies of the device. It is feasible that such degree of variability in physicochemical composition of NTP may greatly affect biological outcome modulated by NTP. That is why it is of unmet need to study in detail mechanistic aspects of NTP-driven cellular responses.

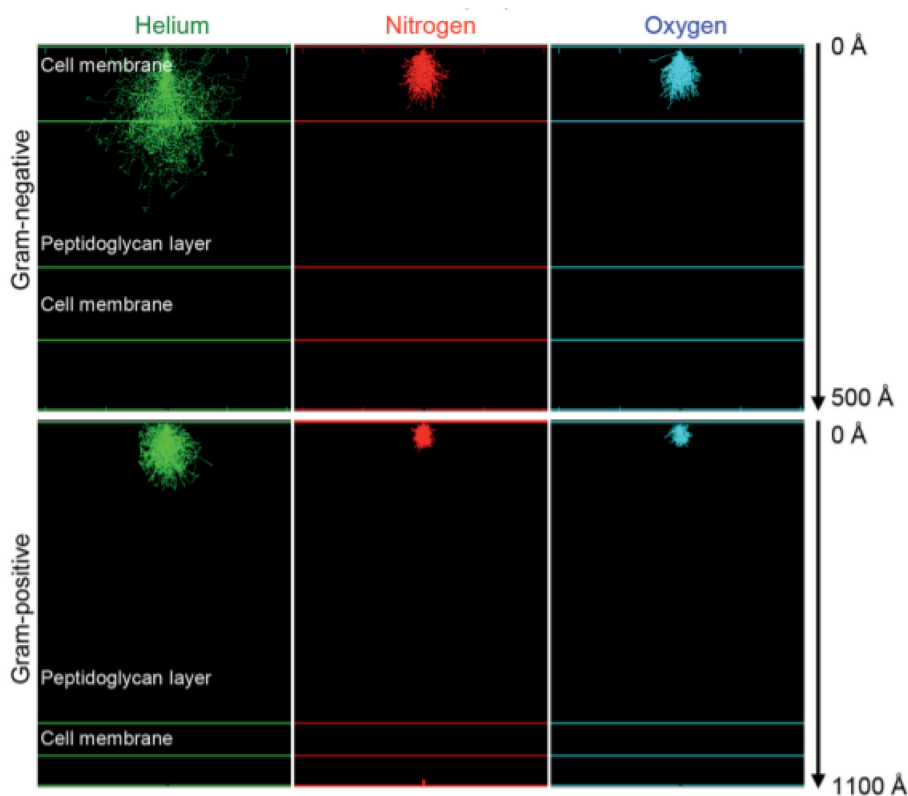


Figure 13 Representation of SRIM simulations: in-depth profiles of He (green panel), N (red panel) and O (blue panel) ions penetration into Gram-positive or Gram-negative bacterial wall models. The total number of ions is 10 000. Reprinted from *RCS Advances*, Vol. 6 (Oleg Lunov, Vitalii Zablotskii Olexander Churpita, Ales Jäger, Leoš Polívka, Eva Syková, Natalia Terebova, Andrei Kulikov, Šárka Kubinová, Alexandr Dejneka, *Towards the understanding of non-thermal air plasma action: effects on bacteria and fibroblasts*, Pages 25286-25292) [202] Copyright (2016) with permission from Royal Society of Chemistry.

4.1.2. Analysis of cell viability post NTP treatment

Over the years, the anti-cancer effects of non-thermal plasma have been shown on various types of cancer *in vitro* and *in vivo* (Table 5). However, only few studies compared the NTP effects using distinct cell lines of the same tumour model. Moreover, only small number of studies analysed the NTP effects on liver cancer cell lines [139, 203]. In our study, we used 3 genetically and morphologically distinct liver cancer cell lines HepG2, Huh7 and Alexander and analysed the effects of air non-thermal plasma treatment. For this study, we chose the air NTP because of its accessibility and easy handling (Appendix I). Firstly, we analysed the proliferation rate of Huh7 and HepG2 cells 48h and 72h after plasma exposure (Fig. 14A,B). We observed time-dependent and dose-dependent anti-proliferative effects of NTP on both cell lines. Surprisingly, HepG2 cells showed higher level of resistance in comparison to Huh7 (Fig.15A).

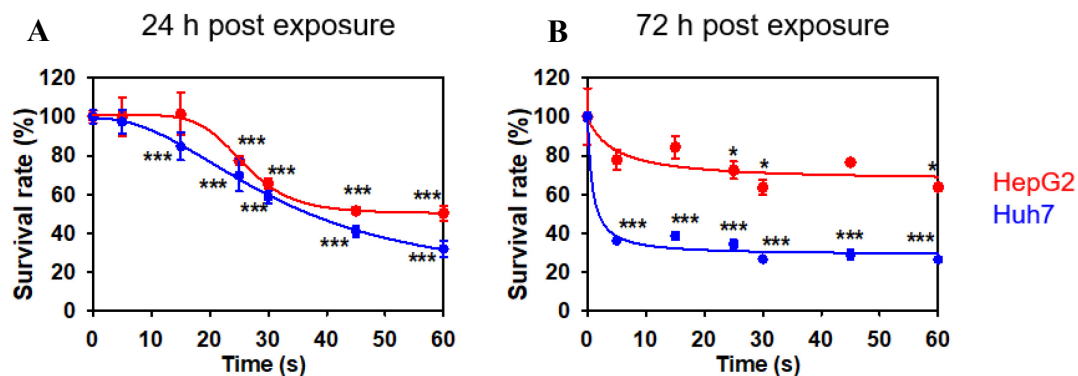


Figure 14 Plasma treatment induced cytotoxic effects in HepG2 and Huh7 cell lines. Survival rate of HepG2 and Huh7 cells analysed by WST-1 reagent 24h (A) and 72h (B) post plasma treatment. The data were normalized to controls (no exposure), which were set as 100%. Readings were done in quadruplicates, data are presented as mean \pm SEM, $n=3$; * $P < 0.05$, *** $P < 0.001$. Reprinted from open access article [204] under the terms of the Creative Commons Attribution-NonCommercial-NoDerivatives 4.0 International License (CC BY-NC-ND).

Moreover, we confirmed the cytotoxic effects of NTP by clonogenic assay which is based on colony formation. Huh7 and HepG2 cells were irradiated with plasma and 5 days after stained with crystal violet as described in Appendix I. We observed the decreased number of colonies of Huh7 post plasma treatment as a sign of reduced tumorigenicity. Whereas, plasma treatment had only minor impact on colony formation of HepG2 cells (Figure 15B).

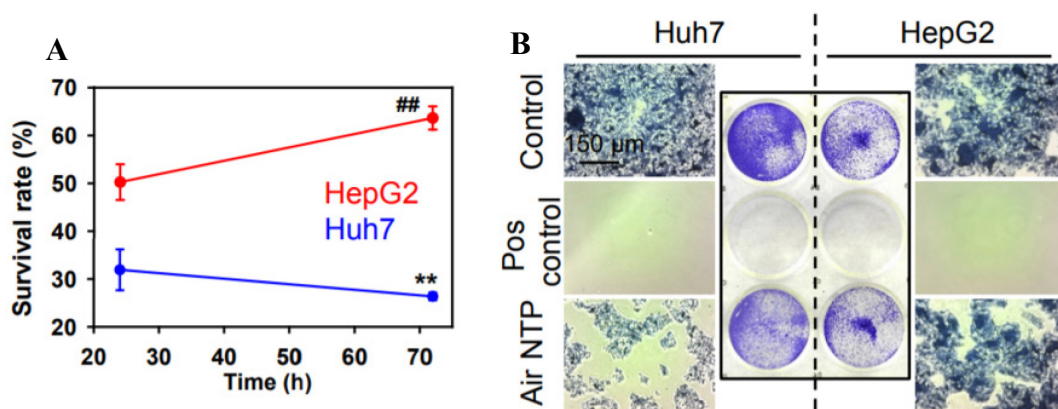


Figure 15 Plasma treatment reduced tumorigenicity of Huh7. (A) Comparison of survival rates of HepG2 and Huh7 cells 24- 72h post plasma treatment. Data are evaluated as in Fig 14; ## $P < 0.01$, ** $P < 0.01$ (B) Reduced formation of colonies in Huh7 cells post NTP treatment. As positive control 20% Ethanol was used. Reprinted from open access article [204] under the terms of the Creative Commons Attribution-NonCommercial-NoDerivatives 4.0 International License (CC BY-NC-ND).

4.1.3. Detection of cellular ROS and Superoxide

As mentioned above, synergistic effect of chemically active particles is responsible for plasma-mechanism of action [70, 88, 89, 101]. In particular, RONS are major

contributors to the eukaryotic cellular response to NTP treatment [116-119]. In order to see the accumulation of intracellular ROS and Superoxide post plasma treatment we used two specific fluorescent probes, one for total ROS and one for Superoxide. We noticed dose-dependent accumulation of both ROS (Fig.16A) and Superoxide (Fig.16B) higher in Huh7 than in HepG2 cells post NTP treatment. Interestingly, we observed excessive nuclear accumulation of Superoxide in Huh7 cells (Fig 16C). Indeed, abundant Superoxide production and accumulation are linked to mitochondrial damage and following cell death execution [5, 205, 206].

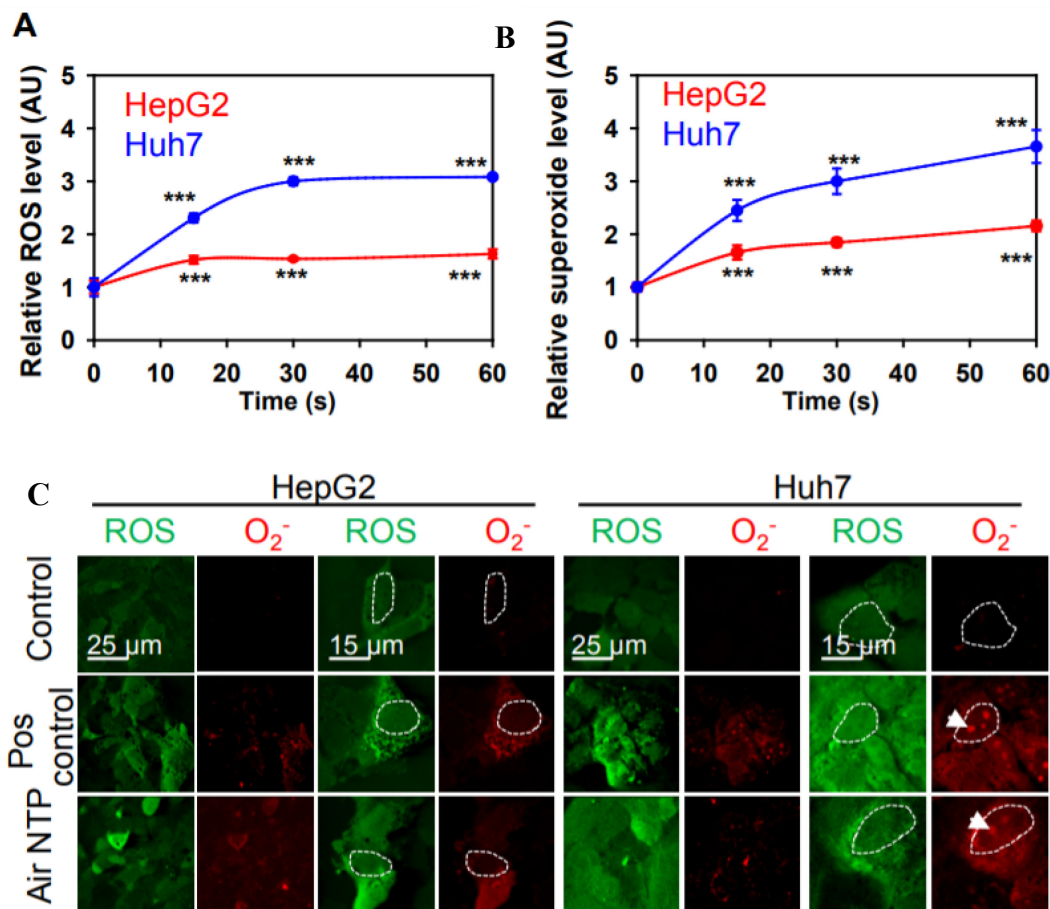


Figure 16 Accumulation of ROS and Superoxide in HepG2 and Huh7 post NTP treatment. (A) ROS and (B) Superoxide production in HepG2 and Huh7 cells 6h post plasma treatment. Accumulation of ROS and Superoxide were measured spectrofluorometrically by using cellular ROS/Superoxide detection assay kit. Readings were done in quadruplicates, data are present as mean \pm SEM, $n = 3$, $***P < 0.001$. (C) Subcellular localization of ROS/Superoxide. Cells were stained with ROS/Superoxide detection assay kit after NTP treatment and imaged by confocal microscopy. Representative images are shown. $500\mu\text{M H}_2\text{O}_2$ was used as positive control. Reprinted from open access article[204] under the terms of the Creative Commons Attribution-NonCommercial-NoDerivatives 4.0 International License (CC BY-NC-ND).

In order to verify the involvement of ROS in plasma-mediated response in cells we used N-acetylcysteine, a well-known ROS scavenger. As it is seen from the

figure 17 the addition of N-acetyl cysteine attenuated the cytotoxic effects of plasma (Fig.17).

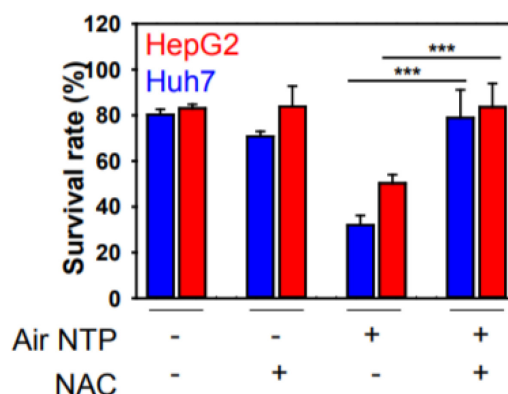


Figure 17 N-acetyl cysteine attenuated the cytotoxic effects of NTP. Survival rate of Huh7 and HepG2 24h post plasma treatment (60s) in combination with NAC analysed by WST-1 assay. Data are assessed as in Fig 14 *** $P < 0.001$. Reprinted from open access article [204] under the terms of the Creative Commons Attribution-NonCommercial-NoDerivatives 4.0 International License (CC BY-NC-ND).

4.1.4. Analysis of mitochondria post NTP treatment

It is widely known that primary intracellular source of ROS are mitochondria and their electron transport chain (ETC) [5]. Moreover, under stress stimuli, mitochondria elevate ROS production and induce subsequently cell death signalling (64,68,75). Indeed, only small number of studies examined the plasma effects on mitochondria of cells [207]. In order to study the mitochondrial activity in HepG2 and Huh7 cells post NTP treatment, we used JC-1 staining. Microscopical analysis of cells labelled with JC-1 revealed changes in mitochondrial dynamics and morphology of Huh7 cells post plasma treatment (Fig.18A). We noticed the excessive rate of fission, swelling and increased circularity of mitochondria in Huh7 cells post plasma treatment (Fig.18A). On the other hand, plasma treatment had no effects on mitochondrial dynamics of HepG2 cells (Fig. 18A). Moreover, we analysed the mitochondrial membrane potential ($\Delta m\Phi$) of cells post NTP treatment by JC-1 staining, which exhibits accumulation into mitochondria dependent on their potential. Quantification of the total red fluorescence of JC-1 shows the decreased $\Delta m\Phi$ of Huh7 cells post plasma treatment, whereas no alterations were noticed in HepG2 cells (Fig. 18B).

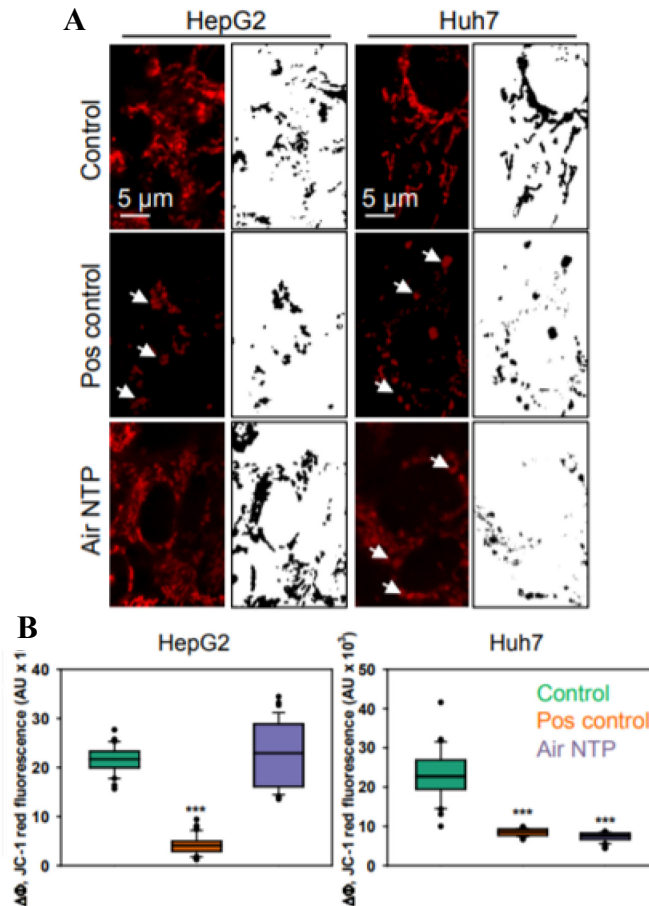


Figure 18 NTP treatment induced changes in mitochondrial membrane potential and mitochondrial dynamics. (A) Representative confocal images of mitochondrial shape of HepG2 and Huh7 cells post plasma treatment marked with JC-1. Cells were stained with JC-1 5h post NTP treatment. 20% Ethanol for 20 min was used as positive control. Arrows indicate circulated mitochondria. (B) Quantification of total red fluorescence of JC-1 from pictures described in A. The data are showed as mean \pm SEM, n= 30-50 cells; ***P< 0.001. Reprinted from open access article[204] under the terms of the Creative Commons Attribution-NonCommercial-NoDerivatives 4.0 International License (CC BY-NC-ND).

In fact, dysregulation of mitochondrial homeostasis and changes in their function and dynamics are linked with generation of ROS and oxidative stress [17]. Therefore, we labelled cells post plasma treatment with MitoTracker®Red CM-H2 XROS, a fluorescent probe staining specifically mitochondria- originated ROS. This staining showed elevated level of ROS in both cell lines after plasma, but at significantly higher extend in Huh7 cells (Fig.19A, B).

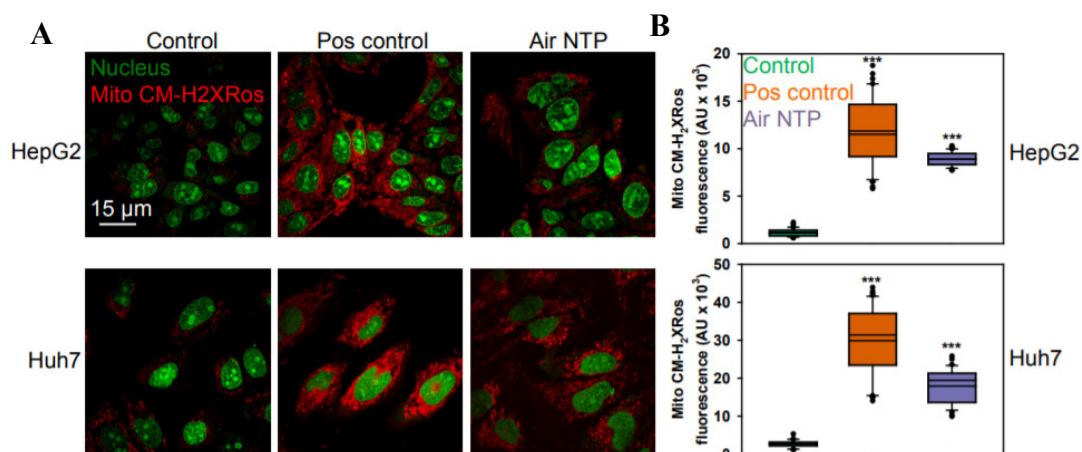


Figure 19 Increased production of mitochondria- mediated ROS post NTP treatment. (A) Representative confocal images of mitochondrial- mediated ROS of HepG2 and Huh7 cells post plasma treatment marked with MitoTracker®red CM-H2 XRos. Cells were stained 5h post NTP treatment, SYTO 13 (green dye) was used to counterstain nuclei. (B)Quantification of fluorescence intensity from pictures described in A. The data are showed as mean \pm SEM, $n= 30-50$ cells; *** $P < 0.001$. Reprinted from open access article[204] under the terms of the Creative Commons Attribution-NonCommercial-NoDerivatives 4.0 International License (CC BY-NC-ND).

Additionally, we assess the lysosomal stability in both cell lines and observed no changes post NTP treatment [Appendix I](#). Detailed analysis of mitochondria and lysosomes of Huh7 and HepG2 cells post plasma treatment is described in [Appendix I](#).

4.1.5. Detection of apoptotic cell death

The previous data set suggested that mitochondria act as main sensor of cells in response to plasma treatment. It is known that mitochondrial fission is associated with cell death activation [11, 16, 22], especially with apoptosis. Thus, in order to reveal if plasma treatment led to apoptosis in Huh7 cells we stained the cells with Annexin V- AlexaFluor 488 and propidium iodide (PI). NTP treatment induced higher level of Annexin V binding, a sign of early apoptosis, and only small portion of Huh7 with PI incorporated in nuclei (Fig 20). Contrary, we noticed slightly elevated accumulation of PI in the nuclei of HepG2 post NTP treatment, as a sign of late apoptotic stage or necrosis (Fig. 20). Additionally, we analysed the activation of Caspase3/7 which act as executionary caspase in mitochondria-mediated apoptotic cell death. Consistently with the previous data, confocal microscopy imaging (Fig.21A) and fluorometric analysis (Fig.21B) revealed the Caspase 3/7 activation in Huh7 cells post plasma treatment without any detectable changes in HepG2 cells (Fig. 21A,B). Detailed description can be found in [Appendix I](#).

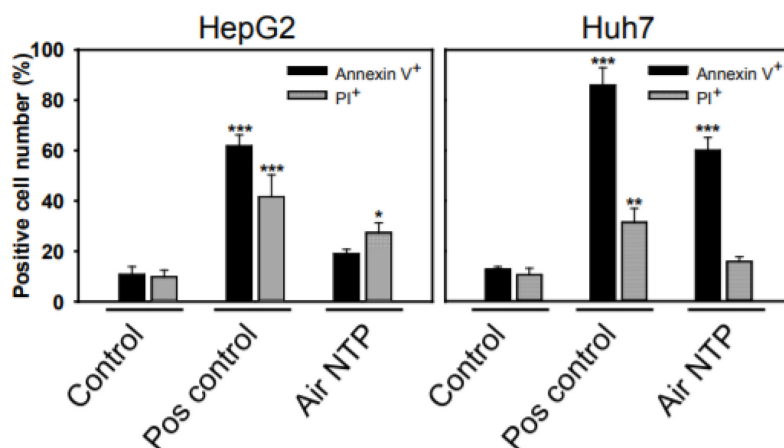


Figure 20 Quantification of the Annexin V and PI in Huh7 and HepG2 cells post NTP treatment. Cells were stained with dyes 6h post NTP treatment (60sec), Hoechst was used for nucleus counterstaining. After, cells were imaged by fluorescent microscope and analysed as described in [Appendix I](#). Staurosporine (2 μ M) was used as positive control. Data are presented as means \pm SEM, $n = 5$; * $P < 0.05$, ** $P < 0.01$, *** $P < 0.001$. Reprinted from open access article [204] under the terms of the Creative Commons Attribution-NonCommercial-NoDerivatives 4.0 International License (CC BY-NC-ND).

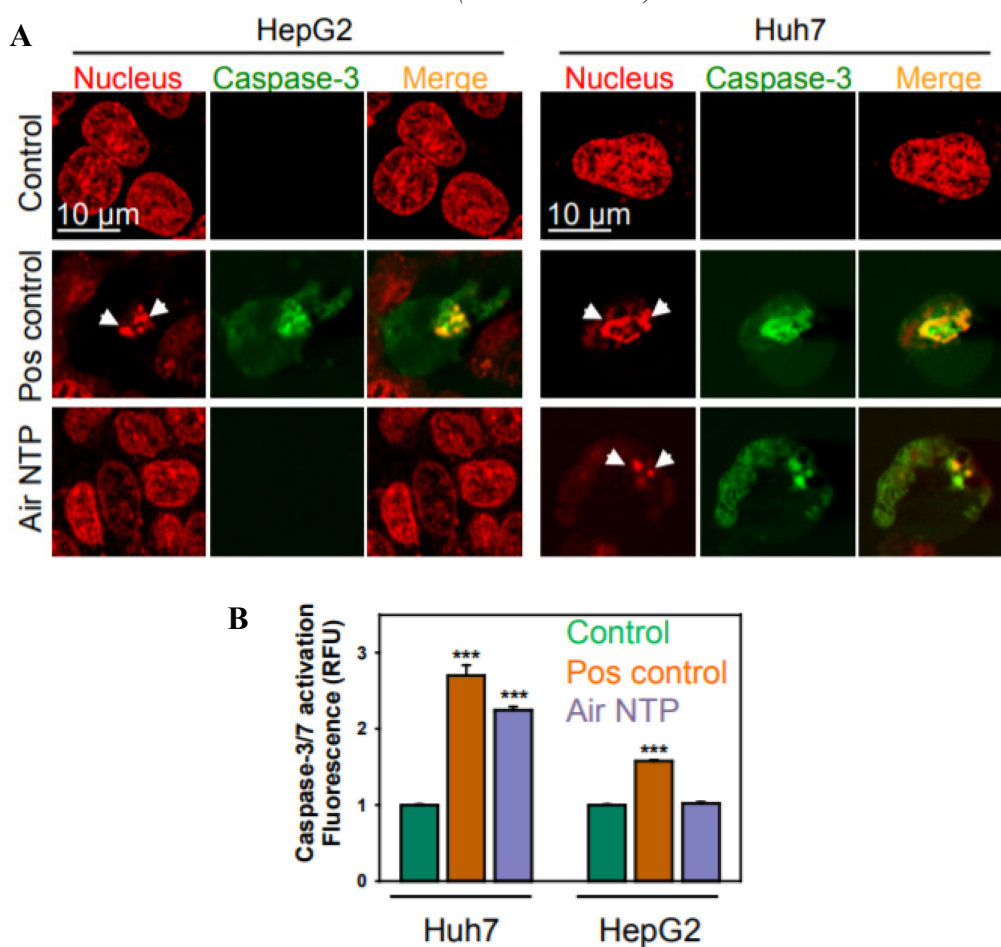


Figure 21 Analysis of Caspase 3/7 in HepG2 and Huh7 cells treated with NTP. (A) Representative confocal microscopy images of HepG2 and Huh7 cells stained with CellEvent™ Caspase-3/7 Green Assay Kit and imaged 6h post NTP treatment (60sec).

*NucRed™ Live 647 ReadyProbes™ Reagent (red dye) was used to counterstain nuclei. Staurosporine (2 μM) was used as positive control. Arrows designate nuclear fragmentation. (B) Quantification of Caspase 3/7 in Huh7 and HepG2 cells post NTP treatment. Cells were stained as described in A and fluorescence intensity was measured by microplate reader. Data are presented as means ± SEM, n = 4; ***P < 0.001. Reprinted from open access article [204] under the terms of the Creative Commons Attribution-NonCommercial-NoDerivatives 4.0 International License (CC BY-NC-ND).*

Additionally, in [Appendix I](#) we examined the effect of NTP on another liver cancer cell line, i.e., Alexander cells. Plasma treatment led to dose-dependent reduction of viability of Alexander cells, similarly as in Huh7 cells (Fig.22A). Moreover, binding of Annexin V and activation of caspase 3/7 in Alexander cells post NTP treatment confirmed apoptotic cell death (Fig.22B, C).

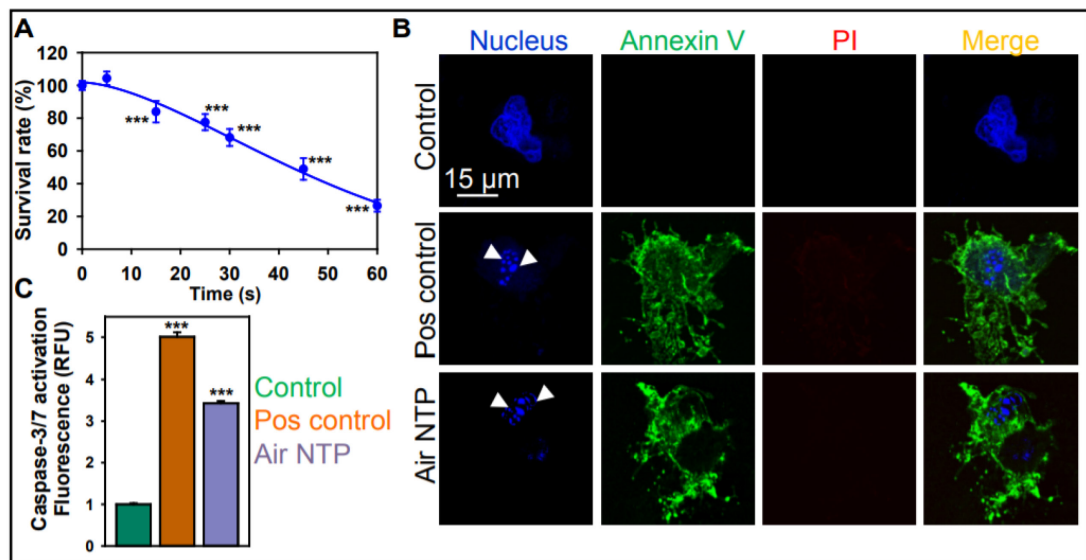


Figure 22 NTP treatment induced apoptotic cell death in Alexander cells. (A) Survival rate of Alexander cells analysed by WST-1 24h post plasma treatment. Data are evaluated as in Fig14, ***P < 0.001. (B) Representative confocal microscopy images of Alexander cells stained with annexin V in green, PI in red and NucRed in blue, 6h post plasma treatment (60sec). Staurosporine (2 μM) was used as positive control. Arrows designate nuclear fragmentation. (C) Quantification of caspase 3/7 activation in Alexander cells post NTP treatment. Cells were stained with CellEvent™ Caspase-3/7Green Assay Kit and fluorescence intensity was measured by microplate reader. Data are presented as means ± SEM, n = 4; ***P < 0.001. Reprinted from open access article [204] under the terms of the Creative Commons Attribution-NonCommercial-NoDerivatives 4.0 International License (CC BY-NC-ND).

4.1.6. Analysis of cellular signalling post plasma treatment

In order to reveal the cellular signalling and identify the key molecular targets in Huh7 and HepG2 cells post plasma treatment we performed the immunoblot analysis. NTP treatment led to decreased p53 expression in Huh7 cells, whereas there was no effect observed in HepG2 cells (Fig.23). Indeed, p53 is tumour suppressor and is involved in cell death activation [50]. However, mutant p53 (mutp53) stimulates the cancer

progression, promotes metastasis and chemoresistance of many cancer types, including HCC [49, 52]. Therefore, a number of therapeutic approaches is targeting the mutated p53 in order to eradicate the cancer. In fact, Alexander and Huh7 cells possess mutated form of p53, whereas p53 of HepG2 cells is a wild type [208]. Moreover, HepG2 cells have elevated level of an anti-apoptotic Bcl-2 protein, which is involved in the response to oxidative stress [135]. We noticed the excessive up-regulation of Bcl-2 protein in HepG2 post NTP treatment, what could be a possible explanation for higher resistance of HepG2 to plasma (Fig. 23). Additionally, we analysed the effects of H₂O₂, one of the major components of air plasma, on cellular signalling of HepG2 and Huh7. Western blot analysis revealed the down-regulation of p53 in both cell lines simultaneously with transversion of LC3A/B post H₂O₂, suggesting the autophagic cell death (Fig. 23).

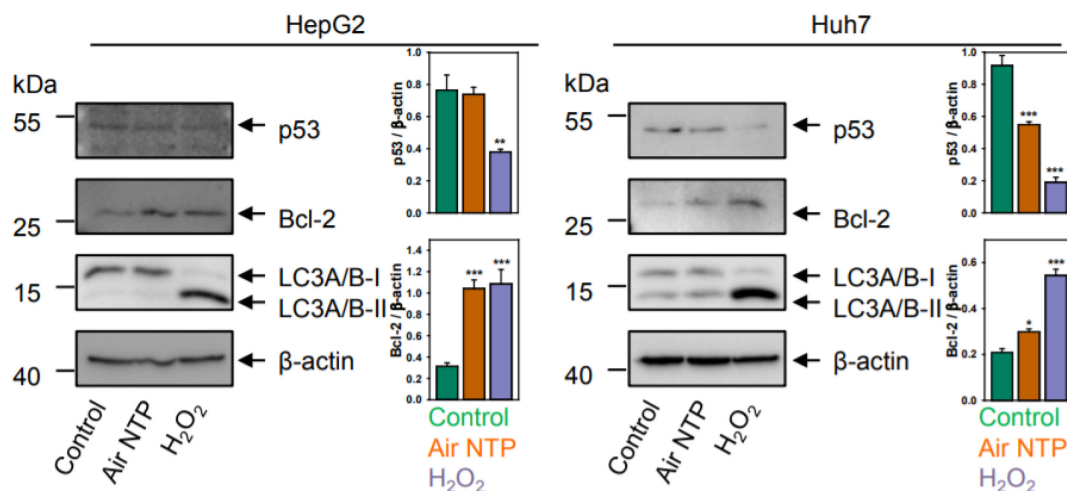


Figure 23 Changes in p53, Bcl-2 and LC-3 protein signalling in HepG2 and Huh7 cells post plasma treatment. HepG2 and Huh7 cells were treated with plasma for 60 sec and 4h later proteins were isolated. Densitometric quantification of p53 and Bcl2 is shown, * $P < 0.05$, ** $P < 0.01$, *** $P < 0.001$, mean \pm SEM, $n = 3$. Actin – control of equal protein loading. Reprinted from open access article [204] under the terms of the Creative Commons Attribution-NonCommercial-NoDerivatives 4.0 International License (CC BY-NC-ND).

In addition, we focus on other proteins involved in the cross-talk of different types of cell death, namely mTOR1 and STAT1. We observed no changes in mTOR activity after NTP and H₂O₂ treatments (Fig.24). On the other hand, we noticed up-regulation of pSTAT1 in both cell lines after exposure to H₂O₂ and down-regulation of pSTAT1 in Huh7 post plasma treatment. Contrary, there was no effect on STAT1 in HepG2 exposed to plasma (Fig.24A). Detailed description of the western blot analysis together with full immunoblots are shown in [Appendix I](#). Depending on the conditions, STAT1 act as a tumour suppressor however it could also contribute to the

tumour progression [209]. Moreover, we compared the basal expression of p53 and Bcl-2 proteins in all cell lines and human liver. Protein analysis showed that HepG2 cells have the highest Bcl-2 level among all three cell lines (Fig.24B). In fact, p53 is highly expressed in Huh7 cells in comparison to HepG2 and Alexander cells (Fig. 24B).

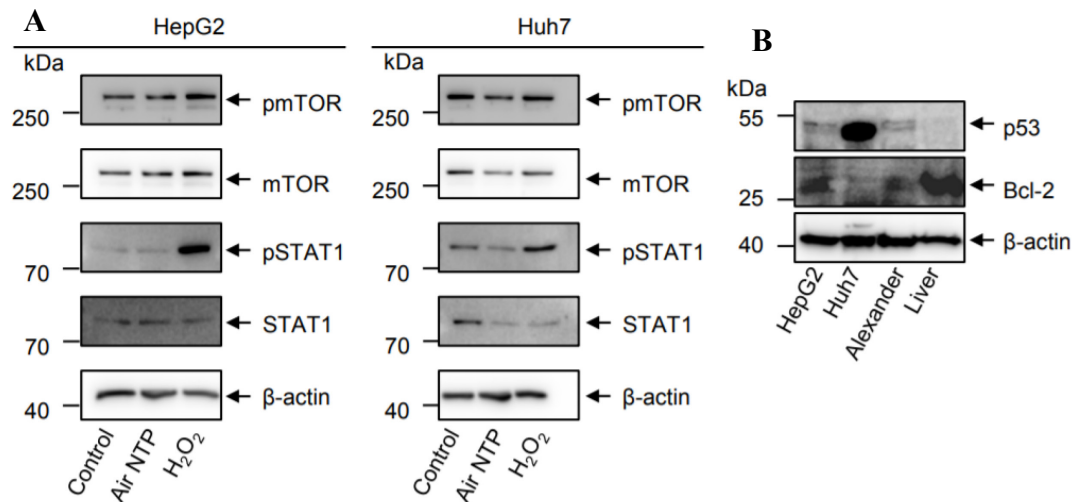


Figure 24 Changes in mTOR and STAT-1 protein signalling in HepG2 and Huh7 cells post plasma treatment. (A) HepG2 and Huh7 cells were treated with plasma for 60 sec and 4h later proteins were isolated. Actin – control of equal protein loading. (B) Comparison of p53 and Bcl-2 protein expression in HepG2, Huh7 and Alexander cells and human liver. Actin – control of equal protein loading. Reprinted from open access article [204] under the terms of the Creative Commons Attribution-NonCommercial-NoDerivatives 4.0 International License (CC BY-NC-ND).

Furthermore, we compared the viability of all tested cell lines after plasma exposure and revealed that cells with mutated p53, namely Alexander and Huh7 cells were more sensitive to plasma (Fig.25A). Contrary, HepG2 with their elevated level of Bcl-2 showed high resistance to cell death- mediated by plasma (Fig.25A). In order to uncover the Bcl-2 involvement in HepG2 resistance to plasma treatment we used specific pharmacological inhibitor of Bcl-2. Indeed, in combination with Bcl-2 inhibitor plasma treatment led to excessive cell death in HepG2 cells (Fig.25B).

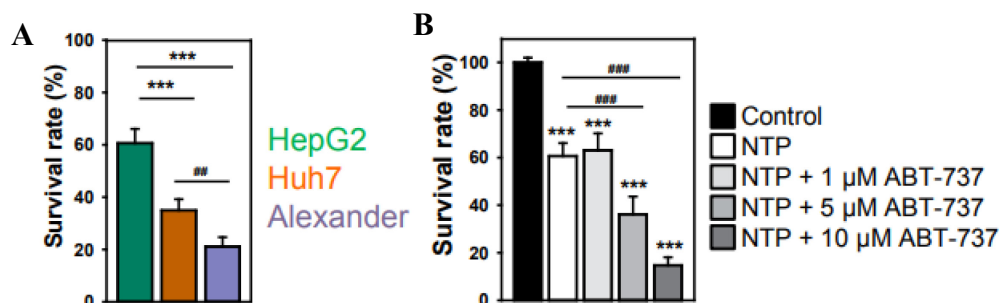


Figure 25 NTP treatment led to different response in cells (A) Comparison of viability of HepG2, Alexander and Huh7 cells post plasma treatment. Cells were analysed 24h after plasma treatment (60sec) as described in Fig.14 and Fig.22A. (B) Inhibition of Bcl-2 sensitized the HepG2 cells to plasma treatment. HepG2 were treated with NTP (60sec) in combination with different concentrations of Bcl-2 inhibitor (ABT-737) and analysed with WST-1 after 24h as described earlier. Data are presented as a mean \pm SEM, n=3, ###P< 0.001, ***P<0.001. Reprinted from open access article [204] under the terms of the Creative Commons Attribution-NonCommercial-NoDerivatives 4.0 International License (CC BY-NC-ND).

In the conclusion, in **Appendix I** we revealed the molecular mechanisms of plasma treatment in human liver cancer cell lines. We showed that cellular response to NTP-treatment is mediated via p53-Bcl-2 signalling pathway. In Huh7 and Alexander cells, plasma treatment triggered excessive ROS production, oxidative stress and mitochondrial damage mediating p53-dependent apoptosis. Whereas elevated levels of antiapoptotic protein Bcl-2 protected HepG2 cells from cell death triggered by plasma (Fig. 26).

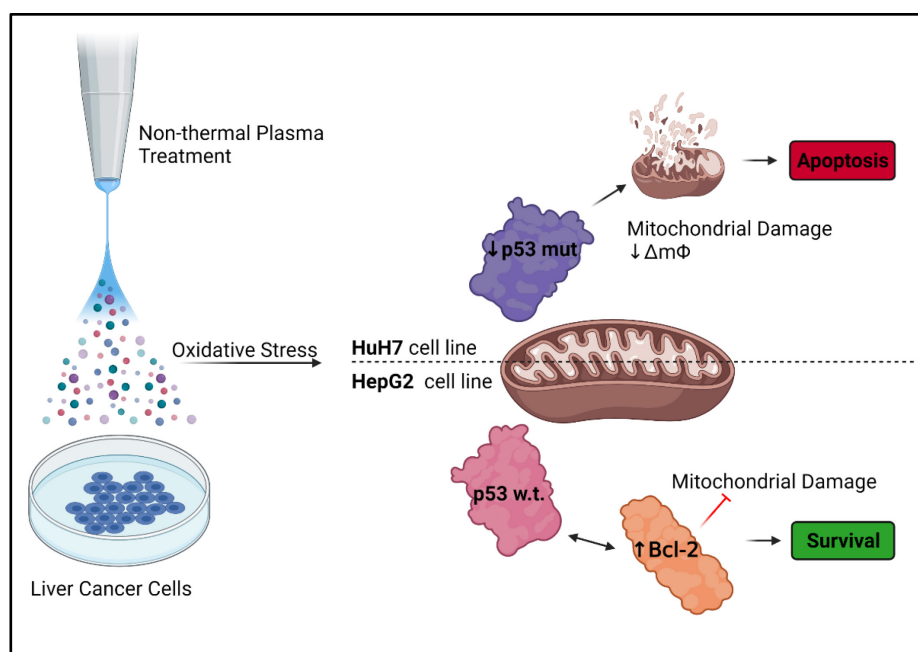


Figure 26 Schematic illustration of the molecular mechanisms in Huh7 and HepG2 cells post NTP treatment. Adapted from figure 11C from [204] **Appendix I**.

4.2. Laser light irradiation with living cells

4.2.1. Laser light characterization

In order to produce laser light for direct cells irradiation in media we used previously described system [169] (Fig.27A, B). Optical circuits contain 3 laser diode modules, LDI-405-FP-20-E-8-SM03-FA-CW, LDI-520-FP-20-E-3-SM03-FA-CW and LDI-650-FP-20-E-18-SM04-FA-CW (LasersCom, LLC, Belarus) with a fibre output of blue light at 398nm, green light at 505nm and red light at 650nm respectively

(Fig.27C). Single-mode optical fibre of the SMF-28 type (Corning) with a reduced diameter at the output end was used for delivery of the irradiation to the cells [169], **Appendix II**.

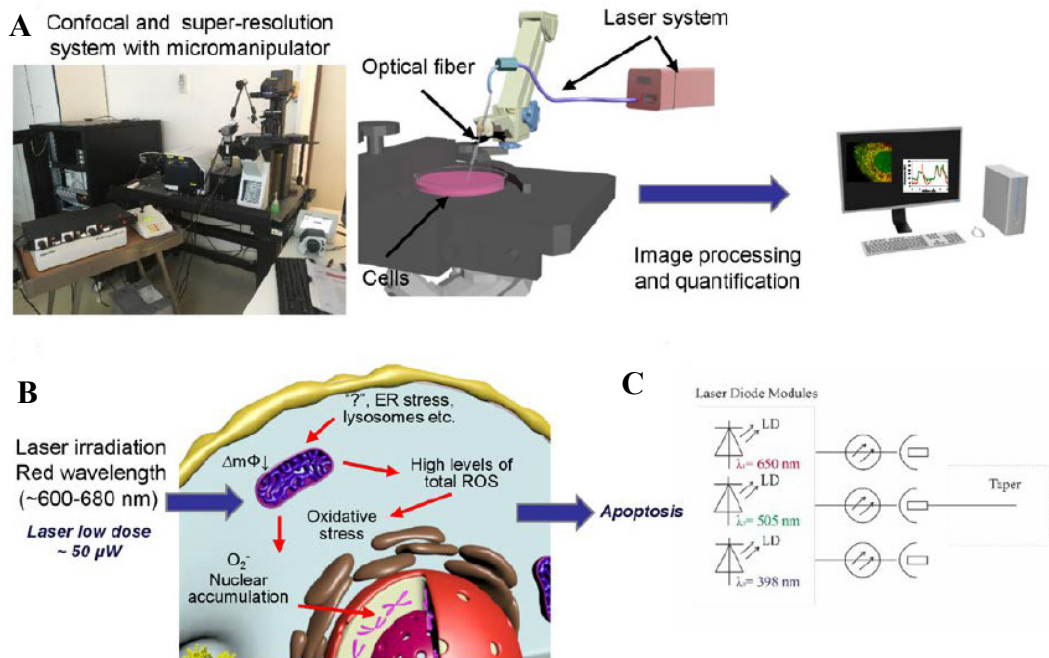


Figure 27 (A) Schematic illustration of the system. (B) Schematic illustration of the proposed molecular mechanisms of laser light irradiation on cells, $\Delta m\Phi$ – mitochondrial membrane potential. (C) Scheme of the used laser system, LD-laser diode. Reprinted by permission from Springer Nature Switzerland AG. Cellular and Molecular Life Sciences, Vol. 77, Mariia Lunova, Barbora Smolková, Mariia Uzhytchak, Klára Žofie Janoušková, Milan Jirsa, Daria Egorova, Andrei Kulikov, Šárka Kubinová, Alexandr Dejneka, Oleg Lunov, Light-induced modulation of the mitochondrial respiratory chain activity: possibilities and limitations, Pages 2815–2838 [210] Copyright © 2019.

Furthermore, we set up the output laser power at $\sim 50 \mu\text{W}$ for all three wavelengths, which was measured by an optical power meter PM100D (Thorlabs). In addition, the laser radiation divergence at wavelengths of 398nm, 505nm and 650nm at the end of the taper was determined by a beam-profiling camera Spiricon SP620U (Ophir-Spiricon) (Fig.28A). Based on the divergence of radiation, we assessed the dependence of the power density (irradiance) in the distance for $50\mu\text{W}$ (Fig. 28B). In a chosen area cells were irradiated with the power density of $< 1 \text{ kW}/\text{cm}^2$. The detailed description of the laser system is presented in **Appendix II**.

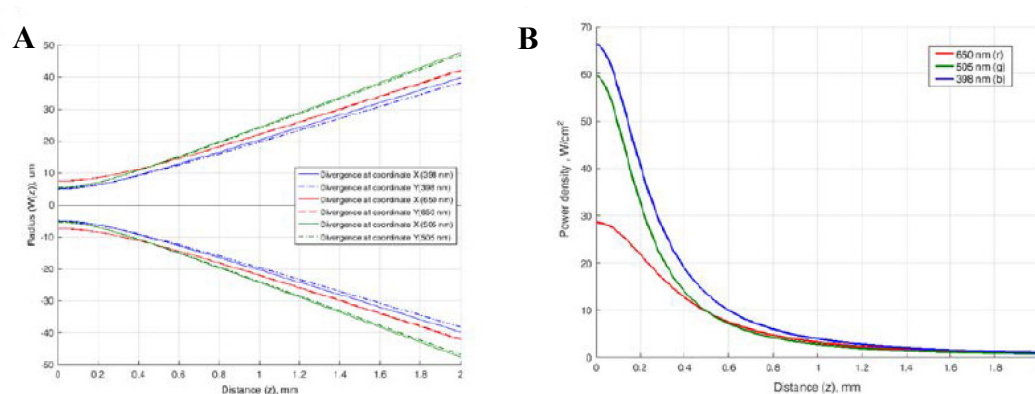


Figure 28 Characterisation of the laser light (A) Laser radiation divergence at wavelengths of 398nm, 505nm and 650nm at the end of the taper. (B) Power density of the used taper for wavelengths of 398nm, 505nm and 650nm. Reprinted by permission from Springer Nature Switzerland AG. *Cellular and Molecular Life Sciences*, Vol. 77, Mariia Lunova, Barbora Smolková, Mariia Uzhytchak, Klára Žofie Janoušková, Milan Jirsa, Daria Egorova, Andrei Kulikov, Šárka Kubinová, Alexandr Dejneka, Oleg Lunov, *Light-induced modulation of the mitochondrial respiratory chain activity: possibilities and limitations*, Pages 2815–2838 [210] Copyright © 2019.

4.2.2. Analysis of cell death post laser irradiation

Over the years, several reports have shown the phototoxic effects of high-fluence low power (HFLP) lasers on various cellular models (Table 6). In our previous study we revealed that red laser power of $\sim 50 \mu\text{W}$ triggered apoptotic cell death whereas 1 mW induced necrotic cell death [169]. Indeed, the laser power of $\sim 50 \mu\text{W}$ is very commonly utilized in biomedical applications. Thus, in our study we used one laser power of $\sim 50 \mu\text{W}$ with corresponding power density of $< 1 \text{ kW}/\text{cm}^2$ (Appendix II). Knowing that such low power laser irradiation of “red” light (i.e., 650 nm) induces signs of apoptosis, we wanted to uncover in details molecular mechanisms of such apoptotic events and verify whether that response is wavelength dependent. Therefore, we assessed the effects of three different wavelengths (398nm, 505nm, 650nm), which are most frequently used in LLLT, on three hepatic cancer cell lines Alexander, HepG2 and Huh7. Firstly, we analysed the impact of laser irradiation on cellular viability by using LIVE/DEAD® Viability/Cytotoxicity Kit assay. We observed increased cytotoxic effects of blue (398nm) and red (650nm) laser irradiation on Alexander and Huh7 cells. On the other hand, green (505nm) laser had no impact on viability of Alexander and Huh7 cells (Fig.29). Moreover, laser irradiation at neither tested wavelength led to cell death execution in HepG2 cells (Fig.29).

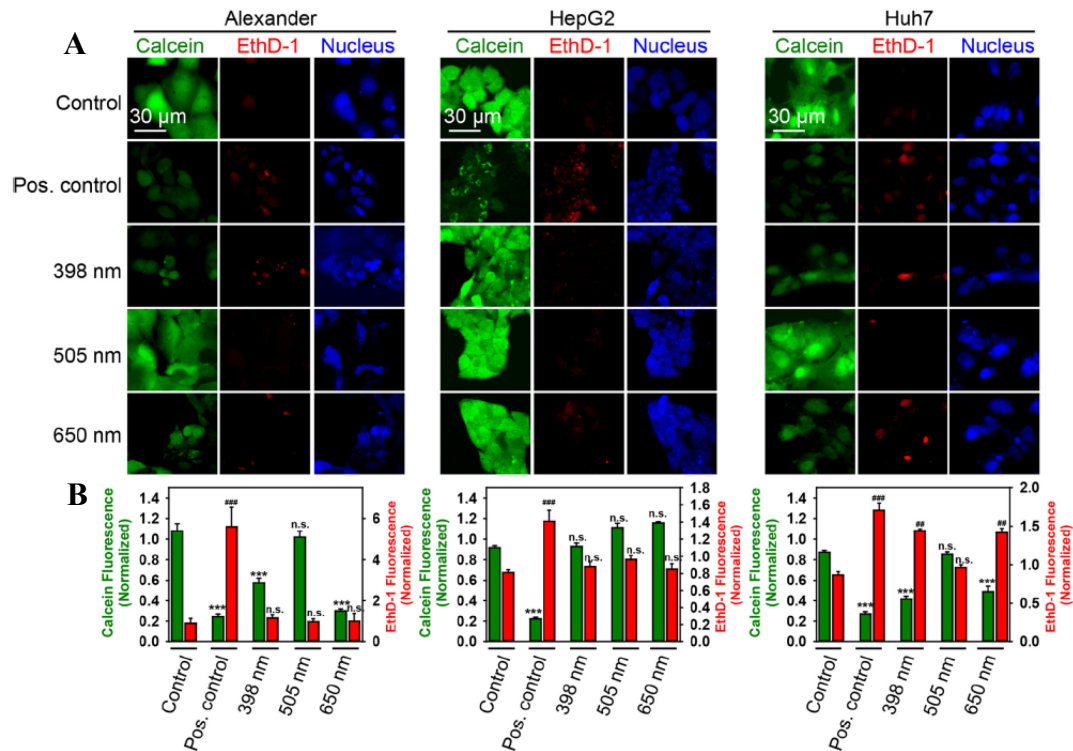


Figure 29 HFLP laser irradiation led to cell death execution in Alexander and Huh7 cells. (A) Representative confocal microscopy images of Alexander, HepG2 and Huh7 cells post laser irradiation. Cells were irradiated with laser (50 μ W) of different wavelengths 398,505 and 650nm for 1h. Cells were labelled with calcein-AM (green) and ethidium homodimer (red) of LIVE/DEAD® Viability/Cytotoxicity Kit and imaged by laser scanning confocal microscopy. NucRed™ Live 647 ReadyProbes™ Reagent (blue) was used to counterstain nuclei. 20% ethanol for 30 min was used as a positive control. (B) Quantification of fluorescent intensity of calcein-AM and ethidium homodimer. Data are expressed as mean \pm SEM n = 3., **p < 0.01, ***p < 0.001 for Calcein-AM, ###p < 0.001 for Ethidium. Reprinted by permission from Springer Nature Switzerland AG. Cellular and Molecular Life Sciences, Vol. 77, Mariia Lunova, Barbora Smolková, Mariia Uzhytchak, Klára Žofie Janoušková, Milan Jirsa, Daria Egorova, Andrei Kulikov, Šárka Kubinová, Alexandr Dejneka, Oleg Lunov, Light-induced modulation of the mitochondrial respiratory chain activity: possibilities and limitations, Pages 2815–2838 [210] Copyright © 2019.

Our previous study revealed that red laser irradiation of wavelength 655nm and similar laser power triggered apoptotic cell death in Huh7 cells [169]. Thus, we focus on analysis of the biochemical signalling leading to increased cytotoxicity in Alexander and Huh7 cells post laser irradiation. We noticed the early signs of apoptosis, the increased binding of Annexin V and Caspase-3 activation, in Alexander and Huh7 cells post treatment with blue and red laser irradiation. In line with cytotoxicity data, laser irradiation led neither to Annexin V binding nor to Caspase-3 activation in HepG2 cells. Detailed description and data are shown in [Appendix II](#).

4.2.3. Analysis of mitochondria post laser irradiation

Over the years, number of studies have proposed mitochondria as the sensor of low-power light [167, 181]. Previously, we and others have shown that HFLP lasers can trigger apoptotic cell death in cells via the mitochondrial signalling [169, 178, 180]. Therefore, in order to study mitochondrial involvement in response to laser irradiation in all three cell lines we used JC-1 staining.

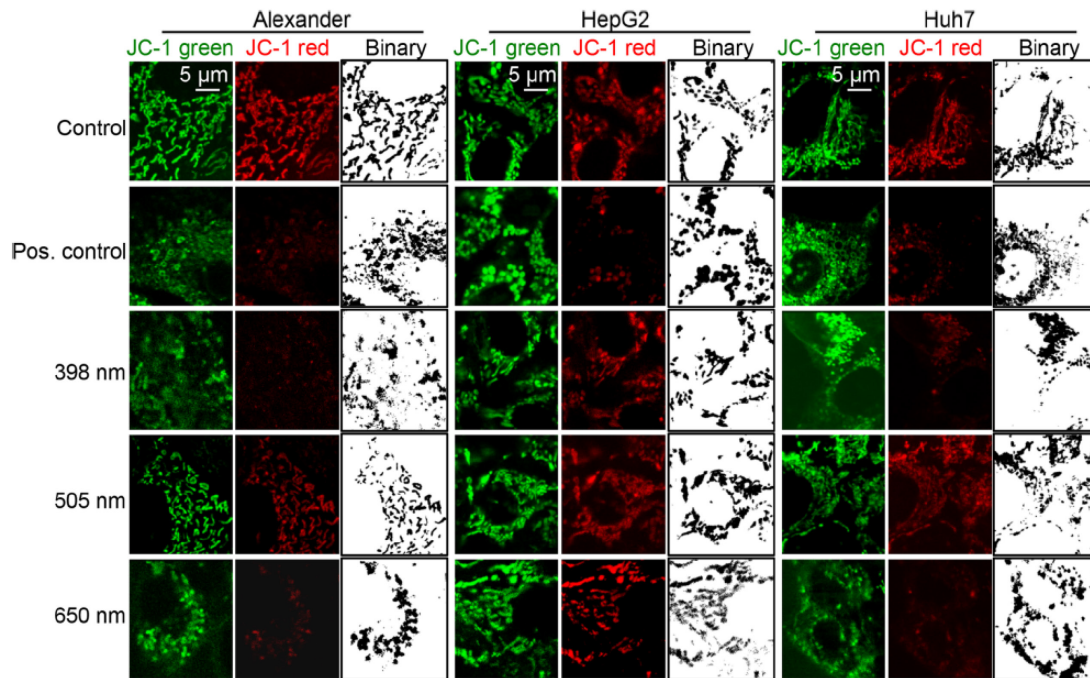


Figure 30 HFLP laser irradiation induced the changes in mitochondrial dynamics and mitochondrial membrane potential. Representative confocal images and binarized pictures of cells post laser irradiation of different wavelengths (398nm, 505nm, 650nm) for 30min and labelled with JC-1. 20% ethanol was used as positive control. Reprinted by permission from Springer Nature Switzerland AG. *Cellular and Molecular Life Sciences*, Vol. 77, Mariia Lunova, Barbora Smolková, Mariia Uzhytchak, Klára Žofie Janoušková, Milan Jirsa, Daria Egorova, Andrei Kulikov, Šárka Kubinová, Alexandr Dejneka, Oleg Lunov, Light-induced modulation of the mitochondrial respiratory chain activity: possibilities and limitations, Pages 2815–2838 [210] Copyright © 2019.

By using confocal microscopy imaging, we revealed the drop of red fluorescence intensity of JC-1 in Alexander and Huh7 after blue and red laser irradiation (Fig.30). The reduction of red fluorescence is characteristic for decrease in mitochondrial membrane potential ($\Delta m\Phi$). Moreover, we observed changes in mitochondrial dynamics, especially excessive mitochondrial fission in Alexander and Huh7 cells (Fig.30). In line with previous data, treatment with green laser did not affect the mitochondrial function of both cell lines (Fig.30). Additionally, any laser irradiation did not lead to mitochondria impairment in HepG2 cells (Fig.30).

Quantitative analysis of mitochondrial membrane potential and dynamics of all cell lines post laser irradiation is shown in Fig.31. Detailed description of analysis is written in [Appendix II](#).

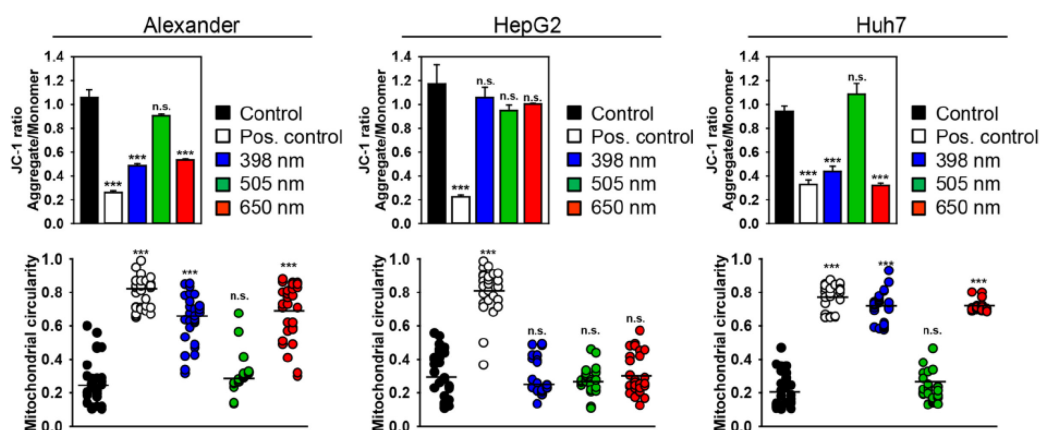


Figure 31 Quantification of mitochondrial membrane potential and dynamics in cells post HFLP laser irradiation. Images described in Fig.30 were processed and JC-1 fluorescence was quantified. Data are presented as mean \pm SEM, $n = 3$, *** $p < 0.001$. Analysis of circularity: data are presented as mean \pm SEM, $n = 30-50$ cells, *** $p < 0.001$. Reprinted by permission from Springer Nature Switzerland AG. Cellular and Molecular Life Sciences, Vol. 77, Mariia Lunova, Barbora Smolková, Mariia Uzhytchak, Klára Žofie Janoušková, Milan Jirsa, Daria Egorova, Andrei Kulikov, Šárka Kubinová, Alexandr Dejneka, Oleg Lunov, Light-induced modulation of the mitochondrial respiratory chain activity: possibilities and limitations, Pages 2815–2838 [210] Copyright © 2019.

Next, we aimed to study the effect of laser irradiation only in Alexander and Huh7 cells, as we did not observe any changes in mitochondria functionality and viability of HepG2. Moreover, we examined the impact of blue and red lasers, as green laser irradiation did not affect the cells. Firstly, we were interested in kinetics of mitochondrial shape and $\Delta m\Phi$ upon laser irradiation. Therefore, we used a brand-new IXplore SpinSR10 Olympus super resolution imaging system which enables ultrafast imaging at spatial resolution of 120nm [211] [212]. Time-lapse images of mitochondria revealed fragmented and roundish mitochondria 10 minutes after laser irradiation in both cell lines (Fig.32).

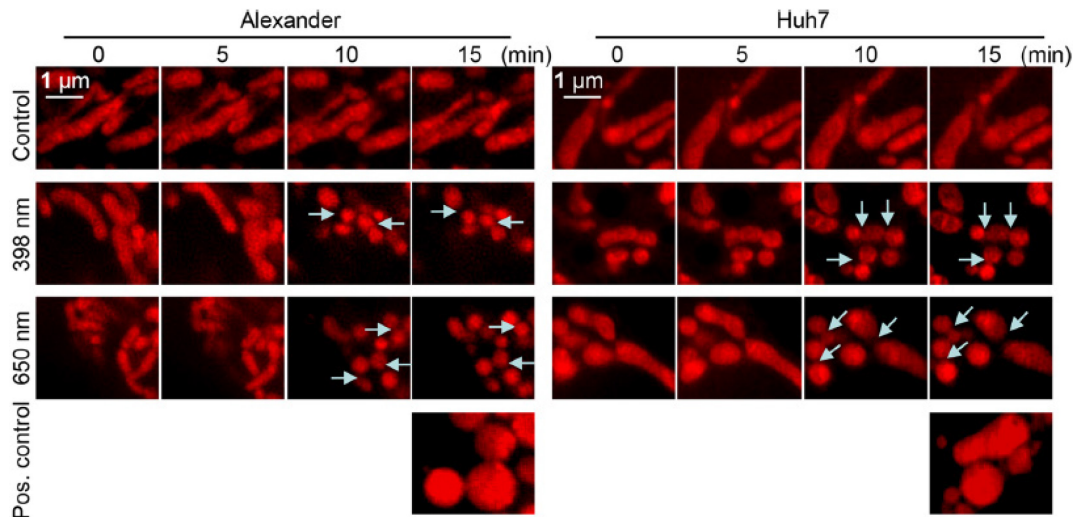


Figure 32 Kinetic analysis of mitochondria of Alexander and Huh7 cells post HFLP laser irradiation. Representative super-resolution time-lapse images of mitochondria of cells irradiated with red and blue lasers. 20% ethanol was used as a positive control. Arrows indicate mitochondrial fission. Reprinted by permission from Springer Nature Switzerland AG. *Cellular and Molecular Life Sciences*, Vol. 77, Mariia Lunova, Barbora Smolková, Mariia Uzhytchak, Klára Žofie Janoušková, Milan Jirsa, Daria Egorova, Andrei Kulikov, Šárka Kubinová, Alexandr Dejneka, Oleg Lunov, *Light-induced modulation of the mitochondrial respiratory chain activity: possibilities and limitations*, Pages 2815–2838 [210] Copyright © 2019.

In addition, we examined the kinetics of mitochondrial membrane potential upon laser irradiation by using time-lapse ratiometric JC-1 imaging analysis. At the end, we observed decrease of $\Delta m\Phi$ in both cell lines post blue and red laser irradiation however the kinetics of the process was different (Fig. 33A). Red laser led to hyperpolarization of mitochondria in both cell lines around 5th minutes, whereas blue laser triggered immediate decrease of $\Delta m\Phi$ in both cell lines (Fig. 33A). Moreover, the kinetic analysis of mitochondrial specific ROS production showed higher accumulation of ROS in both cell lines post blue laser irradiation in comparison to red one (Fig.33B).

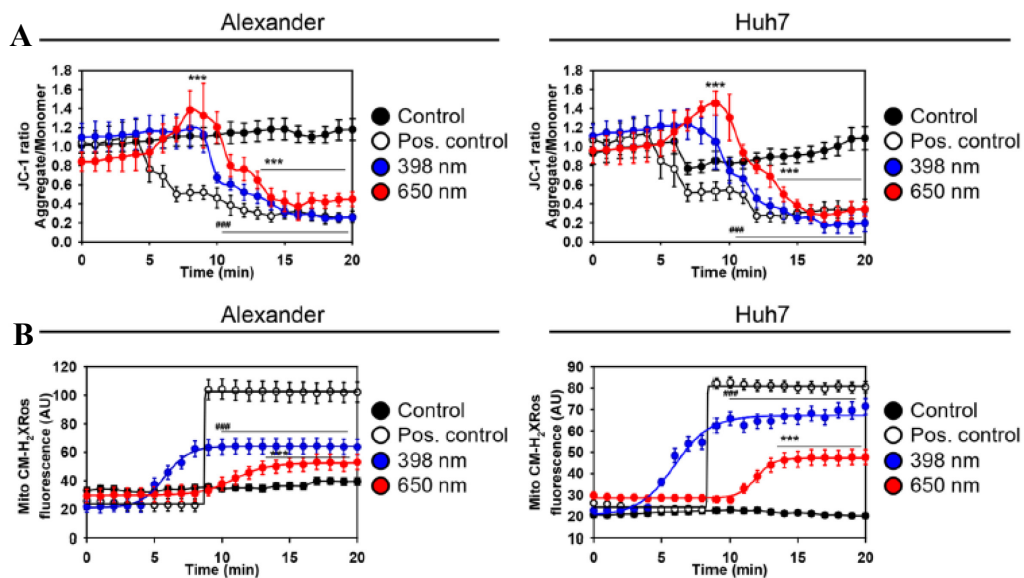


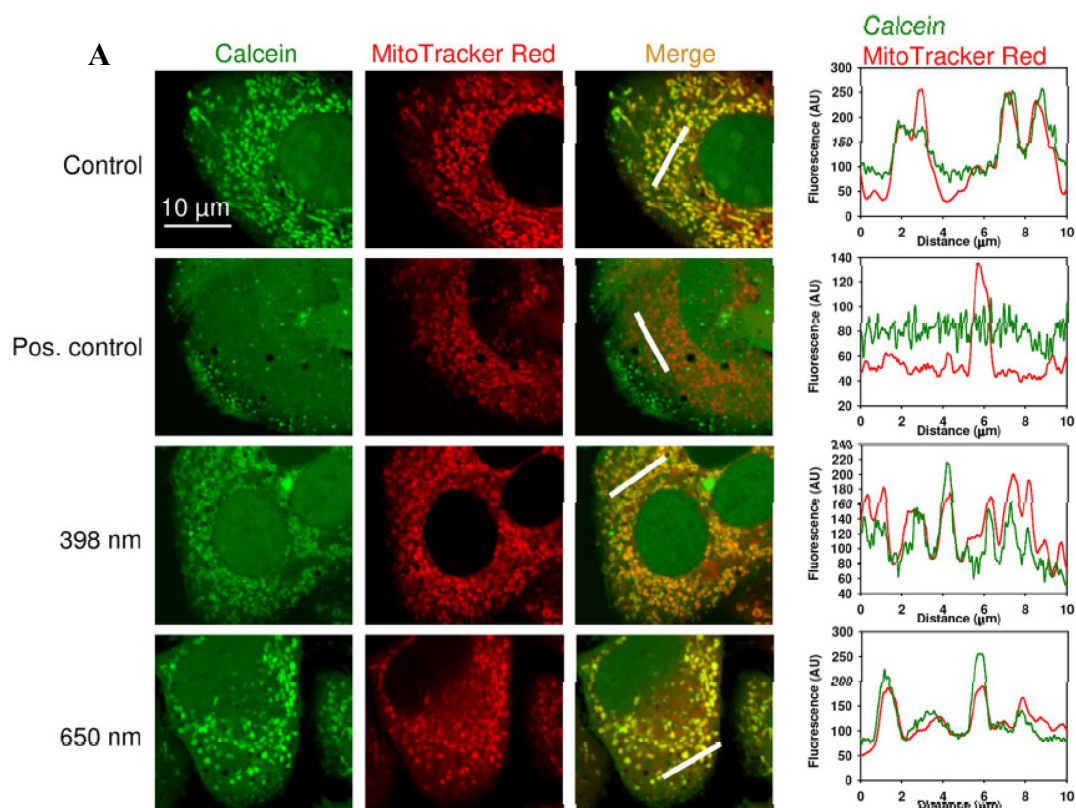
Figure 33 Kinetic analysis of mitochondrial membrane potential and ROS of Alexander and Huh7 cells post HFLP laser irradiation. (A) Quantification of $\Delta m\Phi$ kinetics in Huh7 and Alexander cells post blue and red laser irradiation. Cells were labelled with JC-1 as described previously; 20% Ethanol was used as a positive control. Data are presented as mean \pm SEM, $n = 3$, $t = 0$ timepoint was a control, *** $p < 0.001$. (B) Quantification of kinetics of mitochondrial specific ROS accumulation post blue and red laser irradiation. Cells were labelled with MitoTracker® red CM-H2XROS. H_2O_2 (0.5 mM) was a positive control. Data are presented as mean \pm SEM, $n = 3$, $t = 0$ timepoint was a control, *** $p < 0.001$. Reprinted by permission from Springer Nature Switzerland AG. *Cellular and Molecular Life Sciences*, Vol. 77, Mariia Lunova, Barbora Smolková, Mariia Uzhytchak, Klára Žofie Janoušková, Milan Jirsa, Daria Egorova, Andrei Kulikov, Šárka Kubinová, Alexandr Dejneka, Oleg Lunov, Light-induced modulation of the mitochondrial respiratory chain activity: possibilities and limitations, Pages 2815–2838 [210] Copyright © 2019.

Further, in [Appendix II](#) we analysed the effects of HFLP irradiation on lysosomes and endoplasmic reticulum. In fact, lysosomal dysfunction and ER stress may contribute to mitochondria-related cell death execution [213, 214]. Indeed, we observed neither ER stress nor lysosomal dysfunction in both cell lines post laser irradiation at the time-point of $\Delta m\Phi$ changes ([Appendix II](#)). In conclusion, our data proposed that mitochondria are the main effector and sensor in the cellular response to laser irradiation.

4.2.4. Effects of laser irradiation on mitochondrial electron transport chain

Next, in [Appendix II](#) we performed the analysis of the mitochondrial permeability transition pore (mPTP) opening, in order to validate the function of mitochondria impairment in the cellular response to laser irradiation. Thus, we used technique grounded on accumulation of calcein AM dye and quenching by cobalt ions (Co^{2+}) [215]. Normally, is the calcein localized in all structures of the cell, but the addition of

Co²⁺ is quenching the fluorescence of calcein outside of mitochondria. Only upon mPTP opening and permeabilization of mitochondrial inner membrane, is Co²⁺ penetrating inside the mitochondria what results into quenching of calcein fluorescence ([Appendix II](#)). Our analysis showed no impact of blue or red laser irradiation on mPTP opening in both cell lines (Fig. 34). Calcein of cells irradiated with lasers co-localized with mitochondria similarly as in control cells. We observed calcein quenching from mitochondria only in cells treated with ionomycin (Fig.34). Further, in order to validate the role of mitochondria-associated ROS in cell death triggered by laser irradiation, we used Mito-TEMPO, specific scavenger of mitochondrial ROS [216]. Our data in [Appendix II](#) showed that addition of Mito-TEMPO to cells led to inhibition of mitochondrial-ROS accumulation and stabilization of $\Delta m\Phi$ in Alexander and Huh7 cells after laser irradiation. Moreover, addition of Mito-TEMPO rescued Alexander and Huh7 cells from cell death-mediated by laser irradiation. Data and detailed description are presented in [Appendix II](#).



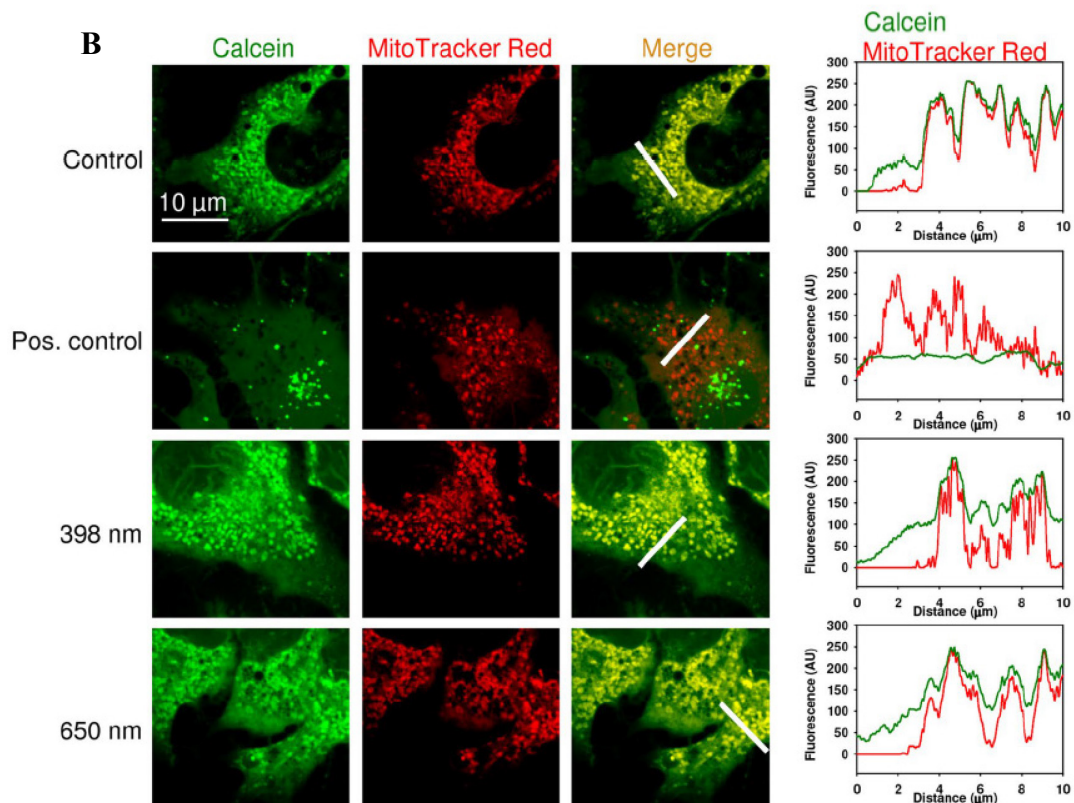


Figure 34 Analysis of mPTP opening post HFLP laser irradiation. Representative confocal images of Alexander (A) and Huh7 (B) cells post blue and red laser irradiation. Cells were labelled with calcein-AM and MitoTracker® Red in the presence of Co^{2+} . $1 \mu\text{M}$ ionomycin was used as a positive control. Reprinted by permission from Springer Nature Switzerland AG. *Cellular and Molecular Life Sciences*, Vol. 77, Mariia Lunova, Barbora Smolková, Mariia Uzhytchak, Klára Žofie Janoušková, Milan Jirsa, Daria Egorova, Andrei Kulikov, Šárka Kubinová, Alexandr Dejneka, Oleg Lunov, *Light-induced modulation of the mitochondrial respiratory chain activity: possibilities and limitations*, Pages 2815–2838 [210] Copyright © 2019.

Taking all data together, in [Appendix II](#) we confirmed the importance of mitochondria in the cellular response to laser irradiation. However, we were interested more in molecular mechanisms behind this response. So far, we could not explain that the distinct kinetic resulted in the same cytotoxic events. In fact, we found a model combining the cytochrome c oxidase (COX), mitochondria, ROS and cell death [185]. This model proposes that either inhibition or activation of COX may lead to increased ROS production, hypo- or hyper-polarization of $\Delta m\Phi$ and cell death [185]. Based on this model, in [Appendix II](#) we suggested that blue laser irradiation inhibited the COX whereas red laser irradiation hyper-activated the COX and finally, both conditions resulted into cell death (Fig.35).

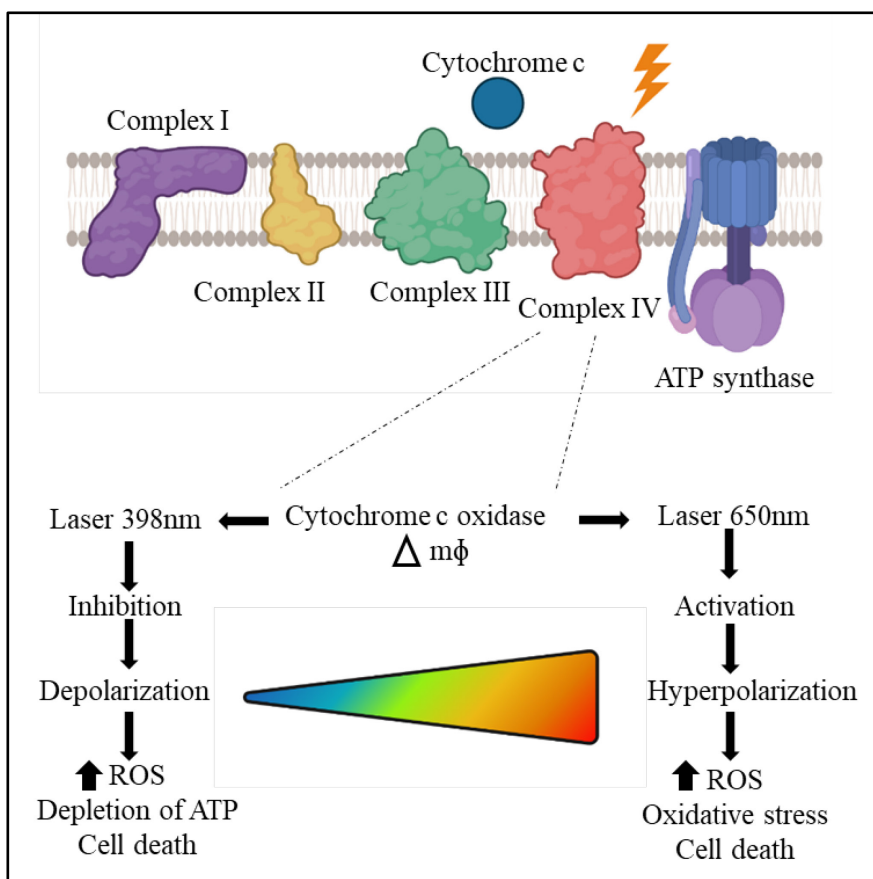


Figure 35 Schematic illustration of the suggested model of the action of blue and red laser irradiation. Adapted from Figure 6D of [210] Appendix II.

In order to confirm the role of COX in the response to laser irradiation we used two inhibitors and one activator of this enzyme. Firstly, we examined the mitochondrial ROS production, $\Delta m\Phi$ and viability after treatment with blue and red irradiation in the presence of specific COX inhibitor, called ADDA-5. Our data showed that co-treatment of cells with ADDA-5 blocked the mitochondrial ROS production, stabilized changes in $\Delta m\Phi$ and rescued both cell lines from cell death triggered by red laser irradiation (Fig.36). The addition of ADDA-5 had no impact on cytotoxic effects of blue laser irradiation (Fig.36). Furthermore, the co-treatment of cells with KCN, a non-specific inhibitor of COX resulted in similar cellular response to laser irradiation. Data are shown in Appendix II. Next, we used the bezafibrate (BZF), a non-selective activator of COX in order to verify the blue laser irradiation response. It is worth noting that co-treatment of both cell lines led to increased ROS level and hyperpolarization of mitochondria (Fig. 37). However, the ROS level and $\Delta m\Phi$ were stabilized after blue laser irradiation proving its ability to inhibit COX (Fig.37). In conclusion, we revealed the mechanism leading to different effects of blue

and red laser irradiation on COX function. Red laser irradiation led to COX activation, whereas blue laser irradiation inhibited the COX function.

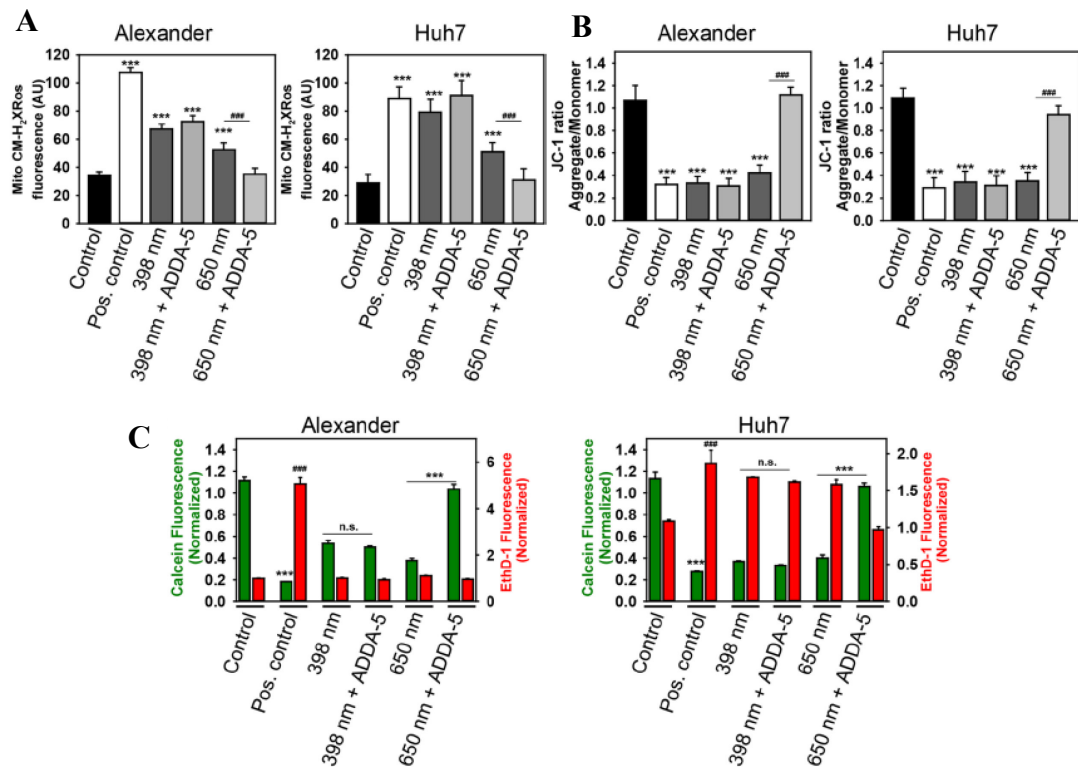


Figure 36 Analysis of the cellular response to blue and red laser irradiation in the presence of COX inhibitor. (A) Analysis of mitochondrial specific ROS. Cells were labelled with MitoTracker® red CM-H₂XRos and irradiated with lasers. (B) Analysis of mitochondrial membrane potential. Cells were labelled with JC-1 and irradiated with lasers. (C) Analysis of cellular viability. Cells were labelled with LIVE/DEAD® Viability/Cytotoxicity Kit as described previously. In A, B, C data are presented as mean ± SEM, n = 3, ***p < 0.001, ###p < 0.00. Reprinted by permission from Springer Nature Switzerland AG. Cellular and Molecular Life Sciences, Vol. 77, Mariia Lunova, Barbora Smolková, Mariia Uzhytchak, Klára Žofie Janoušková, Milan Jirsa, Daria Egorova, Andrei Kulikov, Šárka Kubinová, Alexandr Dejnek, Oleg Lunov, Light-induced modulation of the mitochondrial respiratory chain activity: possibilities and limitations, Pages 2815–2838 [210] Copyright © 2019.

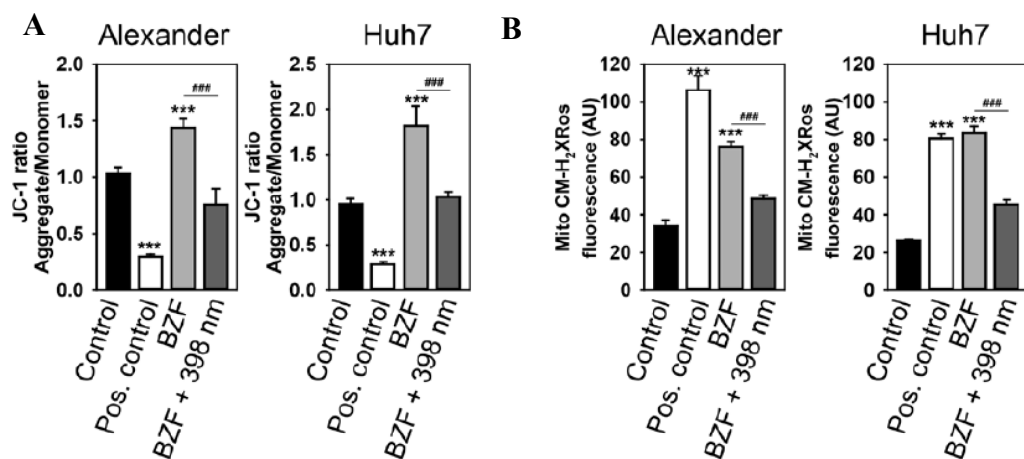


Figure 37 Analysis of cellular response to blue and red laser irradiation in the presence of BZF.

COX activator. (A) Quantitative analysis of mitochondrial membrane potential. Cells were labelled with JC-1 and irradiated with lasers. (B) Quantitative analysis of mitochondrial specific ROS. Cells were labelled with MitoTracker® Red CM-H2XRos and irradiated with lasers. In A, B data are presented as mean \pm SEM, $n = 3$, *** $p < 0.001$, #### $p < 0.001$. Detailed description is presented in [Appendix II](#). Reprinted by permission from Springer Nature Switzerland AG. Cellular and Molecular Life Sciences, Vol. 77, Mariia Lunova, Barbora Smolková, Mariia Uzhytchak, Klára Žofie Janoušková, Milan Jirsa, Daria Egorova, Andrei Kulikov, Šárka Kubinová, Alexandr Dejneka, Oleg Lunov, Light-induced modulation of the mitochondrial respiratory chain activity: possibilities and limitations, Pages 2815–2838 [210] Copyright © 2019.

4.2.5. Up-regulation of Bcl-2 protein stabilized the mitochondria and protected cells from cell death

Data in previous chapter explained the mechanism of action of blue and red laser irradiation in Alexander and Huh7 cells. Further, in [Appendix II](#) we were interested in the reason of HepG2 cells resistance to laser irradiation. We know from the [Appendix I](#) that our three cell lines possess different basal expression of crucial proteins Bcl-2 and p53, involved in cell death regulation. The densitometric quantification of immunoblots confirmed the highest level of Bcl-2 protein in HepG2 cells (Fig.38).

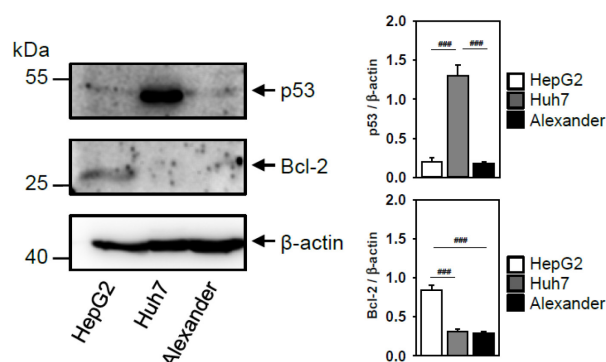


Figure 38 Comparison of the different expression of Bcl-2 and p53 proteins in cells. Graphs presents densitometric quantification of the immunoblots. Data are presented as mean \pm SEM, $n=3$, #### $p < 0.001$. Reprinted by permission from Springer Nature Switzerland AG. Cellular and Molecular Life Sciences, Vol. 77, Mariia Lunova, Barbora Smolková, Mariia Uzhytchak, Klára Žofie Janoušková, Milan Jirsa, Daria Egorova, Andrei Kulikov, Šárka Kubinová, Alexandr Dejneka, Oleg Lunov, Light-induced modulation of the mitochondrial respiratory chain activity: possibilities and limitations, Pages 2815–2838 [210] Copyright © 2019.

In order to verify the role of Bcl-2 protein in resistance of HepG2 cells towards laser irradiation we used specific Bcl-2 inhibitor ABT-737. In fact, co-treatment of cells with ABT-737 and blue and red laser irradiation induced not only the cell death (Fig.39) but also changes in $\Delta m\Phi$ of HepG2 cells (data showed in [Appendix II](#)).

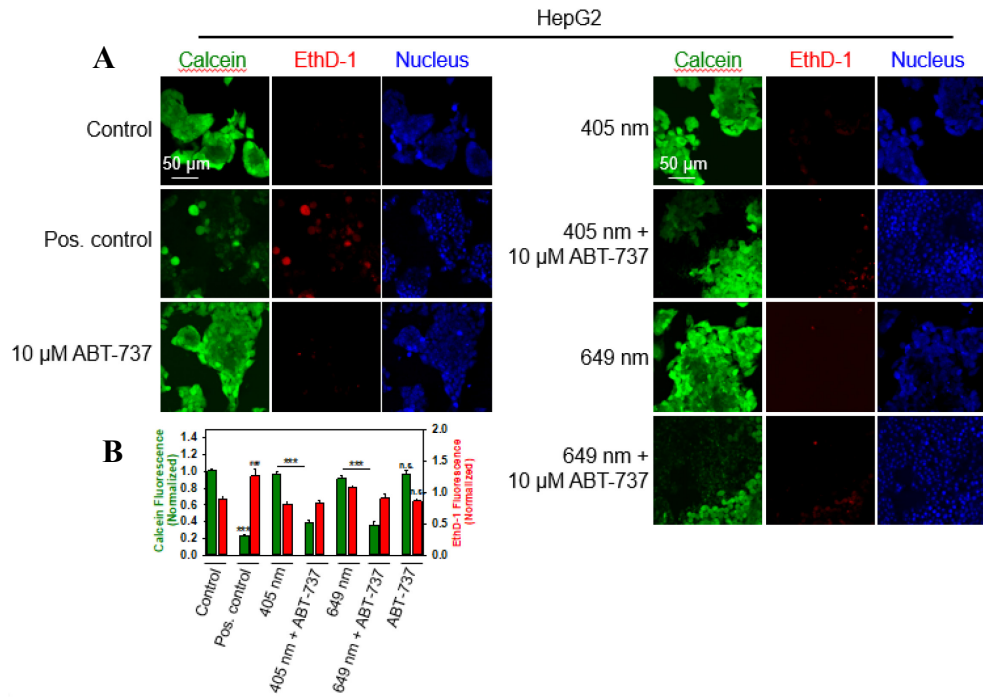


Figure 39 Bcl-2 inhibition restored the resistance of HepG2 cells towards laser irradiation. (A) Representative confocal images of HepG2 cells labelled with LIVE/DEAD® Viability/Cytotoxicity Kit and irradiated with the blue and red lasers with or without the addition of Bcl-2 inhibitor (ABT-737). 20% Ethanol was used as a positive control. (B) Quantification of the fluorescence intensity of the images from A. Data are presented as mean \pm SEM ($n = 3$), *** $p < 0.001$, #### $p < 0.001$. Reprinted by permission from Springer Nature Switzerland AG. Cellular and Molecular Life Sciences, Vol. 77, Mariia Lunova, Barbora Smolková, Mariia Uzhytchak, Klára Žofie Janoušková, Milan Jirsa, Daria Egorova, Andrei Kulikov, Šárka Kubinová, Alexandr Dejneka, Oleg Lunov, Light-induced modulation of the mitochondrial respiratory chain activity: possibilities and limitations, Pages 2815–2838 [210] Copyright © 2019.

In addition, we overexpressed the Bcl-2 protein in Alexander and Huh7 cells by using Bcl-2-GFP plasmid [217] in order to confirm the Bcl-2 function (Fig.39A). Validation of transfection efficiency, detailed description and full blots are showed in [Appendix II](#). We observed neither the increased level of mitochondrial mediated ROS (Fig.40B) nor the cell death (Fig.40C) of Alexander and Huh7 cells overexpressing Bcl-2 protein after blue and red laser irradiation.

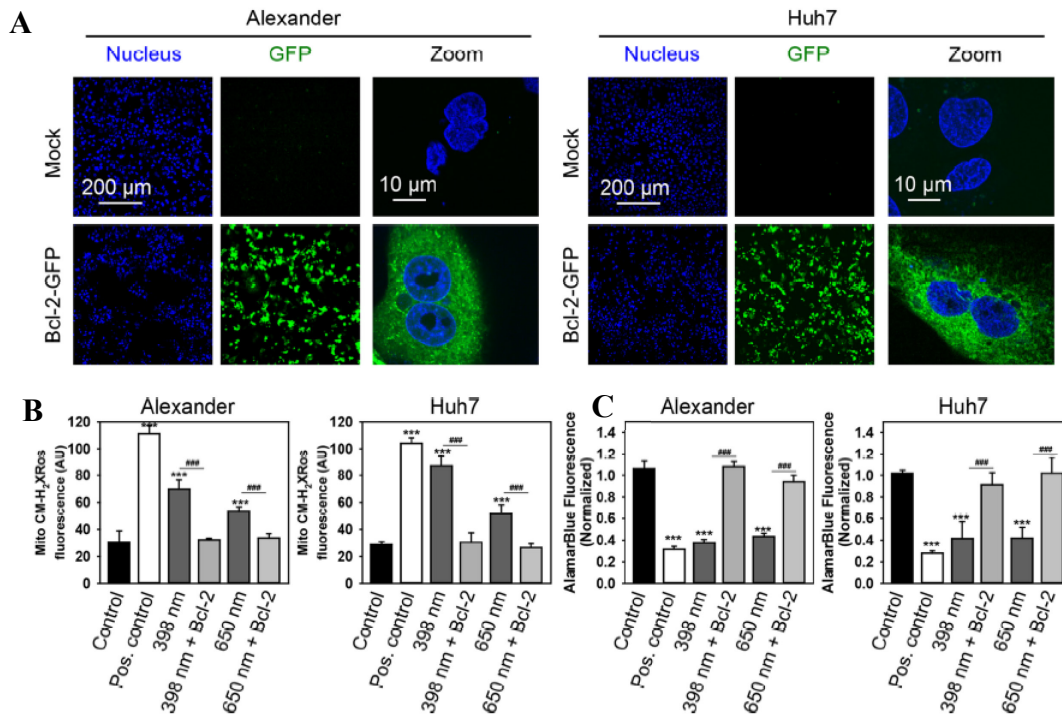


Figure 40 *Bcl-2* overexpression inhibited the cytotoxic effects of blue and red laser irradiation in Alexander and Huh7 cells. (A) Representative confocal images of the Alexander and Huh7 cells with overexpressed *Bcl-2* tagged with GFP. Hoechst33,342 stain was used to counterstain nuclei. (B) Quantitative analysis of mitochondrial specific ROS. Cells overexpressing mock or *Bcl-2*-GFP were labelled with MitoTracker® red CM-H2XROS and irradiated with lasers. (C) Analysis of cellular viability. Cells overexpressing mock or *Bcl-2*-GFP were labelled with alamarBlue and irradiated with lasers. For B, C data are presented as mean \pm SEM, $n = 3$, $***p < 0.001$, $###p < 0.00$. Reprinted by permission from Springer Nature Switzerland AG. Cellular and Molecular Life Sciences, Vol. 77, Mariia Lunova, Barbora Smolková, Mariia Uzhytchak, Klára Žofie Janoušková, Milan Jirsa, Daria Egorova, Andrei Kulikov, Šárka Kubinová, Alexandr Dejneka, Oleg Lunov, Light-induced modulation of the mitochondrial respiratory chain activity: possibilities and limitations, Pages 2815–2838 [210] Copyright © 2019.

Moreover, confocal microscopy imaging revealed that overexpressed *Bcl-2* was localized in cytosol and mitochondria of both cell lines. However, we noticed prevalent translocation of *Bcl-2* to mitochondria upon blue and red laser irradiation (Fig. 41). In fact, it has been shown that anti-apoptotic protein *Bcl-2* may inhibit apoptotic cell death execution in this way [218].

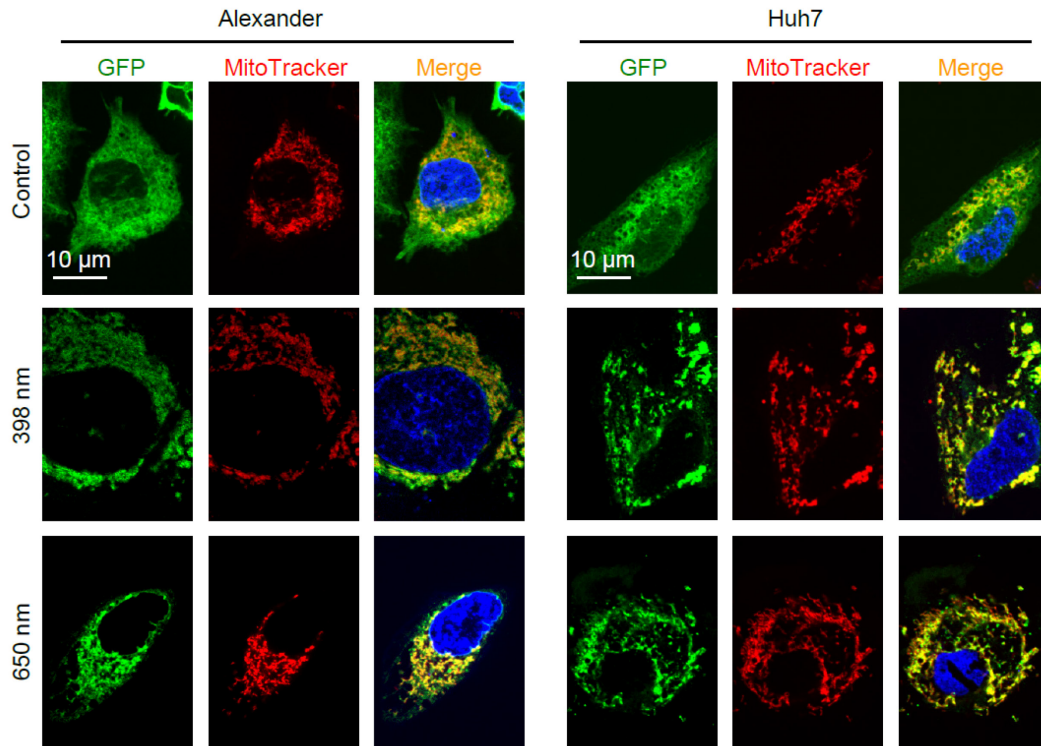


Figure 41 Translocation of Bcl-2 protein to mitochondria inhibited the cell death mediated by red and blue laser irradiation in Alexander and Huh7 cells. Representative confocal images of cells with overexpressed Bcl-2-GFP, labelled with MitoTracker Red after blue and red laser irradiation. Reprinted by permission from Springer Nature Switzerland AG. Cellular and Molecular Life Sciences, Vol. 77, Mariia Lunova, Barbora Smolková, Mariia Uzhytchak, Klára Žofie Janoušková, Milan Jirsa, Daria Egorova, Andrei Kulikov, Šárka Kubinová, Alexandr Dejneka, Oleg Lunov, Light-induced modulation of the mitochondrial respiratory chain activity: possibilities and limitations, Pages 2815–2838 [210] Copyright © 2019.

Taking all data together, in **Appendix II** we revealed the mechanisms of action of laser irradiation in three hepatic cancer cell lines. We showed by various methods that Bcl-2 protein level has a great impact on the cellular response to laser irradiation (Fig.42).

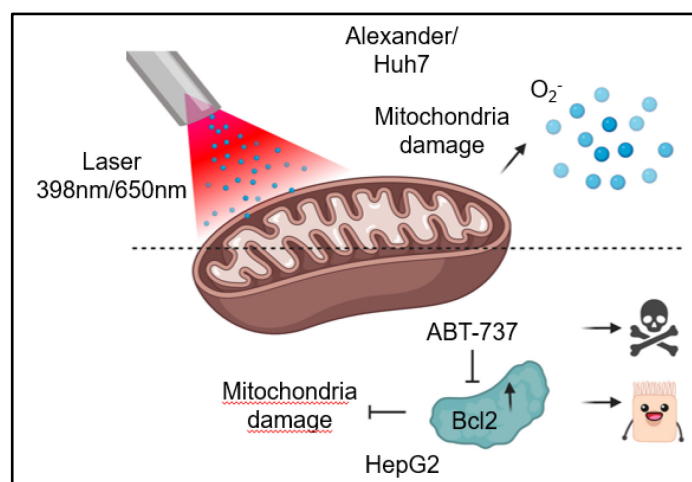


Figure 42 Schematic illustration of the molecular mechanisms in cells post laser irradiation. Adapted from Figure 8D of [210] **Appendix II**.

5. CONCLUSIONS

The presented dissertation thesis focuses on the mechanisms of action of air non-thermal plasma and laser irradiation in three hepatic cancer cell lines. The thesis consists of two main sections, introductory theoretical background and experimental section.

The first section is summarizing the literature depicting the current stage of both fields, plasma medicine and laser therapy from biophysical point of view. In particular, we focused on the mechanism of the cellular response to non-thermal plasma and laser irradiation. Indeed, the background for the theoretical part represents two reviews presented in [Appendix III](#) and [Appendix IV](#). Here, we critically assessed the current knowledge in both fields, described the recent progress but also specified the limitations and challenges.

Second experimental section is divided into two parts. In order to achieve all goals, various advanced techniques of molecular biology and biochemistry have been used. In particular, cellular signalling was analysed by different microscopical methods, from standard optical microscopy to utilization of a brand-new high resolution spinning disk confocal microscopy IXplore SpinSR (Olympus) and by western blot analysis. In the first part, we revealed the molecular mechanisms of action of air non-thermal plasma in hepatic cancer cell lines, namely HepG2, Huh7 and Alexander. We uncovered that cellular response to NTP is dependent on the p53/Bcl2 signalling pathway. Moreover, we showed that NTP treatment led to mitochondria-mediated p53-dependent apoptosis in Huh7 cells, whereas elevated level of Bcl-2 protein saved HepG2 cells from NTP- triggered cell death ([Appendix I](#)). Second part of the experimental section described the cytochrome c oxidase as the key cellular target of high-fluence low power laser irradiation of different wavelengths in above mentioned hepatic cancer cell lines. We showed that blue and red laser irradiation induced apoptotic cell death in Alexander and Huh7 cells. Further, we revealed the mechanism of action of blue and red laser irradiation on COX function. Blue laser irradiation led to COX inhibition, whereas red laser irradiation activated the function of COX. Furthermore, we showed that elevated level of Bcl-2 protein protected HepG2 cells from cell death and contributed to the resistance to laser irradiation ([Appendix II](#)).

We hope that our work and critical analysis will help researchers to overcome challenges and develop in the future better controlled, safer, and more robust NTP- and laser-based treatment modalities. Presented work resulted into 4 publications published in indexed peer-reviewed journals, several conference contributions and lectures.

BIBLIOGRAPHY

1. Trachootham, D., J. Alexandre, and P. Huang, *Targeting cancer cells by ROS-mediated mechanisms: a radical therapeutic approach?* Nat Rev Drug Discov, 2009. **8**(7): p. 579-91.
2. Sies, H. and D.P. Jones, *Reactive oxygen species (ROS) as pleiotropic physiological signalling agents.* Nat Rev Mol Cell Biol, 2020. **21**(7): p. 363-383.
3. Fang, F.C., *Antimicrobial reactive oxygen and nitrogen species: concepts and controversies.* Nat Rev Microbiol, 2004. **2**(10): p. 820-32.
4. Adams, L., M.C. Franco, and A.G. Estevez, *Reactive nitrogen species in cellular signaling.* Exp Biol Med (Maywood), 2015. **240**(6): p. 711-7.
5. Dickinson, B.C. and C.J. Chang, *Chemistry and biology of reactive oxygen species in signaling or stress responses.* Nat Chem Biol, 2011. **7**(8): p. 504-11.
6. Di Mascio, P., et al., *Singlet Molecular Oxygen Reactions with Nucleic Acids, Lipids, and Proteins.* Chem Rev, 2019. **119**(3): p. 2043-2086.
7. Lerner, R.A. and A. Eschenmoser, *Ozone in biology.* Proc Natl Acad Sci U S A, 2003. **100**(6): p. 3013-5.
8. Winter, J., et al., *Bleach activates a redox-regulated chaperone by oxidative protein unfolding.* Cell, 2008. **135**(4): p. 691-701.
9. Perillo, B., et al., *ROS in cancer therapy: the bright side of the moon.* Exp Mol Med, 2020. **52**(2): p. 192-203.
10. Forman, H.J., F. Ursini, and M. Maiorino, *An overview of mechanisms of redox signaling.* J Mol Cell Cardiol, 2014. **73**: p. 2-9.
11. Vakifahmetoglu-Norberg, H., A.T. Ouchida, and E. Norberg, *The role of mitochondria in metabolism and cell death.* Biochem Biophys Res Commun, 2017. **482**(3): p. 426-431.
12. Tait, S.W. and D.R. Green, *Mitochondria and cell death: outer membrane permeabilization and beyond.* Nat Rev Mol Cell Biol, 2010. **11**(9): p. 621-32.
13. Spinelli, J.B. and M.C. Haigis, *The multifaceted contributions of mitochondria to cellular metabolism.* Nat Cell Biol, 2018. **20**(7): p. 745-754.
14. Mishra, P. and D.C. Chan, *Mitochondrial dynamics and inheritance during cell division, development and disease.* Nat Rev Mol Cell Biol, 2014. **15**(10): p. 634-46.
15. Friedman, J.R. and J. Nunnari, *Mitochondrial form and function.* Nature, 2014. **505**(7483): p. 335-43.
16. Giacomello, M., et al., *The cell biology of mitochondrial membrane dynamics.* Nat Rev Mol Cell Biol, 2020. **21**(4): p. 204-224.
17. Willems, P.H., et al., *Redox Homeostasis and Mitochondrial Dynamics.* Cell Metab, 2015. **22**(2): p. 207-18.
18. Chen, H., A. Chomyn, and D.C. Chan, *Disruption of fusion results in mitochondrial heterogeneity and dysfunction.* J Biol Chem, 2005. **280**(28): p. 26185-92.
19. Pickles, S., P. Vigie, and R.J. Youle, *Mitophagy and Quality Control Mechanisms in Mitochondrial Maintenance.* Curr Biol, 2018. **28**(4): p. R170-R185.
20. Lemasters, J.J., *Selective mitochondrial autophagy, or mitophagy, as a targeted defense against oxidative stress, mitochondrial dysfunction, and aging.* Rejuvenation Res, 2005. **8**(1): p. 3-5.
21. Jiao, H., et al., *Mitocytosis, a migrasome-mediated mitochondrial quality-control process.* Cell, 2021. **184**(11): p. 2896-2910 e13.
22. Bock, F.J. and S.W.G. Tait, *Mitochondria as multifaceted regulators of cell death.* Nat Rev Mol Cell Biol, 2020. **21**(2): p. 85-100.
23. Wallace, D.C., *Mitochondria and cancer.* Nat Rev Cancer, 2012. **12**(10): p. 685-98.
24. Chan, D.C., *Mitochondria: dynamic organelles in disease, aging, and development.* Cell, 2006. **125**(7): p. 1241-52.

25. Murphy, M.P. and R.C. Hartley, *Mitochondria as a therapeutic target for common pathologies*. Nature Reviews Drug Discovery, 2018. **17**(12): p. 865-886.
26. Schrader, M. and H.D. Fahimi, *Peroxisomes and oxidative stress*. Biochimica Et Biophysica Acta-Molecular Cell Research, 2006. **1763**(12): p. 1755-1766.
27. Brigelius-Flohe, R. and M. Maiorino, *Glutathione peroxidases*. Biochim Biophys Acta, 2013. **1830**(5): p. 3289-303.
28. Fukai, T. and M. Ushio-Fukai, *Superoxide dismutases: role in redox signaling, vascular function, and diseases*. Antioxid Redox Signal, 2011. **15**(6): p. 1583-606.
29. Shields, H.J., A. Traa, and J.M. Van Raamsdonk, *Beneficial and Detrimental Effects of Reactive Oxygen Species on Lifespan: A Comprehensive Review of Comparative and Experimental Studies*. Frontiers in Cell and Developmental Biology, 2021. **9**.
30. Ribas, V., C. Garcia-Ruiz, and J.C. Fernandez-Checa, *Glutathione and mitochondria*. Front Pharmacol, 2014. **5**: p. 151.
31. Otterbein, L.E., et al., *Carbon monoxide has anti-inflammatory effects involving the mitogen-activated protein kinase pathway*. Nat Med, 2000. **6**(4): p. 422-8.
32. Atkuri, K.R., et al., *N-Acetylcysteine--a safe antidote for cysteine/glutathione deficiency*. Curr Opin Pharmacol, 2007. **7**(4): p. 355-9.
33. Murphy, M.P., et al., *Unraveling the Biological Roles of Reactive Oxygen Species*. Cell Metabolism, 2011. **13**(4): p. 361-366.
34. Winterbourn, C.C., *Reconciling the chemistry and biology of reactive oxygen species*. Nature Chemical Biology, 2008. **4**(5): p. 278-286.
35. Barnham, K.J., C.L. Masters, and A.I. Bush, *Neurodegenerative diseases and oxidative stress*. Nat Rev Drug Discov, 2004. **3**(3): p. 205-14.
36. Tell, G., C. Vascotto, and C. Tiribelli, *Alterations in the redox state and liver damage: Hints from the EASL Basic School of Hepatology*. Journal of Hepatology, 2013. **58**(2): p. 365-374.
37. Vander Heiden, M.G., L.C. Cantley, and C.B. Thompson, *Understanding the Warburg effect: the metabolic requirements of cell proliferation*. Science, 2009. **324**(5930): p. 1029-33.
38. Harris, I.S. and J.S. Brugge, *CANCER The enemy of my enemy is my friend*. Nature, 2015. **527**(7577): p. 170-171.
39. Gorrini, C., I.S. Harris, and T.W. Mak, *Modulation of oxidative stress as an anticancer strategy*. Nature Reviews Drug Discovery, 2013. **12**(12): p. 931-947.
40. Hayes, J.D. and A.T. Dinkova-Kostova, *The Nrf2 regulatory network provides an interface between redox and intermediary metabolism*. Trends in Biochemical Sciences, 2014. **39**(4): p. 199-218.
41. Canning, P., F.J. Sorrell, and A.N. Bullock, *Structural basis of Keap1 interactions with Nrf2*. Free Radical Biology and Medicine, 2015. **88**: p. 101-107.
42. Hayes, J.D., et al., *Cancer Chemoprevention Mechanisms Mediated Through the Keap1-Nrf2 Pathway*. Antioxidants & Redox Signaling, 2010. **13**(11): p. 1713-1748.
43. Lister, A., et al., *Nrf2 is overexpressed in pancreatic cancer: implications for cell proliferation and therapy*. Molecular Cancer, 2011. **10**.
44. De Nicola, G.M., et al., *Oncogene-induced Nrf2 transcription promotes ROS detoxification and tumorigenesis*. Nature, 2011. **475**(7354): p. 106-U128.
45. Hayes, J.D. and M. McMahon, *NRF2 and KEAP1 mutations: permanent activation of an adaptive response in cancer*. Trends in Biochemical Sciences, 2009. **34**(4): p. 176-188.
46. Totoki, Y., et al., *Trans-ancestry mutational landscape of hepatocellular carcinoma genomes*. Nature Genetics, 2014. **46**(12): p. 1267-1273.
47. Sporn, M.B. and K.T. Liby, *NRF2 and cancer: the good, the bad and the importance of context*. Nature Reviews Cancer, 2012. **12**(8): p. 564-571.

48. Kandoth, C., et al., *Mutational landscape and significance across 12 major cancer types*. Nature, 2013. **502**(7471): p. 333-+.
49. Mantovani, F., L. Collavin, and G. Del Sal, *Mutant p53 as a guardian of the cancer cell*. Cell Death and Differentiation, 2019. **26**(2): p. 199-212.
50. Eriksson, S.E., et al., *p53 as a hub in cellular redox regulation and therapeutic target in cancer*. Journal of Molecular Cell Biology, 2019. **11**(4): p. 330-341.
51. Zhang, C., et al., *Tumour-associated mutant p53 drives the Warburg effect*. Nature Communications, 2013. **4**.
52. Rebouissou, S. and J.C. Nault, *Advances in molecular classification and precision oncology in hepatocellular carcinoma*. Journal of Hepatology, 2020. **72**(2): p. 215-229.
53. Mari, M., et al., *Redox Control of Liver Function in Health and Disease*. Antioxidants & Redox Signaling, 2010. **12**(11): p. 1295-1331.
54. Loguercio, C. and A. Federico, *Oxidative stress in viral and alcoholic hepatitis*. Free Radic Biol Med, 2003. **34**(1): p. 1-10.
55. Cardin, R., et al., *DNA oxidative damage in leukocytes correlates with the severity of HCV-related liver disease: validation in an open population study*. J Hepatol, 2001. **34**(4): p. 587-92.
56. Browning, J.D. and J.D. Horton, *Molecular mediators of hepatic steatosis and liver injury*. J Clin Invest, 2004. **114**(2): p. 147-52.
57. Marchesini, G., et al., *Nonalcoholic fatty liver, steatohepatitis, and the metabolic syndrome*. Hepatology, 2003. **37**(4): p. 917-23.
58. Mari, M., et al., *Mitochondrial free cholesterol loading sensitizes to TNF- and Fas-mediated steatohepatitis*. Cell Metab, 2006. **4**(3): p. 185-98.
59. Fernandez-Checa, J.C., et al., *Advanced preclinical models for evaluation of drug-induced liver injury - consensus statement by the European Drug-Induced Liver Injury Network [PRO-EURO-DILI-NET]*. J Hepatol, 2021. **75**(4): p. 935-959.
60. Villanueva, A., *Hepatocellular Carcinoma*. N Engl J Med, 2019. **380**(15): p. 1450-1462.
61. Llovet, J.M., et al., *Hepatocellular carcinoma*. Nat Rev Dis Primers, 2021. **7**(1): p. 6.
62. Lluís, J.M., et al., *Dual role of mitochondrial reactive oxygen species in hypoxia signaling: Activation of nuclear factor-kappa B via c-SRC- and oxidant-dependent cell death*. Cancer Research, 2007. **67**(15): p. 7368-7377.
63. Denko, N.C., *Hypoxia, HIF1 and glucose metabolism in the solid tumour*. Nature Reviews Cancer, 2008. **8**(9): p. 705-713.
64. Trachootham, D., et al., *Selective killing of oncogenically transformed cells through a ROS-mediated mechanism by beta-phenylethyl isothiocyanate*. Cancer Cell, 2006. **10**(3): p. 241-252.
65. Montero, J., et al., *Mitochondrial cholesterol contributes to chemotherapy resistance in hepatocellular carcinoma*. Cancer Research, 2008. **68**(13): p. 5246-5256.
66. Dongiovanni, P., et al., *Iron in fatty liver and in the metabolic syndrome: a promising therapeutic target*. J Hepatol, 2011. **55**(4): p. 920-32.
67. Le Gal, K., et al., *Antioxidants can increase melanoma metastasis in mice*. Sci Transl Med, 2015. **7**(308): p. 308re8.
68. Halliwell, B., *The antioxidant paradox*. Lancet, 2000. **355**(9210): p. 1179-1180.
69. Bairati, I., et al., *Randomized trial of antioxidant vitamins to prevent acute adverse effects of radiation therapy in head and neck cancer patients*. Journal of Clinical Oncology, 2005. **23**(24): p. 5805-5813.
70. Weltmann, K.D. and T. von Woedtke, *Plasma medicine-current state of research and medical application*. Plasma Physics and Controlled Fusion, 2017. **59**(1).
71. Yun, S.H. and S.J.J. Kwok, *Light in diagnosis, therapy and surgery*. Nature Biomedical Engineering, 2017. **1**(1).

72. Longley, D.B., D.P. Harkin, and P.G. Johnston, *5-Fluorouracil: Mechanisms of action and clinical strategies*. Nature Reviews Cancer, 2003. **3**(5): p. 330-338.
73. Simunek, T., et al., *Anthracycline-induced cardiotoxicity: Overview of studies examining the roles of oxidative stress and free cellular iron*. Pharmacological Reports, 2009. **61**(1): p. 154-171.
74. Montero, A.J., et al., *Phase 2 study of neoadjuvant treatment with NOV-002 in combination with doxorubicin and cyclophosphamide followed by docetaxel in patients with HER-2 negative clinical stage II-IIIc breast cancer*. Breast Cancer Research and Treatment, 2012. **132**(1): p. 215-223.
75. Lo, M., et al., *Potential use of the anti-inflammatory drug, sulfasalazine, for targeted therapy of pancreatic cancer*. Current Oncology, 2010. **17**(3): p. 9-16.
76. Guan, J., et al., *The xc- cystine/glutamate antiporter as a potential therapeutic target for small-cell lung cancer: use of sulfasalazine*. Cancer Chemother Pharmacol, 2009. **64**(3): p. 463-72.
77. Marullo, R., et al., *Cisplatin induces a mitochondrial-ROS response that contributes to cytotoxicity depending on mitochondrial redox status and bioenergetic functions*. PLoS One, 2013. **8**(11): p. e81162.
78. Zhang, Q., et al., *Involvement of reactive oxygen species in 2-methoxyestradiol-induced apoptosis in human neuroblastoma cells*. Cancer Letters, 2011. **313**(2): p. 201-210.
79. Denmeade, S.R., et al., *Engineering a Prostate-Specific Membrane Antigen-Activated Tumor Endothelial Cell Prodrug for Cancer Therapy (vol 4, 143er4, 2012)*. Science Translational Medicine, 2012. **4**(143).
80. Zhu, J.X., et al., *Using cyclooxygenase-2 inhibitors as molecular platforms to develop a new class of apoptosis-inducing agents*. Jnci-Journal of the National Cancer Institute, 2002. **94**(23): p. 1745-1757.
81. Fribley, A., Q.H. Zeng, and C.Y. Wang, *Proteasome inhibitor PS-341 induces a apoptosis through induction of endoplasmic reticulum stress-reactive oxygen species in head and neck squamous cell carcinoma cells*. Molecular and Cellular Biology, 2004. **24**(22): p. 9695-9704.
82. Miller, W.H., et al., *Mechanisms of action of arsenic trioxide*. Cancer Research, 2002. **62**(14): p. 3893-3903.
83. Yoshida, T., et al., *Mitochondrial dysfunction, a probable cause of persistent oxidative stress after exposure to ionizing radiation*. Free Radical Research, 2012. **46**(2): p. 147-153.
84. Keevil, S.F., *Physics and medicine: a historical perspective*. Lancet, 2012. **379**(9825): p. 1517-24.
85. Melzer, A., et al., *Physics and Medicine 3 The importance of physics to progress in medical treatment*. Lancet, 2012. **379**(9825): p. 1534-1543.
86. Kong, M.G., et al., *Plasma medicine: an introductory review*. New Journal of Physics, 2009. **11**.
87. Langmuir, I., *Oscillations in Ionized Gases*. Proc Natl Acad Sci U S A, 1928. **14**(8): p. 627-37.
88. Lu, X., et al., *Reactive species in non-equilibrium atmospheric-pressure plasmas: Generation, transport, and biological effects*. Physics Reports-Review Section of Physics Letters, 2016. **630**: p. 1-84.
89. Scholtz, V., et al., *Nonthermal plasma - A tool for decontamination and disinfection*. Biotechnology Advances, 2015. **33**(6): p. 1108-1119.
90. De Geyter, N. and R. Morent, *Nonthermal Plasma Sterilization of Living and Nonliving Surfaces*. Annual Review of Biomedical Engineering, Vol 14, 2012. **14**: p. 255-274.
91. Laroussi, M., *Low-Temperature Plasmas for Medicine?* Ieee Transactions on Plasma Science, 2009. **37**(6): p. 714-725.

92. Laroussi, M., et al., *Low-Temperature Plasma for Biology, Hygiene, and Medicine: Perspective and Roadmap*. Ieee Transactions on Radiation and Plasma Medical Sciences, 2022. **6**(2): p. 127-157.
93. Lieberman, M.A. and A.J. Lichtenberg, *Principles of Plasma Discharges and Materials Processing, 2nd Edition*. Principles of Plasma Discharges and Materials Processing, 2nd Edition, 2005: p. 1-757.
94. Fridman, G., et al., *Blood coagulation and living tissue sterilization by floating-electrode dielectric barrier discharge in air*. Plasma Chemistry and Plasma Processing, 2006. **26**(4): p. 425-442.
95. Kalghatgi, S.U., et al., *Mechanism of blood coagulation by nonthermal atmospheric pressure dielectric barrier discharge plasma*. Ieee Transactions on Plasma Science, 2007. **35**(5): p. 1559-1566.
96. Stoffels, E., et al., *Plasma needle: a non-destructive atmospheric plasma source for fine surface treatment of (bio)materials*. Plasma Sources Science & Technology, 2002. **11**(4): p. 383-388.
97. Winter, J., R. Brandenburg, and K.D. Weltmann, *Atmospheric pressure plasma jets: an overview of devices and new directions*. Plasma Sources Science & Technology, 2015. **24**(6).
98. Sladek, R.E.J. and E. Stoffels, *Deactivation of Escherichia coli by the plasma needle*. Journal of Physics D-Applied Physics, 2005. **38**(11): p. 1716-1721.
99. Tanaka, H., et al., *State of the art in medical applications using non-thermal atmospheric pressure plasma*. Reviews of Modern Plasma Physics, 2017. **1**(1).
100. Reuter, S., T. von Woedtke, and K.D. Weltmann, *The kINPen-a review on physics and chemistry of the atmospheric pressure plasma jet and its applications*. Journal of Physics D-Applied Physics, 2018. **51**(23).
101. von Woedtke, T., et al., *Plasmas for medicine*. Physics Reports, 2013. **530**(4): p. 291-320.
102. Gilmore, B.F., et al., *Cold Plasmas for Biofilm Control: Opportunities and Challenges*. Trends in Biotechnology, 2018. **36**(6): p. 627-638.
103. Lunov, O., et al., *Cell death induced by ozone and various non-thermal plasmas: therapeutic perspectives and limitations*. Scientific Reports, 2014. **4**.
104. Lunov, O., et al., *Chemically different non-thermal plasmas target distinct cell death pathways*. Scientific Reports, 2017. **7**.
105. Privat-Maldonado, A., et al., *ROS from Physical Plasmas: Redox Chemistry for Biomedical Therapy*. Oxidative Medicine and Cellular Longevity, 2019. **2019**.
106. Moreau, S., et al., *Using the flowing afterglow of a plasma to inactivate Bacillus subtilis spores: Influence of the operating conditions*. Journal of Applied Physics, 2000. **88**(2): p. 1166-1174.
107. Sinha, R.P. and D.P. Hader, *UV-induced DNA damage and repair: a review*. Photochemical & Photobiological Sciences, 2002. **1**(4): p. 225-236.
108. Lunov, O., et al., *Non-thermal plasma kills bacteria: Scanning electron microscopy observations*. Applied Physics Letters, 2015. **106**(5).
109. Kostov, K.G., et al., *Bacterial sterilization by a dielectric barrier discharge (DBD) in air*. Surface & Coatings Technology, 2010. **204**(18-19): p. 2954-2959.
110. Park, J.Y., et al., *Plasma-Functionalized Solution: A Potent Antimicrobial Agent for Biomedical Applications from Antibacterial Therapeutics to Biomaterial Surface Engineering*. Acs Applied Materials & Interfaces, 2017. **9**(50): p. 43470-43477.
111. Laroussi, M. and F. Leipold, *Evaluation of the roles of reactive species, heat, and UV radiation in the inactivation of bacterial cells by air plasmas at atmospheric pressure*. International Journal of Mass Spectrometry, 2004. **233**(1-3): p. 81-86.

112. Lee, K.Y., et al., *Sterilization of Escherichia coli and MRSA using microwave-induced argon plasma at atmospheric pressure*. Surface & Coatings Technology, 2005. **193**(1-3): p. 35-38.
113. Laroussi, M., *Nonthermal decontamination of biological media by atmospheric-pressure plasmas: Review, analysis, and prospects*. IEEE Transactions on Plasma Science, 2002. **30**(4): p. 1409-1415.
114. Lunov, O., et al., *The interplay between biological and physical scenarios of bacterial death induced by non-thermal plasma*. Biomaterials, 2016. **82**: p. 71-83.
115. Fridman, G., et al., *Comparison of direct and indirect effects of non-thermal atmospheric-pressure plasma on bacteria*. Plasma Processes and Polymers, 2007. **4**(4): p. 370-375.
116. Kalghatgi, S., et al., *Effects of Non-Thermal Plasma on Mammalian Cells*. Plos One, 2011. **6**(1).
117. Ahn, H.J., et al., *Targeting Cancer Cells with Reactive Oxygen and Nitrogen Species Generated by Atmospheric-Pressure Air Plasma*. Plos One, 2014. **9**(1).
118. Partecke, L.I., et al., *Tissue Tolerable Plasma (TTP) induces apoptosis in pancreatic cancer cells in vitro and in vivo*. BMC Cancer, 2012. **12**.
119. Schmidt, A. and S. Bekeschus, *Redox for Repair: Cold Physical Plasmas and Nrf2 Signaling Promoting Wound Healing*. Antioxidants, 2018. **7**(10).
120. Smolková, B., et al., *Critical Analysis of Non-Thermal Plasma-Driven Modulation of Immune Cells from Clinical Perspective*. International Journal of Molecular Sciences, 2020. **21**(17).
121. Al-Abduly, A. and P. Christensen, *An in situ and downstream study of non-thermal plasma chemistry in an air fed dielectric barrier discharge (DBD)*. Plasma Sources Science & Technology, 2015. **24**(6).
122. Jablonowski, H. and T. von Woedtke, *Research on plasma medicine-relevant plasma-liquid interaction: What happened in the past five years?* Clinical Plasma Medicine, 2015. **3**(2): p. 42-52.
123. Smolková, B., et al., *A Critical Review on Selected External Physical Cues and Modulation of Cell Behavior: Magnetic Nanoparticles, Non-thermal Plasma and Lasers*. Journal of Functional Biomaterials, 2018. **10**(1).
124. Holmstrom, K.M. and T. Finkel, *Cellular mechanisms and physiological consequences of redox-dependent signalling*. Nature Reviews Molecular Cell Biology, 2014. **15**(6): p. 411-421.
125. D'Autreaux, B. and M.B. Toledano, *ROS as signalling molecules: mechanisms that generate specificity in ROS homeostasis*. Nature Reviews Molecular Cell Biology, 2007. **8**(10): p. 813-824.
126. Nathan, C. and A. Cunningham-Bussell, *Beyond oxidative stress: an immunologist's guide to reactive oxygen species*. Nature Reviews Immunology, 2013. **13**(5): p. 349-361.
127. Sthijns, M.M.J.P.E., et al., *Time in Redox Adaptation Processes: From Evolution to Hormesis*. International Journal of Molecular Sciences, 2016. **17**(10).
128. Dezest, M., et al., *Mechanistic insights into the impact of Cold Atmospheric Pressure Plasma on human epithelial cell lines*. Scientific Reports, 2017. **7**.
129. Schmidt, A., et al., *Nrf2 signaling and inflammation are key events in physical plasma-spurred wound healing*. Theranostics, 2019. **9**(4): p. 1066-1084.
130. Lu, H., et al., *Bacterial inactivation by high-voltage atmospheric cold plasma: influence of process parameters and effects on cell leakage and DNA*. Journal of Applied Microbiology, 2014. **116**(4): p. 784-794.
131. Kim, S.J. and T.H. Chung, *Cold atmospheric plasma jet-generated RONS and their selective effects on normal and carcinoma cells*. Scientific Reports, 2016. **6**.

132. Liedtke, K.R., et al., *Cold Physical Plasma Selectively Elicits Apoptosis in Murine Pancreatic Cancer Cells In Vitro and In Ovo*. *Anticancer Research*, 2018. **38**(10): p. 5655-5663.
133. Van der Paal, J., et al., *Hampering Effect of Cholesterol on the Permeation of Reactive Oxygen Species through Phospholipids Bilayer: Possible Explanation for Plasma Cancer Selectivity*. *Scientific Reports*, 2017. **7**.
134. Yang, H., et al., *Effects of atmospheric pressure cold plasma on human hepatocarcinoma cell and its 5-fluorouracil resistant cell line*. *Physics of Plasmas*, 2015. **22**(12).
135. Kang, S.U., et al., *Nonthermal plasma induces head and neck cancer cell death: the potential involvement of mitogen-activated protein kinase-dependent mitochondrial reactive oxygen species*. *Cell Death & Disease*, 2014. **5**(2): p. e1056-e1056.
136. Kaushik, N., et al., *Non-thermal plasma with 2-deoxy-D-glucose synergistically induces cell death by targeting glycolysis in blood cancer cells*. *Sci Rep*, 2015. **5**: p. 8726.
137. Bekeschus, S., et al., *Tumor cell metabolism correlates with resistance to gas plasma treatment: The evaluation of three dogmas*. *Free Radic Biol Med*, 2021. **167**: p. 12-28.
138. Van Boxem, W., et al., *Anti-cancer capacity of plasma-treated PBS: effect of chemical composition on cancer cell cytotoxicity*. *Sci Rep*, 2017. **7**(1): p. 16478.
139. Ma, Y., et al., *Non-thermal atmospheric pressure plasma preferentially induces apoptosis in p53-mutated cancer cells by activating ROS stress-response pathways*. *PLoS One*, 2014. **9**(4): p. e91947.
140. Azzariti, A., et al., *Plasma-activated medium triggers cell death and the presentation of immune activating danger signals in melanoma and pancreatic cancer cells*. *Sci Rep*, 2019. **9**(1): p. 4099.
141. Liu, Y., et al., *Selective effects of non-thermal atmospheric plasma on triple-negative breast normal and carcinoma cells through different cell signaling pathways*. *Sci Rep*, 2017. **7**(1): p. 7980.
142. Lin, A., et al., *Nanosecond-Pulsed DBD Plasma-Generated Reactive Oxygen Species Trigger Immunogenic Cell Death in A549 Lung Carcinoma Cells through Intracellular Oxidative Stress*. *Int J Mol Sci*, 2017. **18**(5).
143. Wolff, C.M., et al., *Combination Treatment with Cold Physical Plasma and Pulsed Electric Fields Augments ROS Production and Cytotoxicity in Lymphoma*. *Cancers (Basel)*, 2020. **12**(4).
144. Liedtke, K.R., et al., *Non-thermal plasma-treated solution demonstrates antitumor activity against pancreatic cancer cells in vitro and in vivo*. *Sci Rep*, 2017. **7**(1): p. 8319.
145. Mizuno, K., et al., *Anti-tumor immune response induced by nanosecond pulsed streamer discharge in mice*. *Journal of Physics D-Applied Physics*, 2017. **50**(12).
146. Lin, A., et al., *Non-Thermal Plasma as a Unique Delivery System of Short-Lived Reactive Oxygen and Nitrogen Species for Immunogenic Cell Death in Melanoma Cells*. *Adv Sci (Weinh)*, 2019. **6**(6): p. 1802062.
147. Bekeschus, S., et al., *Medical Gas Plasma Jet Technology Targets Murine Melanoma in an Immunogenic Fashion*. *Adv Sci (Weinh)*, 2020. **7**(10): p. 1903438.
148. Yan, D., et al., *Toward understanding the selective anticancer capacity of cold atmospheric plasma--a model based on aquaporins (Review)*. *Biointerphases*, 2015. **10**(4): p. 040801.
149. Keidar, M., *Plasma for cancer treatment*. *Plasma Sources Science and Technology*, 2015. **24**(3).

150. Bauer, G. and D.B. Graves, *Mechanisms of Selective Antitumor Action of Cold Atmospheric Plasma-Derived Reactive Oxygen and Nitrogen Species*. Plasma Processes and Polymers, 2016. **13**(12): p. 1157-1178.
151. Papadopoulos, M.C. and S. Saadoun, *Key roles of aquaporins in tumor biology*. Biochim Biophys Acta, 2015. **1848**(10 Pt B): p. 2576-83.
152. Glorieux, C., et al., *Regulation of catalase expression in healthy and cancerous cells*. Free Radic Biol Med, 2015. **87**: p. 84-97.
153. Frtus, A., et al., *Analyzing the mechanisms of iron oxide nanoparticles interactions with cells: A road from failure to success in clinical applications*. J Control Release, 2020. **328**: p. 59-77.
154. Ehrenstein, M.R. and C. Mauri, *If the treatment works, do we need to know why?: the promise of immunotherapy for experimental medicine*. Journal of Experimental Medicine, 2007. **204**(10): p. 2249-2252.
155. Dai, X., et al., *Cold Atmospheric Plasma: A Promising Controller of Cancer Cell States*. Cancers (Basel), 2020. **12**(11).
156. Bekeschus, S., et al., *The plasma jet kINPen – A powerful tool for wound healing*. Clinical Plasma Medicine, 2016. **4**(1): p. 19-28.
157. Isbary, G., et al., *A first prospective randomized controlled trial to decrease bacterial load using cold atmospheric argon plasma on chronic wounds in patients*. British Journal of Dermatology, 2010. **163**(1): p. 78-82.
158. Daeschlein, G., et al., *Skin and wound decontamination of multidrug-resistant bacteria by cold atmospheric plasma coagulation*. JDDG: Journal der Deutschen Dermatologischen Gesellschaft, 2015. **13**(2): p. 143-149.
159. Freund, E. and S. Bekeschus, *Gas Plasma-Oxidized Liquids for Cancer Treatment: Preclinical Relevance, Immuno-Oncology, and Clinical Obstacles*. IEEE Transactions on Radiation and Plasma Medical Sciences, 2021. **5**(6): p. 761-774.
160. Van Loenhout, J., et al., *Cold Atmospheric Plasma-Treated PBS Eliminates Immunosuppressive Pancreatic Stellate Cells and Induces Immunogenic Cell Death of Pancreatic Cancer Cells*. Cancers (Basel), 2019. **11**(10).
161. *Correction: Consensus guidelines for the definition, detection and interpretation of immunogenic cell death*. J Immunother Cancer, 2020. **8**(1).
162. Hasse, S., et al., *Plasma Treatment Limits Human Melanoma Spheroid Growth and Metastasis Independent of the Ambient Gas Composition*. Cancers (Basel), 2020. **12**(9).
163. Koritzer, J., et al., *Restoration of sensitivity in chemo-resistant glioma cells by cold atmospheric plasma*. PLoS One, 2013. **8**(5): p. e64498.
164. Rasouli, M., et al., *Combining Nanotechnology and Gas Plasma as an Emerging Platform for Cancer Therapy: Mechanism and Therapeutic Implication*. Oxidative Medicine and Cellular Longevity, 2021. **2021**: p. 1-20.
165. Tanaka, H., et al., *Plasma-Treated Solutions (PTS) in Cancer Therapy*. Cancers (Basel), 2021. **13**(7).
166. Shi, J., et al., *Cancer nanomedicine: progress, challenges and opportunities*. Nat Rev Cancer, 2017. **17**(1): p. 20-37.
167. Chung, H., et al., *The nuts and bolts of low-level laser (light) therapy*. Ann Biomed Eng, 2012. **40**(2): p. 516-33.
168. Zein, R., W. Selting, and M.R. Hamblin, *Review of light parameters and photobiomodulation efficacy: dive into complexity*. J Biomed Opt, 2018. **23**(12): p. 1-17.
169. Lynnyk, A., et al., *Manipulating the mitochondria activity in human hepatic cell line Huh7 by low-power laser irradiation*. Biomed Opt Express, 2018. **9**(3): p. 1283-1300.
170. Waldchen, S., et al., *Light-induced cell damage in live-cell super-resolution microscopy*. Sci Rep, 2015. **5**: p. 15348.

171. Soares, D.M., et al., *Effects of laser therapy on the proliferation of human periodontal ligament stem cells*. *Lasers in Medical Science*, 2013. **30**(3): p. 1171-1174.
172. Yang, D., et al., *Effects of light-emitting diode irradiation on the osteogenesis of human umbilical cord mesenchymal stem cells in vitro*. *Sci Rep*, 2016. **6**: p. 37370.
173. Ong, W.K., et al., *The activation of directional stem cell motility by green light-emitting diode irradiation*. *Biomaterials*, 2013. **34**(8): p. 1911-20.
174. Arany, P.R., et al., *Photoactivation of endogenous latent transforming growth factor-beta1 directs dental stem cell differentiation for regeneration*. *Sci Transl Med*, 2014. **6**(238): p. 238ra69.
175. Khan, I., E. Tang, and P. Arany, *Molecular pathway of near-infrared laser phototoxicity involves ATF-4 orchestrated ER stress*. *Sci Rep*, 2015. **5**: p. 10581.
176. Chen, A.C., et al., *Low-level laser therapy activates NF-kB via generation of reactive oxygen species in mouse embryonic fibroblasts*. *PLoS One*, 2011. **6**(7): p. e22453.
177. Rajendran, N.K., N.N. Hourelid, and H. Abrahamse, *Photobiomodulation reduces oxidative stress in diabetic wounded fibroblast cells by inhibiting the FOXO1 signaling pathway*. *Journal of Cell Communication and Signaling*, 2020. **15**(2): p. 195-206.
178. Liang, W.Z., et al., *Selective cytotoxic effects of low-power laser irradiation on human oral cancer cells*. *Lasers Surg Med*, 2015. **47**(9): p. 756-64.
179. Wang, Y., et al., *Photobiomodulation (blue and green light) encourages osteoblastic-differentiation of human adipose-derived stem cells: role of intracellular calcium and light-gated ion channels*. *Sci Rep*, 2016. **6**: p. 33719.
180. Wu, S., et al., *High fluence low-power laser irradiation induces mitochondrial permeability transition mediated by reactive oxygen species*. *J Cell Physiol*, 2009. **218**(3): p. 603-11.
181. de Freitas, L.F. and M.R. Hamblin, *Proposed Mechanisms of Photobiomodulation or Low-Level Light Therapy*. *IEEE J Sel Top Quantum Electron*, 2016. **22**(3).
182. Sutherland, J.C., *Biological effects of polychromatic light*. *Photochem Photobiol*, 2002. **76**(2): p. 164-70.
183. Karu, T.I., et al., *Absorption measurements of a cell monolayer relevant to phototherapy: reduction of cytochrome c oxidase under near IR radiation*. *J Photochem Photobiol B*, 2005. **81**(2): p. 98-106.
184. Mason, M.G., P. Nicholls, and C.E. Cooper, *Re-evaluation of the near infrared spectra of mitochondrial cytochrome c oxidase: Implications for non invasive in vivo monitoring of tissues*. *Biochimica Et Biophysica Acta-Bioenergetics*, 2014. **1837**(11): p. 1882-1891.
185. Huttemann, M., et al., *Regulation of mitochondrial respiration and apoptosis through cell signaling: cytochrome c oxidase and cytochrome c in ischemia/reperfusion injury and inflammation*. *Biochim Biophys Acta*, 2012. **1817**(4): p. 598-609.
186. Karu, T.I., *Mitochondrial signaling in mammalian cells activated by red and near-IR radiation*. *Photochem Photobiol*, 2008. **84**(5): p. 1091-9.
187. Wu, S.A., et al., *Cancer Phototherapy via Selective Photoinactivation of Respiratory Chain Oxidase to Trigger a Fatal Superoxide Anion Burst*. *Antioxidants & Redox Signaling*, 2014. **20**(5): p. 733-746.
188. Hawkins, D. and H. Abrahamse, *Biological effects of helium-neon laser irradiation on normal and wounded human skin fibroblasts*. *Photomed Laser Surg*, 2005. **23**(3): p. 251-9.
189. Kokol, R., et al., *685-nm low level laser therapy of venous leg ulcers. No improvement of wound healing. Randomised, placebo-controlled, double-blind study*. *Hautarzt*, 2005. **56**(6): p. 570-575.
190. Anneroth, G., et al., *The effect of low-energy infra-red laser radiation on wound healing in rats*. *Br J Oral Maxillofac Surg*, 1988. **26**(1): p. 12-7.

191. Youan, B.B., *Chronopharmaceutical drug delivery systems: Hurdles, hype or hope?* Adv Drug Deliv Rev, 2010. **62**(9-10): p. 898-903.
192. Jayakumar, M.K.G., N.M. Idris, and Y. Zhang, *Remote activation of biomolecules in deep tissues using near-infrared-to-UV upconversion nanotransducers*. Proceedings of the National Academy of Sciences of the United States of America, 2012. **109**(22): p. 8483-8488.
193. Masic, I., M. Miokovic, and B. Muhamedagic, *Evidence based medicine - new approaches and challenges*. Acta Inform Med, 2008. **16**(4): p. 219-25.
194. *Mechanism matters*. Nat Med, 2010. **16**(4): p. 347.
195. Masters, J.R., *HeLa cells 50 years on: the good, the bad and the ugly*. Nat Rev Cancer, 2002. **2**(4): p. 315-9.
196. Marx, V., *Cell-line authentication demystified*. Nat Methods, 2014. **11**(5): p. 483-8.
197. Drexler, H.G. and C.C. Uphoff, *Mycoplasma contamination of cell cultures: Incidence, sources, effects, detection, elimination, prevention*. Cytotechnology, 2002. **39**(2): p. 75-90.
198. Lunova, M., et al., *Expression of Interferons Lambda 3 and 4 Induces Identical Response in Human Liver Cell Lines Depending Exclusively on Canonical Signaling*. Int J Mol Sci, 2021. **22**(5).
199. Frtus, A., et al., *Hepatic Tumor Cell Morphology Plasticity under Physical Constraints in 3D Cultures Driven by YAP-mTOR Axis*. Pharmaceuticals, 2020. **13**(12).
200. Smolkova, B., et al., *Protein Corona Inhibits Endosomal Escape of Functionalized DNA Nanostructures in Living Cells*. Acs Applied Materials & Interfaces, 2021. **13**(39): p. 46375-46390.
201. Dell, R.B., S. Holleran, and R. Ramakrishnan, *Sample size determination (vol 43, pg 207, 2002)*. Ilar Journal, 2003. **44**(3): p. 239-239.
202. Lunov, O., et al., *Towards the understanding of non-thermal air plasma action: effects on bacteria and fibroblasts*. Rsc Advances, 2016. **6**(30): p. 25286-25292.
203. Zhang, X.H., et al., *Ablation of liver cancer cells in vitro by a plasma needle*. Applied Physics Letters, 2008. **93**(2).
204. Smolkova, B., et al., *Non-Thermal Plasma, as a New Physicochemical Source, to Induce Redox Imbalance and Subsequent Cell Death in Liver Cancer Cell Lines*. Cell Physiol Biochem, 2019. **52**(1): p. 119-140.
205. Birnboim, H.C. and M. Kanabuskaminska, *The Production of DNA Strand Breaks in Human-Leukocytes by Superoxide Anion May Involve a Metabolic Process*. Proceedings of the National Academy of Sciences of the United States of America, 1985. **82**(20): p. 6820-6824.
206. Kroemer, G. and J.C. Reed, *Mitochondrial control of cell death*. Nature Medicine, 2000. **6**(5): p. 513-519.
207. Nguyen, N.H., et al., *Anti-cancer efficacy of nonthermal plasma dissolved in a liquid, liquid plasma in heterogeneous cancer cells*. Scientific Reports, 2016. **6**.
208. Cagatay, T. and M. Ozturk, *p53 mutation as a source of aberrant beta-catenin accumulation in cancer cells*. Oncogene, 2002. **21**(52): p. 7971-7980.
209. Yoshida, T., et al., *SOCS1 is a suppressor of liver fibrosis and hepatitis-induced carcinogenesis*. Journal of Experimental Medicine, 2004. **199**(12): p. 1701-1707.
210. Lunova, M., et al., *Light-induced modulation of the mitochondrial respiratory chain activity: possibilities and limitations*. Cell Mol Life Sci, 2020. **77**(14): p. 2815-2838.
211. Hayashi, S., *Resolution doubling using confocal microscopy via analogy with structured illumination microscopy*. Japanese Journal of Applied Physics, 2016. **55**(8).
212. Hayashi, S. and Y. Okada, *Ultrafast superresolution fluorescence imaging with spinning disk confocal microscope optics*. Mol Biol Cell, 2015. **26**(9): p. 1743-51.

213. Boya, P., et al., *Endoplasmic reticulum stress-induced cell death requires mitochondrial membrane permeabilization*. *Cell Death and Differentiation*, 2002. **9**(4): p. 465-467.
214. Boya, P., et al., *Lysosomal membrane permeabilization induces cell death in a mitochondrion-dependent fashion*. *Journal of Experimental Medicine*, 2003. **197**(10): p. 1323-1334.
215. Petronilli, V., et al., *Transient and long-lasting openings of the mitochondrial permeability transition pore can be monitored directly in intact cells by changes in mitochondrial calcein fluorescence*. *Biophysical Journal*, 1999. **76**(2): p. 725-734.
216. Liang, H.L., et al., *SOD1 and MitoTEMPO partially prevent mitochondrial permeability transition pore opening, necrosis, and mitochondrial apoptosis after ATP depletion recovery*. *Free Radical Biology and Medicine*, 2010. **49**(10): p. 1550-1560.
217. Wang, N.S., et al., *Transient expression of wild-type or mitochondrially targeted Bcl-2 induces apoptosis, whereas transient expression of endoplasmic reticulum-targeted Bcl-2 is protective against Bax-induced cell death*. *Journal of Biological Chemistry*, 2001. **276**(47): p. 44117-44128.
218. Kale, J., E.J. Osterlund, and D.W. Andrews, *BCL-2 family proteins: changing partners in the dance towards death*. *Cell Death Differ*, 2018. **25**(1): p. 65-80.

LIST OF FIGURES

Figure 1	Schematic illustration of exogeneous and endogenous sources of ROS.....	3
Figure 2	Schematic illustration of electron transport chain of mitochondria....	5
Figure 3	Comparison of the redox status in normal and cancer cells.....	8
Figure 4	Different stages of liver pathology.....	11
Figure 5	Four states of matter.....	14
Figure 6	Schematic illustration of the potential mechanism of non-thermal plasma in cancer cells.....	19
Figure 7	Scheme of the potential mechanisms.....	25
Figure 8	Major challenges in the field of plasma medicine and laser therapy.	28
Figure 9	Graphs of publication activity plasma medicine.....	30
Figure 10	Graphs of publication activity photobiomodulation.....	31
Figure 11	Schematic illustration and the physicochemical parameters of plasma device. Reprinted from [103].....	38
Figure 12	FT-IR spectra of air, helium NTPs and ozone. Reprinted from [104].....	38
Figure 13	Representation of SRIM simulations. Reprinted from [202].....	40
Figure 14	Plasma treatment induced cytotoxic effects in HepG2 and Huh7 cell lines. Reprinted from Appendix I	41
Figure 15	Plasma treatment reduced tumorigenicity of Huh7. Reprinted from Appendix I	41
Figure 16	Accumulation of ROS and Superoxide in HepG2 and Huh7 post NTP treatment. Reprinted from Appendix I	42
Figure 17	N-acetyl cysteine attenuated the cytotoxic effects of NTP. Reprinted from Appendix I	43
Figure 18	NTP treatment induced changes in mitochondrial membrane potential and mitochondrial dynamics. Reprinted from Appendix I	44
Figure 19	Increased production of mitochondria- mediated ROS post NTP treatment. Reprinted from Appendix I	45
Figure 20	Quantification of the Annexin V and PI in Huh7 and HepG2 cells post NTP treatment. Reprinted from Appendix I	46
Figure 21	Analysis of Caspase 3/7 in HepG2 and Huh7 cells treated with NTP. Reprinted from Appendix I	46
Figure 22	NTP treatment induced apoptotic cell death in Alexander cells. Reprinted from Appendix I	47
Figure 23	Changes in p53, Bcl-2 and LC-3 protein signalling in HepG2 and Huh7 cells post plasma treatment. Reprinted from Appendix I	48

Figure 24	Changes in mTOR and STAT-1 protein signalling in HepG2 and Huh7 cells post plasma treatment. Reprinted from Appendix I49
Figure 25	NTP treatment led to different response in cells. Reprinted from Appendix I49-50
Figure 26	Schematic illustration of the molecular mechanisms in Huh7 and HepG2 cells post NTP treatment. Adapted from figure 11C from Appendix I50
Figure 27	Schematic illustration of the system. Reprinted from Appendix II ..51
Figure 28	Characterisation of the laser. Reprinted from Appendix II52
Figure 29	HFLP laser irradiation led to cell death execution in Alexander and Huh7 cells. Reprinted from Appendix II53
Figure 30	HFLP laser irradiation induced the changes in mitochondrial dynamics and mitochondrial membrane potential. Reprinted from Appendix II54
Figure 31	Quantification of mitochondrial membrane potential and dynamics in cells post HFLP laser irradiation. Reprinted from Appendix II55
Figure 32	Kinetic analysis of mitochondria of Alexander and Huh7 cells post HFLP laser irradiation. Reprinted from Appendix II56
Figure 33	Kinetic analysis of mitochondrial membrane potential and ROS of Alexander and Huh7 cells post HFLP laser irradiation. Reprinted from Appendix II57
Figure 34	Analysis of mPTP opening post HFLP laser irradiation. Reprinted from Appendix II58-59
Figure 35	Schematic illustration of the suggested model of the action of blue and red laser irradiation. Adapted from Figure 6D of Appendix II60
Figure 36	Analysis of the cellular response to blue and red laser irradiation in the presence of COX inhibitor. Reprinted from Appendix II61
Figure 37	Analysis of cellular response to blue and red laser irradiation in the presence of COX activator. Reprinted from Appendix II61
Figure 38	Comparison of the different expression of Bcl-2 and p53 proteins in cells. Reprinted from Appendix II62
Figure 39	Bcl-2 inhibition restored the resistance of HepG2 cells towards laser irradiation. Reprinted from Appendix II63
Figure 40	Bcl-2 overexpression inhibited the cytotoxic effects of blue and red laser irradiation in Alexander and Huh7 cells. Reprinted from Appendix II64
Figure 41	Translocation of Bcl-2 protein to mitochondria inhibited the cell death mediated by red and blue laser irradiation in Alexander and Huh7 cells. Reprinted from Appendix II65

Figure 42 Schematic illustration of the molecular mechanisms in cells post laser irradiation. Adapted from Figure 8D from [Appendix II](#).....65

LIST OF TABLES

Table 1	Major types of reactive oxygen and nitrogen species involved in the biological systems signalling
Table 2	Enzymatic and non-enzymatic antioxidants involved in the ROS regulation
Table 3	Selected therapeutic approaches used for cancer treatment modulating the redox system
Table 4	Summary of NTP interaction with cancer models in vitro and in vivo
Table 5	Summary of interactions of low power light on different biological models in vivo and in vitro
Table 6	Physicochemical parameters of the low voltage and high voltage plasma devices

LIST OF ABBREVIATIONS

·OH	hydroxyl radical
¹ O ₂	singlet molecular oxygen
5-FU	5-fluorouracil
APAP1	apoptotic peptidase activating factor 1
APPJ	atmospheric pressure plasma jet
AREs	antioxidant responsive elements
ATCC	American-Type Culture Collection
ATP	adenosine triphosphate
BCA	bicinchoninic acid
Bcl-2	B-cell lymphoma 2
BZF	bezafibrate
cAMP	cyclin adenosine monophosphate
CO	carbon monoxide
Co ²⁺	cobalt ions
COX	cytochrome c oxidase
CT	computed tomography
CypD	cyclophilin D
Cys	cysteine
DAMPs	damage- associated molecular patters
DBD	dielectric barrier discharge
DUOX	dual- oxidases
EBM	evidence-based medicine
EMEM	Eagle's minimal essential medium
ER	electromagnetic radiation
ER	endoplasmic reticulum
ETC	electron transport chain
FADH ₂	flavin adenine dinucleotide
FBS	fetal bovine serum
FDA	Food and drug administration
Fig.	figure
FITC	fluorescein isothiocyanate
FT-IR	Fourier transform infrared spectroscopy
GFP	green fluorescent protein
GPx	glutathione peroxidase
H ₂ O ₂	hydrogen peroxide
HBV	hepatitis B
HCC	hepatocellular carcinoma
HCV	hepatitis C
HFLP	high-fluence low power
His	histidine
HO	heme oxygenase
HOBr	hypobromous acid
HOCl	hypochlorous acid
HV	high voltage
ICD	immunogenic cell death
IMM	inner mitochondrial membrane
JCRB	Japanese Collection of Research Bioresources
KCN	potassium cyanide
kV	kiloVolt
LASER	light amplification by the stimulated emission of radiation
LED	light-emitting diode
LLLT	low-level laser (light) therapy
LV	low voltage
Met	methionine

MOMP	mitochondrial outer membrane permeabilization
MPTP	mitochondria permeability transition pore
MRI	magnetic resonance imaging
mutp53	mutant p53
N.A.	not assessed
NADPH	nicotinamide adenine dinucleotide phosphate
NAFLD	non-alcoholic fatty liver disease
NASH n	on-alcoholic steatohepatitis
NIH	National Institute of Health
NIR	near infra-red light
NO	nitric oxide
NOS	nitric oxide synthase
Nox	NADPH oxidase
NTP	non-thermal plasma
O ₂ ⁻	superoxide anion radical
O ₃	ozone
OES	optical emission spectroscopy
OMM	outer mitochondrial membrane
ONOO ⁻	peroxynitrite
PBM	photobiomodulation
PBS	phosphate buffered saline
PDT	photodynamic therapy
PI	propidium iodide
Prx	peroxiredoxins
PVDF	polyvinylidene fluoride
RIPA	radioimmunoprecipitation assay buffer
RNS	reactive nitrogen species
ROO [·]	peroxyl radical
ROS	reactive oxygen species
RT	room temperature
SDS-PAGE	sodium dodecyl sulphate- polyacrylamide gel electrophoresis
SEM	standard error mean
SOD	superoxide dismutase
SRIM	Stopping and range of ions in matter
TCA	tricarboxylic acid cycle
TFS	Thermo Fisher Scientific
Trp	tryptophan
TRP	transient receptor potential
Trx	thioredoxin
Tyr	tyrosine
ΔmΦ	mitochondrial membrane potential

LIST OF PUBLICATIONS:

The list consists of 17 publications and 3 submitted manuscripts currently under revision process. Total number of citations (22nd of March 2022) is 162, H- index 8 according Scopus database, and 132, H-index 8 according Web of Science (WoS).

- **Smolková B.**, MacCulloch T., Rockwood T. F., Liu M., Henry S. J. W., Frtús A., Uzhytchak M., Lunova, M. Hof, P. Jurkiewicz, A. Dejneka, N. Stephanopoulos, and O. Lunov, *ACS Appl. Mater. Interfaces* 2021, 13, 39, 46375–46390. IF 9.229
- Lunova M., Kubovciak J., **Smolková B.**, Uzhytchak M., Michalova K., Dejneka A., Strnad P., Lunov O., Jirsa M. *Int. J. Mol. Sci.* 2021, 22(5), 2560. IF 5.924
- Frtús A., **Smolková B.**, Uzhytchak M., Lunova M., Jirsa M., Hof M., Jurkiewicz P., Lozinsky V.I., Wolfová L., Petrenko Y., Kubinová Š. Dejneka A., Lunov O. *Pharmaceuticals* 2020, 13(12), 430. IF 5.863
- **Smolková, B.** Frtús, A., Uzhytchak, M., Lunova, M., Kubinová, Š., Dejneka, A., Lunov, O. *Int. J. Mol. Sci.* 2020, 21, 6226. IF 5.924
- Frtús A, **Smolková B.** Uzhytchak M, Lunova M, Jirsa M, Kubinová Š, Dejneka A, Lunov O. *J. Control. Release* 2020; 328: 59. IF 9.776
- Omelyanchik, A., Gurevich, A., Pshenichnikov, S., Kolesnikova, V., **Smolkova, B.**, Uzhytchak, M., ... Rodionova, V. *Journal of Magnetism and Magnetic Materials* 2020, 166991. IF 2.993
- Levada, K., Pshenichnikov, S., Omelyanchik, A. ...Lunova M., Jirsa M., **Smolková B.**, Uzhytchak M., Dejneka A., Lunov O. *Nano Convergence* 2020,7, 17. IF 8.526
- Uzhytchak, M.; **Smolková, B.**; Lunova, M.; Jirsa, M.; Frtús, A.; Kubinová, Š.; Dejneka, A.; Lunov, O. *Cells* 2020, 9, 1015. IF 6.6
- Víšová, I.; **Smolková, B.**; Uzhytchak, M.; Vrabcová, M.; Chafai, D.E.; Houska, M.; Pastucha, M.; Skládal, P.; Farka, Z.; Dejneka, A.; Vaisocherová-Lísalová, H. *Biomolecules* 2020, 10, 1146. IF 4.879
- Víšová, I.; **Smolková, B.**; Uzhytchak, M.; Vrabcová, M.; Zhigunova, Y.; Houska, M.; Surman, F.; de los Santos Pereira, A.; Lunov, O.; Dejneka, A.; Vaisocherová-Lísalová, H. *Macromol. Biosci.* 2020, 20, 1900351– 1900359. IF 4.979
- Lunova M., **Smolková B.**, Uzhytchak M., Janoušková K.Ž., Jirsa M., Egorova D., Kulikov A., Kubinová Š., Dejneka A., Lunov O. *Cell. Mol. Life Sci.* 2020, 77, 2815–2838. IF 9.261
- Lunov, O.; Uzhytchak, M.; **Smolková, B.**; Lunova, M.; Jirsa, M.; Dempsey, N.M.; Dias, A.L.; Bonfim, M.; Hof, M.; Jurkiewicz, P.; Petrenko, Y.; Kubinová, Š.; Dejneka, A. *Cancers* 2019, 11, 1873. IF 6.126

- Jelinek, M.; Kocourek, T.; Jurek, K.; Jelinek, M.; **Smolková, B.**; Uzhytchak, M.; Lunov, O. *Nanomaterials* 2019, 9, 451. IF 4.324
 - O. Lunov, **B. Smolková**, A. Lynnyk, M. Uzhytchak, Š. Kubinová, A. Dejneka, *Jemná mechanika a optika* 2019, 64/5, 127 - 129.
 - **Smolková, B.**; Uzhytchak, M.; Lynnyk, A.; Kubinová, Š.; Dejneka, A.; Lunov, O., *J. Funct. Biomater.* 2019, 10, 2.
 - Lunova, M.; **Smolková, B.**; Lynnyk, A.; Uzhytchak, M.; Jirsa, M.; Kubinová, Š.; Dejneka, A.; Lunov, O. *Cancers* 2019, 11, 82. IF 6.126
 - **Smolkova, B.**, Lunova, M.; Lynnyk, A.; Uzhytchak, M.; Churpita, O.; Jirsa, M.; Kubinova, S.; Lunov, O.; Dejneka, A., *Cell Physiol. Biochem* 2019. 52(1): p. 119-140. IF 5.5
- Submitted manuscripts:**
- Frtús A., **Smolková B.**, Uzhytchak M., Lunova M., Jirsa, M., Dejneka A., Lunov O., *Lysosomal nanotoxicity: Impact of drug delivery and theranostic systems on lysosomal function.* Under review in *Advanced Drug Delivery Reviews*. IF 15.47
 - Frtús A., **Smolková B.**, Uzhytchak M., Lunova M., Jirsa M., Henry S.J.W., Dejneka A., Stephanopoulos N., Lunov O., *The interactions between DNA nanostructures and cells: A roadmap for successful applications in biomedicine.* Revision in *Acta Biomaterialia*. IF 8.947
 - Uzhytchak M., **Smolková B.**, Frtús A., Stupakov A., Lunova M., Scollo F., Hof M., Jurkiewicz P., Sullivan G.J., Dejneka A., Lunov O., *No evidence for detectable direct effects of magnetic field on cellular autofluorescence,* Under review in *Biochimica et Biophysica Acta (BBA) - Molecular Cell Research* IF 4.739

LIST OF APPENDICES

Appendix I

Smolková, B., Lunova, M.; Lynnyk, A.; Uzhytchak, M.; Churpita, O.; Jirsa, M.; Kubinova, S.; Lunov, O.; Dejneka, A., (2019) *Non-Thermal plasma, as a new physicochemical source, to induce redox imbalance and subsequent cell death in liver cancer cell lines*. Cell Physiol. Biochem 52(1): 119-140.

Contribution: Data acquisition and participation in the data interpretation and analysis, participation in writing and editing of the manuscript.

Appendix II

Lunova M., **Smolková B.**, Uzhytchak M., Janoušková K.Ž., Jirsa M., Egorova D., Kulikov A., Kubinová Š., Dejneka A., Lunov O. (2020) *Light-induced modulation of the mitochondrial respiratory chain activity: possibilities and limitations*. Cell. Mol. Life Sci., 77, 2815–2838.

Contribution: Data acquisition and participation in the data interpretation and analysis, participation in writing and editing of the manuscript.

Appendix III

Smolková, B.; Uzhytchak, M.; Lynnyk, A.; Kubinová, Š.; Dejneka, A.; Lunov, O., (2019), *A critical review on selected external physical cues and modulation of cell behavior: magnetic nanoparticles, non-thermal plasma and lasers*. J.Funct. Biomater. 10, 2.

Contribution: Analysis of the literature, participation in writing and editing of the manuscript.

Appendix IV

Smolková, B. Frtús, A., Uzhytchak, M., Lunova, M., Kubinová, Š., Dejneka, A., Lunov, O. (2020) *Critical Analysis of Non-Thermal Plasma-Driven Modulation of Immune Cells from Clinical Perspective*. Int. J. Mol. Sci., 21, 6226.

Contribution: Analysis of the literature, participation in writing and editing of the manuscript.